


國立交通大學

機械工程學系

碩士論文

藉部分區域穩定理論之

坎-離八卦多重交織導數同步



**Kan-Li Hexagram Multiple Symplectic Derivative
Synchronization by Partial Region Stability Theory**

研究生：張登順

指導教授：戈正銘 教授

中華民國一零一年六月

藉部分區域穩定理論之
坎-離八卦多重交織導數同步

**Kan-Li Hexagram Multiple Symplectic Derivative
Synchronization by Partial Region Stability Theory**

研究生：張登順

Student: Ding-Shun Jhang

指導教授：戈正銘

Advisor: Zheng-Ming Ge



Submitted to Institute of Mechanical Engineering
College of Engineering
National Chiao Tung University
In partial Fulfillment of the Requirement
For the Degree of master of science
In
Mechanical Engineering
June 2012
Hsinchu, Taiwan, Republic of China

中華民國一零一年六月

藉部分區域穩定理論之 坎-離八卦多重交織導數同步

學生：張登順

指導教授：戈正銘

摘要

太極為陰陽之結合，而太極渾沌系統即為陽渾沌系統與陰渾沌系統之合併。陽系統為正數系統，及一般系統，而陰系統則為負數時間之系統。八卦為太極之延伸，每個卦皆有各自對應的方向、圖形、代表物。八卦同步利用它們各自的圖形代表三個不同的渾沌系統，接著再用多重交織同步完成八卦同步。六十四卦為八卦的進階，它分上、下兩部分，這兩部分都代表八卦的一個卦象，而六十四卦同步即為八卦同步的延伸。同步一般是指系統間存在著主僕般的函數關係。而新的渾沌多重交織同步則是原來的系統與其他系統間變為伙伴間的函數關係。最後利用數值模擬來驗證前述計畫。

Kan-Li Hexagram Multiple Symplectic Derivative Synchronization by Partial Region Stability Theory

Student: Ding-Shun Jhang

Advisor: Zheng-Ming Ge

Department of Mechanical Engineering

National Chiao Tung University

Abstract

“Tai Ji”, the great one, is the combination of Yin and Yang, and Tai Ji chaotic system is the combination of “Yang” chaotic system and “Yin” chaotic system. Yang system represents contemporary system, and Yin system means historical system. The eight trigrams, a part of Chinese philosophy, is advance of “Tai Ji”, and they have their own directions, figures, and representations. Trigram synchronization uses three different chaos systems by the figures, and multiple symplectic derivative synchronization is used. Hexagram, advance of the eight trigrams, has two parts, upper and low, which both represent a trigram, and the hexagram synchronization is advance of trigram synchronization. The generalized synchronization is that there exists a functional relationship between the states of the master and those of the slave. A new type of chaotic synchronization, multiple chaotic symplectic synchronization, is obtained with the state variables of the original system and of another different order system as constituents of the functional relation of “partners”. Numerical simulations are provided to verify the effectiveness of the scheme.

誌 謝

此篇論文的完成首先要感謝的是指導教授 戈正銘老師的教誨，老師不但是專業領域上的巨擘，且不只是對專業領域的看法對人生的一些見解也都非常獨特、值得令人學習。而老師的文學方面也十分出眾，不論古文、唐詩都難不了他，讓學生深刻的體會到理工科系出身的文學家有這麼多不是沒道理的，對老師充滿了敬佩。

在做研究的過程中，要感謝的是李仕宇、何俊諺、蔡尚恩、王翔平、江振賓、李泳厚幾位學長們的指導，學長們在我們進來對研究主題還不是很了解時，教了我們研究的方式及程式的寫法，帶領我們成功起步。接著要感謝紀亭宇、李健華及黃啟任同學們的相互勉勵和幫忙，使本篇論文得以順利完成。

接下來要感謝的是我的家人的支持和支援，讓我不用為一些生活雜事擔心，得以專心學習。最後僅以此論文獻給你們。



CONTENTS

CHINESE ABSTRACT.....	iii
ABSTRACT.....	iv
ACKNOWLEDGMENT.....	v
CONTENTS.....	vi
Chapter 1 Introduction.....	1
Chapter 2 Chaos of Yang, Yin, and Tai Ji Rössler Systems.....	4
2-1. Preliminary	4
2-2. Yang Rössler system	4
2-3. Yin Rössler system	5
2-4. Simulation results	6
2-5. Tai Ji Rössler system	12
2-6. Summary.....	13
Chapter 3 Multiple Symplectic Derivative Synchronization of Ge-Ku-Van der Pol-Rössler System with Other Different Systems by Partial Region Stability Theory.....	28
3-1. Preliminary	28
3-2. Strategy of multiple symplectic derivative synchronization	28
3-3. Synchronization by GYC partial region stability theory	29
3-4. Synchronization by traditional method.....	32
3-5. Comparison between new strategy and traditional method.....	33
3-6. Summary.....	35

Chapter 4 Multiple Symplectic Derivative Synchronization of Rössler System and Sprott A System with Variable Time Scales by Partial Region

Stability Theory47

4-1. Preliminary47

4-2. Synchronization of different time on other octant.....47

4-3. Synchronization by traditional method.....49

4-5. Summary.....52

Chapter 5 Kan trigram and Li trigram Multiple Symplectic Derivative

Synchronization by Partial Region Stability Theory64

5-1. Preliminary64

5-2. Synchronization of Yang and Yin systems64

5-3. Kan trigram synchronization67

5-4. Li trigram synchronization69

5-5. Summary.....72

Chapter 6 Kan-Li Hexagram Multiple Symplectic Derivative Synchronization by Partial Region Stability Theory.....88

6-1. Preliminary88

6-2. Systems of Kan-Li hexagram synchronization.....88

6-3. Kan-Li hexagram synchronization by GYC partial region stability theory .91

6-4. Kan-Li hexagram synchronization by traditional Lyapunov function93

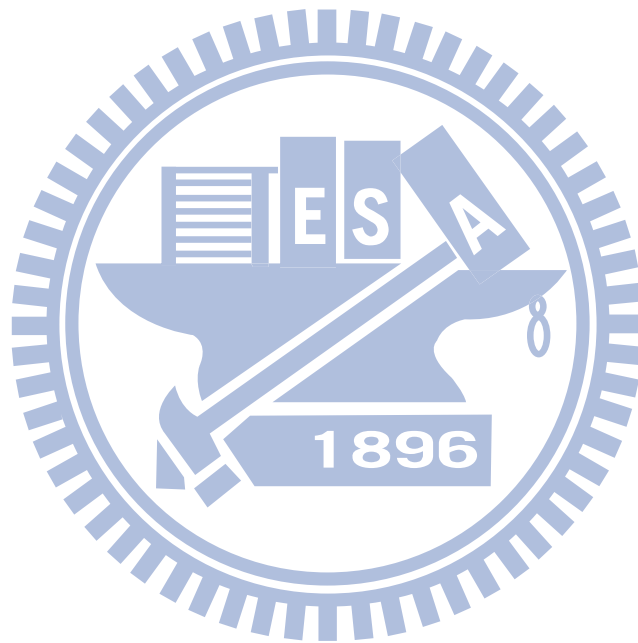
6-5. Kan-Li hexagram synchronization by linear feedback method.....95

6-6. Comparison of synchronization ways.....97

6-7. Summary..... 100

Chapter 7 Conclusions..... 109

References..... 111



Chapter 1

Introduction

Chaos theory, a part of nonlinear dynamics, changes the scientific way of looking at the dynamics of natural and social systems. Since E.N. Lorenz [1] discovered chaos in a simple system of three autonomous ordinary differential equations in 1963, there are lots of articles in studying chaos [2-4]. The phenomenon of chaos has attracted widespread attention amongst physicists, mathematicians, and engineers. Chaos has also been extensively studied in many fields, such as chemical reactions, power converters, biological systems, information processing, secure communications, etc. [5-13].

Chaos synchronization, first proposed by Fujisaka and Yamada in 1983 [14], is a very interesting problem and has been widely studied in recent years [15-23]. Many kinds of chaos synchronization appears, such as symplectic synchronization [24], generalized synchronization [25], complete synchronization [26], phase synchronization [27-28], anticipating synchronization [29-30], lag synchronization [31-32], etc.

This thesis is organized as follows. In Chapter 2, Tai Ji Rössler system is presented, which is combination of Yang Rössler system and Yin Rössler system [33]. Yang Rössler system means contemporary Rössler system [34–36], and Yin Rössler system is historical Rössler system. Tai Ji Rössler system is introduced by time histories and phase portraits and the chaotic behaviors are investigated by bifurcation diagrams, Lyapunov exponents, and tables.

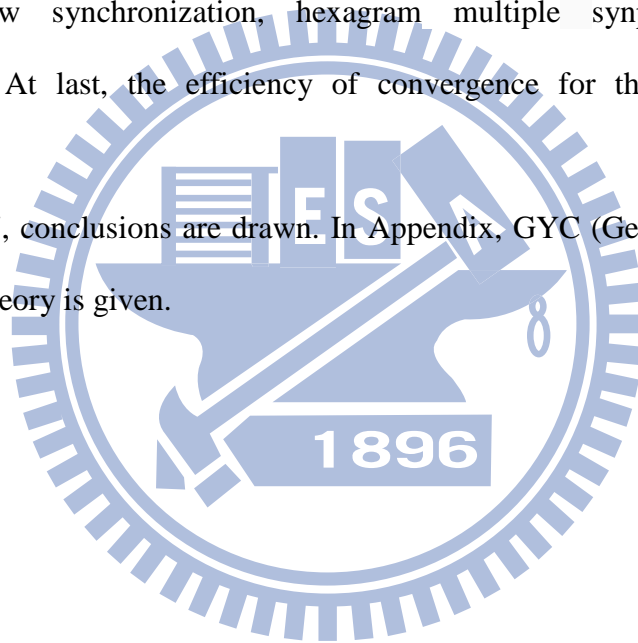
In Chapter 3, a new symplectic synchronization by GYC partial region stability theory is studied. Symplectic synchronization is defined as $y = H(x, y, t)$, where x, y are the state vectors of the “Partner A” and of the “Partner B”, respectively. The final desired state y not only depends upon the “master” system state x but also depends upon the “slave” system state y itself. The symplectic derivative functions is further evolutionary to a more general form, $G(x, y, z, \dots, \dot{x}, \dot{y}, \dot{z}, \dots, \ddot{x}, \ddot{y}, \ddot{z}, \dots, t) = F(x, y, z, \dots, \dot{x}, \dot{y}, \dot{z}, \dots, \ddot{x}, \ddot{y}, \ddot{z}, \dots, t)$, by adding the derivative of the state vectors, and the new synchronization is called “multiple symplectic derivative synchronization”. In simulation examples, Ge-Ku-Van der Pol system [37], Rössler System, Sprott 22, Sprott A, Sprott B and Sprott C [38] are used.

In Chapter 4, multiple symplectic derivative synchronization by GYC partial region stability theory is extended to a more general form. The new strategy of symplectic synchronization not only use the different time scales of chaos system but a new variable, τ . The new multiple symplectic derivative synchronization is proposed as $G(x, y, \dot{x}, \dot{y}, \ddot{x}, \ddot{y}, t, \tau) = F(x, y, \dot{x}, \dot{y}, \ddot{x}, \ddot{y}, t, \tau)$, where τ is a variable time scale, $\tau = \tau(t)$. And the comparison of the new strategy with traditional method, Lyapunov function, is given [39].

In Chapter 5, the eight trigrams are first studied with chaos synchronization. The eight trigrams have their own direction, figure, and representation, and the figures of them are used to complete a new multiple symplectic derivative synchronization, the eight trigrams synchronization, and Kan trigram and Li trigram are selected in this chapter. Trigram has three parts, upper, central, and low, and they represent three different chaos systems separately to complete a two-stages synchronization, linear feedback synchronization, and multiple symplectic derivative synchronization by GYC partial region stability theory.

In Chapter 6, hexagram, advance of the eight trigram, is used to complete a new multiple symplectic derivative synchronization. Hexagram has two parts, upper and low, and they both represent a trigram. For example, the upper part of Kan-Li hexagram, used in this thesis, is Kan trigram and the low part of it is Li trigram. The Kan-Li hexagram multiple symplectic derivative synchronization is based on Kan trigram synchronization and Li trigram synchronization by combining them. Three different synchronization way, Lyapunov function by GYC partial region stability theory, traditional Lyapunov function, and linear feedback method, are used to complete a new synchronization, hexagram multiple synplectic derivative synchronization. At last, the efficiency of convergence for the three ways are compared.

In Chapter 7, conclusions are drawn. In Appendix, GYC (Ge-Yao-Chen) partial region stability theory is given.



Chapter 2

Chaos of Yang, Yin, and Tai Ji Rössler Systems

2-1. Preliminary

The Yang Rössler system has been analyzed in detail, there are no article in looking into the history Rössler system which is called Yin Rössler system. By the combination of Yang Rössler system and Yin Rössler system, which is called “Tai Ji” Rössler system, i.e. the “Great One” Rössler system, the exhaustive behaviors of Rössler system for $-\infty < t < \infty$ are presented.

This chapter is presented as follows. In Section 2, Yang Rössler system is shown. In Section 3, Yin Rössler system is presented. In Section 4, behaviors of chaos of Rössler system is proposed. In Section 5, Tai Ji Rössler system is shown. In Section 6, summary is drawn.

2-2. Yang Rössler system

Before introducing the Yin Rössler equation, the Yang Rössler system can be recalled as follows:

$$\begin{cases} \frac{dx_1(t)}{dt} = -(x_2(t) + x_3(t)) \\ \frac{dx_2(t)}{dt} = x_1(t) + ax_2(t) \\ \frac{dx_3(t)}{dt} = b + x_1(t)x_3(t) - cx_3(t) \end{cases} \quad (2-1)$$

When initial condition $(x_{10}, x_{20}, x_{30}) = (0.3, 0.1, 0.5)$ and parameters $a = 0.15$ and $b = 0.2$ and $c = 10$, chaos of the Yang Rössler system appears. The chaotic time histories and 2D and 3D phase portraits are behavior shown in Figs. 2-1 and 2-2.

2-3. Yin Rössler system

Yin Rössler equations are:

$$\begin{cases} \frac{dx_1(-t)}{d-t} = -(x_2(-t) + x_3(-t)) \\ \frac{dx_2(-t)}{d-t} = x_1(-t) + ax_2(-t) \\ \frac{dx_3(-t)}{d-t} = b + x_1(-t)x_3(-t) - cx_3(-t) \end{cases} \quad (2-2)$$

When initial condition $(x_{10}, x_{20}, x_{30}) = (0.3, 0.1, 0.5)$ and parameters $a = -0.15$ and $b = -0.2$ and $c = -10$, chaos of the Yin Rössler system appears. The chaotic behavior of Eq. (2-2) is shown in Figs. 2-3 and 2-4. It is clear that in the left-hand sides of Eq. (2-2), the derivatives are taken with the back-time.

Table 2-1 shows the behaviors of Yin Rössler system in different part with initial condition $(x_{10}, x_{20}, x_{30}) = (0.3, 0.1, 0.5)$.

Table 2-1 Dynamic behaviors of Yin Rössler system for different signs of parameters

a	b	c	states
+	+	+	Approach to infinity
+	+	-	Approach to a point
+	-	+	Chaos and periodic
+	-	-	Approach to a point
-	+	+	Approach to infinity
-	+	-	Approach to infinity
-	-	+	Approach to infinity
-	-	-	Chaos and periodic

2-4. Simulation results

In order to study the difference and similarity between Yang and Yin Rössler system, the bifurcation diagram and Lyapunov exponents are used. The simulation results are divided into the following three parts :

Part 1 :

Parameter a is varied and b, c are fixed, the simulation results are shown in Figs. 2-5 and 2-6, and Tables 2-2 and 2-3.

Tables 2-2 and 2-3 show the difference between Yang and Yin Rössler systems with different ranges of parameter a and, the behaviors of them are varied with parameter a , become either chaos or Periodic trajectory. Table 2-2 shows that when parameter a are 0.0030 ~ 0.1014, 0.1240 ~ 0.1311, 0.1519 ~ 0.1532, 0.2238 ~ 0.2249, 0.2616 ~ 0.2663, and 0.3251 ~ 0.3256, Yang Rössler system are periodic trajectories. When parameter a are 0.1014 ~ 0.1240, 0.1311 ~ 0.1519, 0.1532 ~ 0.2238, 0.2249 ~ 0.2616, 0.2663 ~ 0.3251, and 0.3256 ~ 0.3750, the chaotic behavior is shown in Yang Rössler system. And Table 2-3 shows that when parameter a are (-0.0030) ~ (-0.1131), (-0.1244) ~ (-0.1311), (-0.1518) ~ (-0.1532), (-0.2239) ~ (-0.2255), (-0.2613) ~ (-0.2670), and (-0.3255) ~ (-0.3257), Yin Rössler system are periodic trajectories. When parameter a are (-0.1131) ~ (-0.1244), (-0.1311) ~ (-0.1518), (-0.1532) ~ (-0.2239), (-0.2255) ~ (-0.2613), (-0.2670) ~ (-0.3255), and (-0.3257) ~ (-0.3750), chaos appears. Comparing Tables 2-2 and 2-3, it can be found out that there are only two cases, chaos and periodic trajectory, in the Yang Rössler system for parameter a in range 0.003 to 0.375, and there exists chaotic behavior and periodic trajectory in Yin Rössler system with parameter a in range -0.375 to -0.003.

Part 2 :

Parameter b is varied and a, c are fixed, the simulation results are shown in Figs. 2-7 and 2-8, and Tables 2-4 and 2-5.

Tables 2-4 and 2-5 show the difference between Yang and Yin Rössler systems with different ranges of parameter b and, the behaviors of them are varied with parameter b , become either chaos or Periodic trajectory. Table 2-4 shows that when parameter b are 0.050 ~ 0.443, 0.553 ~ 0.761, 0.771 ~ 0.949, and 0.956 ~ 1.100, chaos appears. When parameter b are 0.443 ~ 0.553, 0.761 ~ 0.771, 0.949 ~ 0.956, and 1.100 ~ 3.050, Yang Rössler system are periodic trajectories. Table 2-5 shows that when parameter b are (-0.050) ~ (-0.167), (-0.171) ~ (-0.457), (-0.554) ~ (-0.762), (-0.767) ~ (-0.948), and (-0.958) ~ (-1.076), the chaotic behavior is shown in Yin Rössler system. When parameter b are (-0.167) ~ (-0.171), (-0.457) ~ (-0.554), (-0.762) ~ (-0.767), (-0.948) ~ (-0.958), and (-1.076) ~ (-3.050), the behaviors of Yin Rössler system are periodic trajectories. Comparing Tables 2-4 and 2-5, it can be found out that there are only two cases, chaos and periodic trajectory, in the Yang Rössler system for parameter b in range 0.05 to 3.05, and there exists chaotic behavior and periodic trajectory in Yin Rössler system with parameter b in range -3.05 to -0.05.

Part 3 :

Parameter b is varied and a, c are fixed, the simulation results are shown in Figs. 2-9 and 2-10, and Tables 2-6 and 2-7.

Tables 6 and 7 show the different dynamics between Yang and Yin Rössler systems with different ranges of parameter c . Table 2-6 shows that when parameter c are 3.000 ~ 5.930, 6.215 ~ 6.225, 6.740 ~ 6.775, 7.595 ~ 7.975, 8.930 ~ 8.940, and 10.315 ~ 10.380, Yang Rössler system are periodic trajectories. When 5.930 ~ 6.215, 6.225 ~

6.740, 6.775 ~ 7.595, 7.975 ~ 8.930, 8.940 ~ 10.315, and 10.380 ~ 11.000, chaos appears. Table 2-7 shows that when parameter c are (-5.930) ~ (-6.225), (-6.240) ~ (-6.750), (-6.755) ~ (-7.560), (-8.090) ~ (-8.920), (8.940) ~ (-10.265), and (-10.295) ~ (-11.000), the chaotic behavior is shown in Yin Rössler system. When parameter c are (-3.000) ~ (-5.930), (-6.225) ~ (-6.240), (-6.750) ~ (-6.755), (-7.560) ~ (-8.090), (-8.920) ~ (-8.940), and (-10.265) ~ (-10.295), the behaviors of Yin Rössler system are periodic trajectories. Comparing Tables 2-6 and 2-7, it can be found out that there are only two cases, chaos and periodic trajectory, in the Yang Rössler system for parameter c in range 3 to 11, and there exists chaotic behavior and periodic trajectory in Yin Rössler system with parameter c in range -11 to -3.

Table 2-2 Range of parameter a of Yang chaos of Rössler system

Values of a	Behaviors of Yang Chaos
0.0030 ~ 0.1014	Periodic trajectory
0.1014 ~ 0.1240	Chaos
0.1240 ~ 0.1311	Periodic trajectory
0.1311 ~ 0.1519	Chaos
0.1519 ~ 0.1532	Periodic trajectory
0.1532 ~ 0.2238	Chaos
0.2238 ~ 0.2249	Periodic trajectory
0.2249 ~ 0.2616	Chaos
0.2616 ~ 0.2663	Periodic trajectory
0.2663 ~ 0.3251	Chaos
0.3251 ~ 0.3256	Periodic trajectory
0.3256 ~ 0.3750	Chaos

Table 2-3 Range of parameter a of Yin chaos of Rössler system

Values of a	Behaviors of Yin Chaos
-0.0030 ~ -0.1131	Periodic trajectory
-0.1131 ~ -0.1244	Chaos
-0.1244 ~ -0.1311	Periodic trajectory
-0.1311 ~ -0.1518	Chaos
-0.1518 ~ -0.1532	Periodic trajectory
-0.1532 ~ -0.2239	Chaos
-0.2239 ~ -0.2255	Periodic trajectory
-0.2255 ~ -0.2613	Chaos
-0.2613 ~ -0.2670	Periodic trajectory
-0.2670 ~ -0.3255	Chaos
-0.3255 ~ -0.3257	Periodic trajectory
-0.3257 ~ -0.3750	Chaos

Table 2-4 Range of parameter b of Yang chaos of Rössler system

Values of b	Behaviors of Yang Chaos
0.050 ~ 0.443	Chaos
0.443 ~ 0.553	Periodic trajectory
0.553 ~ 0.761	Chaos
0.761 ~ 0.771	Periodic trajectory
0.771 ~ 0.949	Chaos
0.949 ~ 0.956	Periodic trajectory
0.956 ~ 1.100	Chaos
1.100 ~ 3.050	Periodic trajectory

Table 2-5 Range of parameter b of Yin chaos of Rossler system

Values of b	Behaviors of Yin Chaos
-0.050 ~ -0.167	Chaos
-0.167 ~ -0.171	Periodic trajectory
-0.171 ~ -0.457	Chaos
-0.457 ~ -0.554	Periodic trajectory
-0.554 ~ -0.762	Chaos
-0.762 ~ -0.767	Periodic trajectory
-0.767 ~ -0.948	Chaos
-0.948 ~ -0.958	Periodic trajectory
-0.958 ~ -1.076	Chaos
-1.076 ~ -3.050	Periodic trajectory

Table 2-6 Range of parameter c of Yang chaos of Rossler system

Values of c	Behaviors of Yang Chaos
3.000 ~ 5.930	Periodic trajectory
5.930 ~ 6.215	Chaos
6.215 ~ 6.225	Periodic trajectory
6.225 ~ 6.740	Chaos
6.740 ~ 6.775	Periodic trajectory
6.775 ~ 7.595	Chaos
7.595 ~ 7.975	Periodic trajectory
7.975 ~ 8.930	Chaos
8.930 ~ 8.940	Periodic trajectory
8.940 ~ 10.315	Chaos
10.315 ~ 10.380	Periodic trajectory
10.380 ~ 11.000	Chaos

Table 2-7 Range of parameter c of Yin chaos of Rossler system

Values of c	Behaviors of Yin Chaos
-3.000 ~ -5.930	Periodic trajectory
-5.930 ~ -6.225	Chaos
-6.225 ~ -6.240	Periodic trajectory
-6.240 ~ -6.750	Chaos
-6.750 ~ -6.755	Periodic trajectory
-6.755 ~ -7.560	Chaos
-7.560 ~ -8.090	Periodic trajectory
-8.090 ~ -8.920	Chaos
-8.920 ~ -8.940	Periodic trajectory
-8.940 ~ -10.265	Chaos
-10.265 ~ -10.295	Periodic trajectory
-10.295 ~ -11.000	Chaos

2-5. Tai Ji Rössler system

For comparing the difference and similarity between Yang and Yin Rössler system, the Tai Ji Rössler system and the error equation are created.

The Tai Ji Rössler systems are created from the combination of Yang and Yin Rössler systems. And the Tai Ji Rössler system is shown in Figs. 2-11 and 2-12 and the comparison of bifurcation diagram of Yang and Yin Rössler system is shown from Figs. 2-13 to Figs. 2-15.

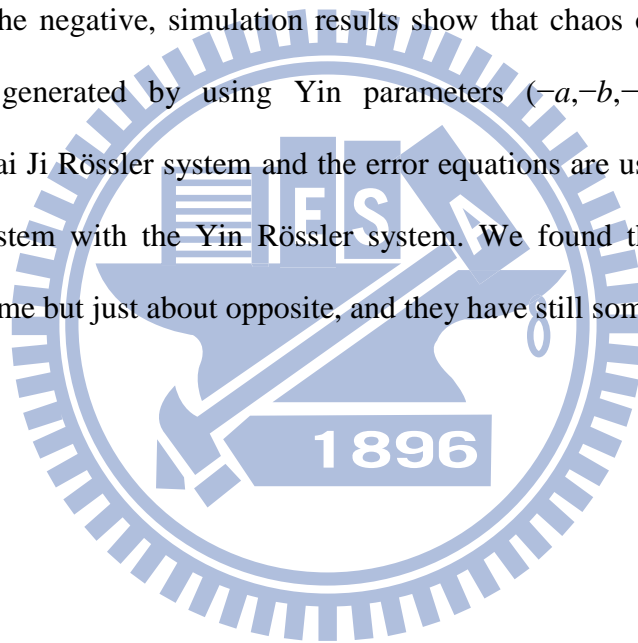
The error equations are:

$$\begin{cases} e_1 = x_{Yin1} - x_{Yang1} \\ e_2 = x_{Yin2} - x_{Yang2} \\ e_3 = x_{Yin3} - x_{Yang3} \end{cases} \quad (2-3)$$

where x_{Yang1} , x_{Yang2} , and x_{Yang3} are x_1 , x_2 , and x_3 of Yang Rössler system with initial condition $(x_{10}, x_{20}, x_{30}) = (0.3, 0.1, 0.5)$ and parameters $a = 0.15$ and $b = 0.2$ and $c = 10$, and x_{Yin1} , x_{Yin2} , and x_{Yin3} are x_1 , x_2 , and x_3 of Yin Rössler system with initial condition $(x_{10}, x_{20}, x_{30}) = (0.3, 0.1, 0.5)$ and parameters $a = -0.15$ and $b = -0.2$ and $c = -10$. The time histories of Eq. (2-3) is shown in Figs. 2-16.

2-6. Summary

The Tai Ji Rössler system are firstly introduced in this chapter. When the time is taken back into the negative, simulation results show that chaos of the Yin Rössler system can be generated by using Yin parameters $(-a, -b, -c)$. By numerical simulation, the Tai Ji Rössler system and the error equations are used to compare the Yang Rössler system with the Yin Rössler system. We found that Yang and Yin would most be same but just about opposite, and they have still some differences.



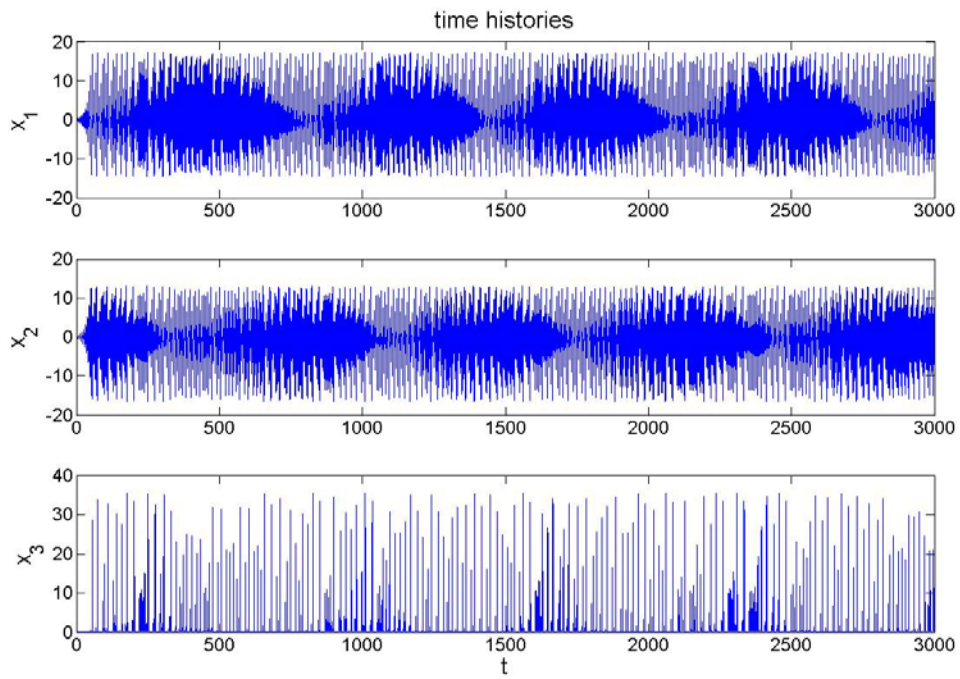
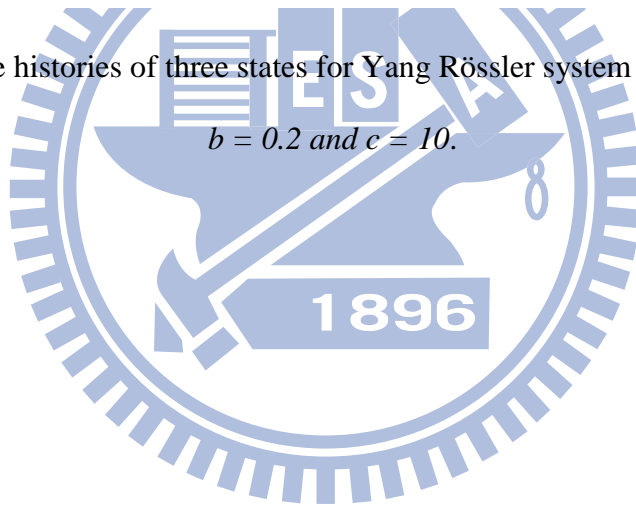


Fig. 2-1 Time histories of three states for Yang Rössler system with $a = 0.15$,
 $b = 0.2$ and $c = 10$.



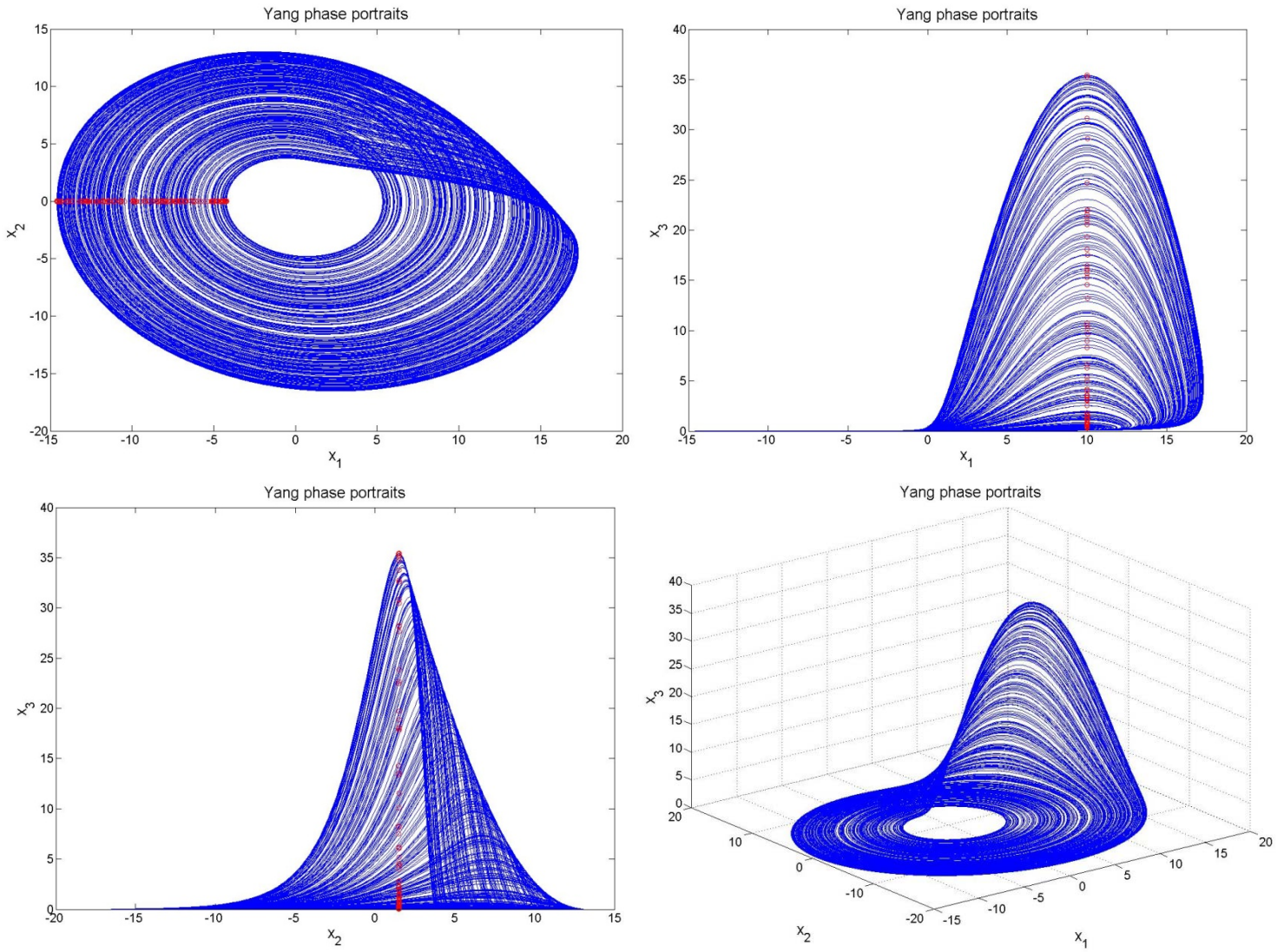


Fig. 2-2 Projections of phase portrait of chaotic Yang Rössler system with $a=0.15$, $b = 0.2$ and $c = 10$.

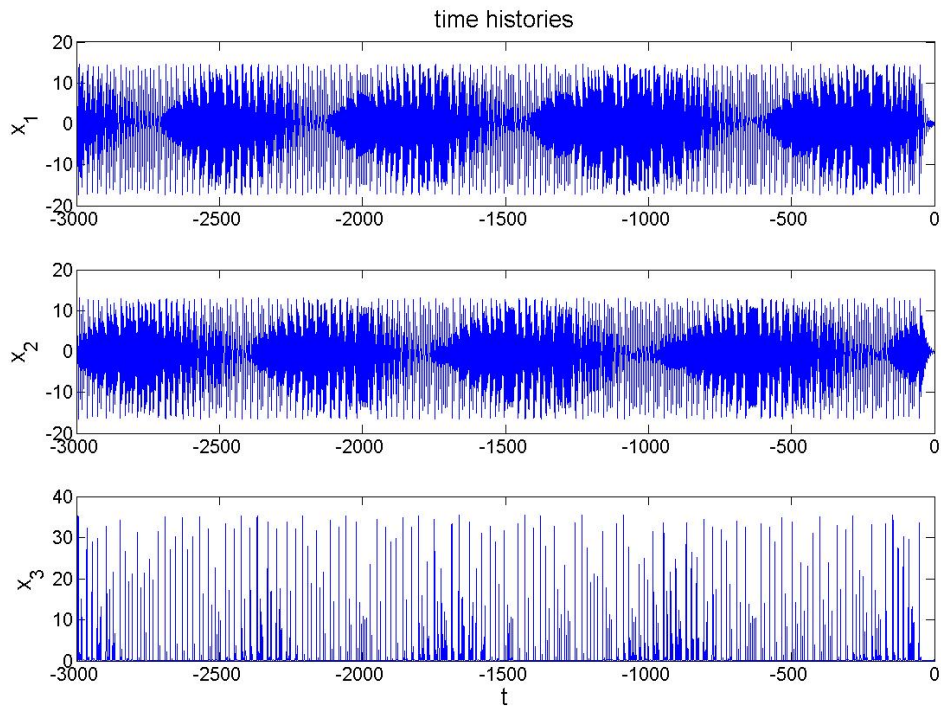
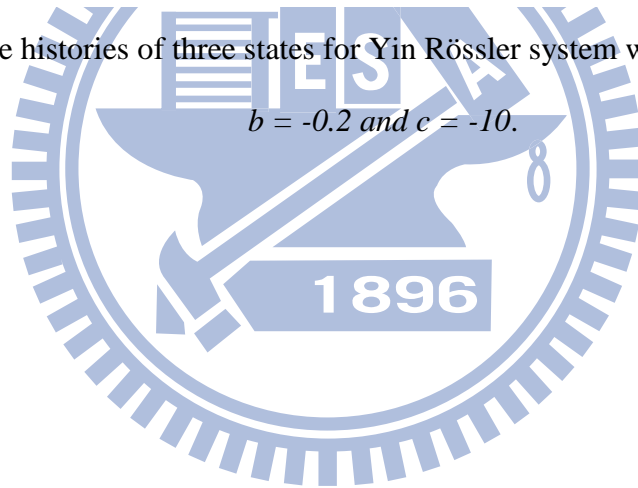


Fig. 2-3 Time histories of three states for Yin Rössler system with $a = -0.15$,
 $b = -0.2$ and $c = -10$.



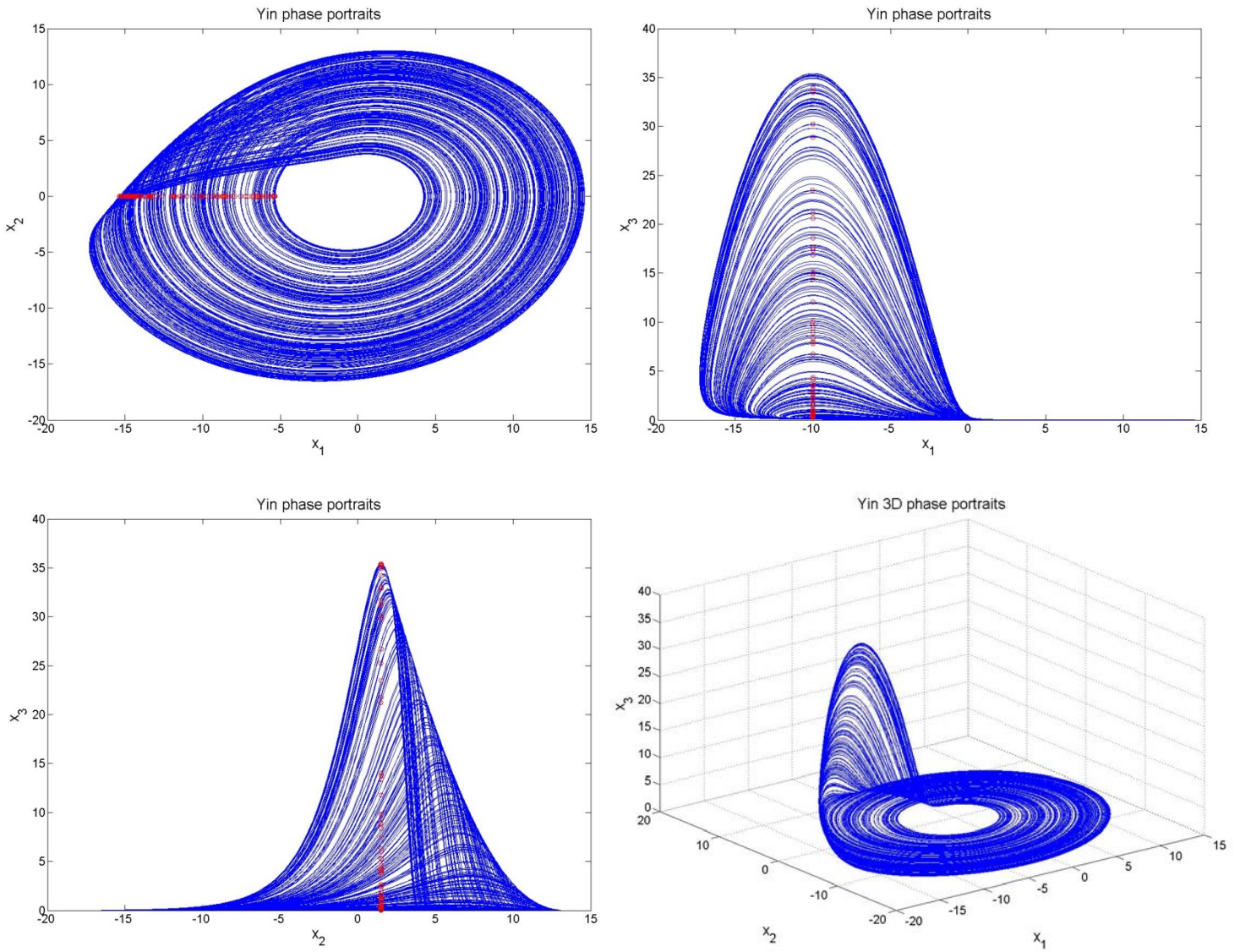


Fig. 2-4 Projections of phase portrait of chaotic Yin Rössler system with
 $a = -0.15$, $b = -0.2$ and $c = -10$.

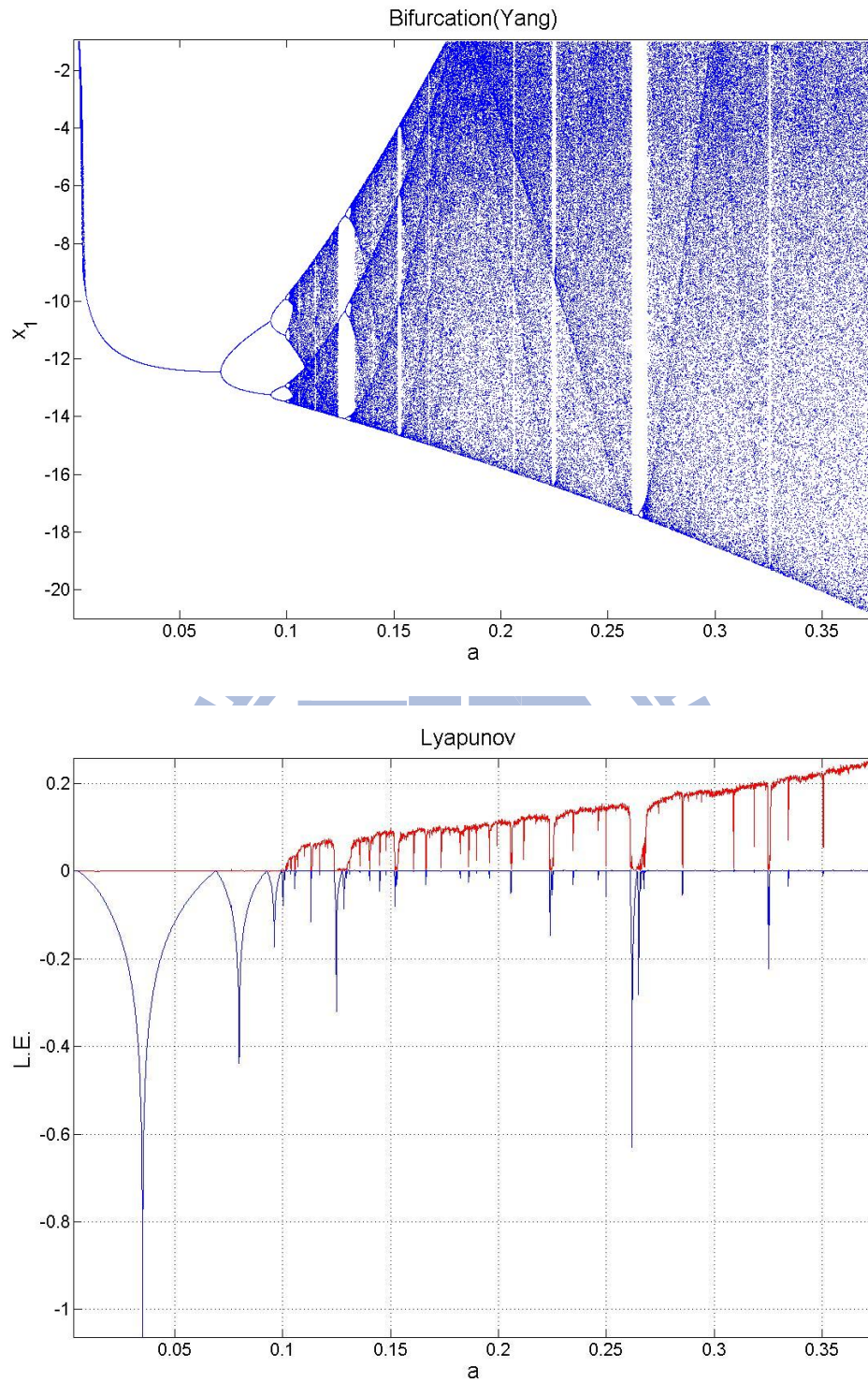


Fig. 2-5 Bifurcation diagram and Lyapunov exponents of chaotic Yang Rössler system with $b = 0.2$ and $c = 10$.

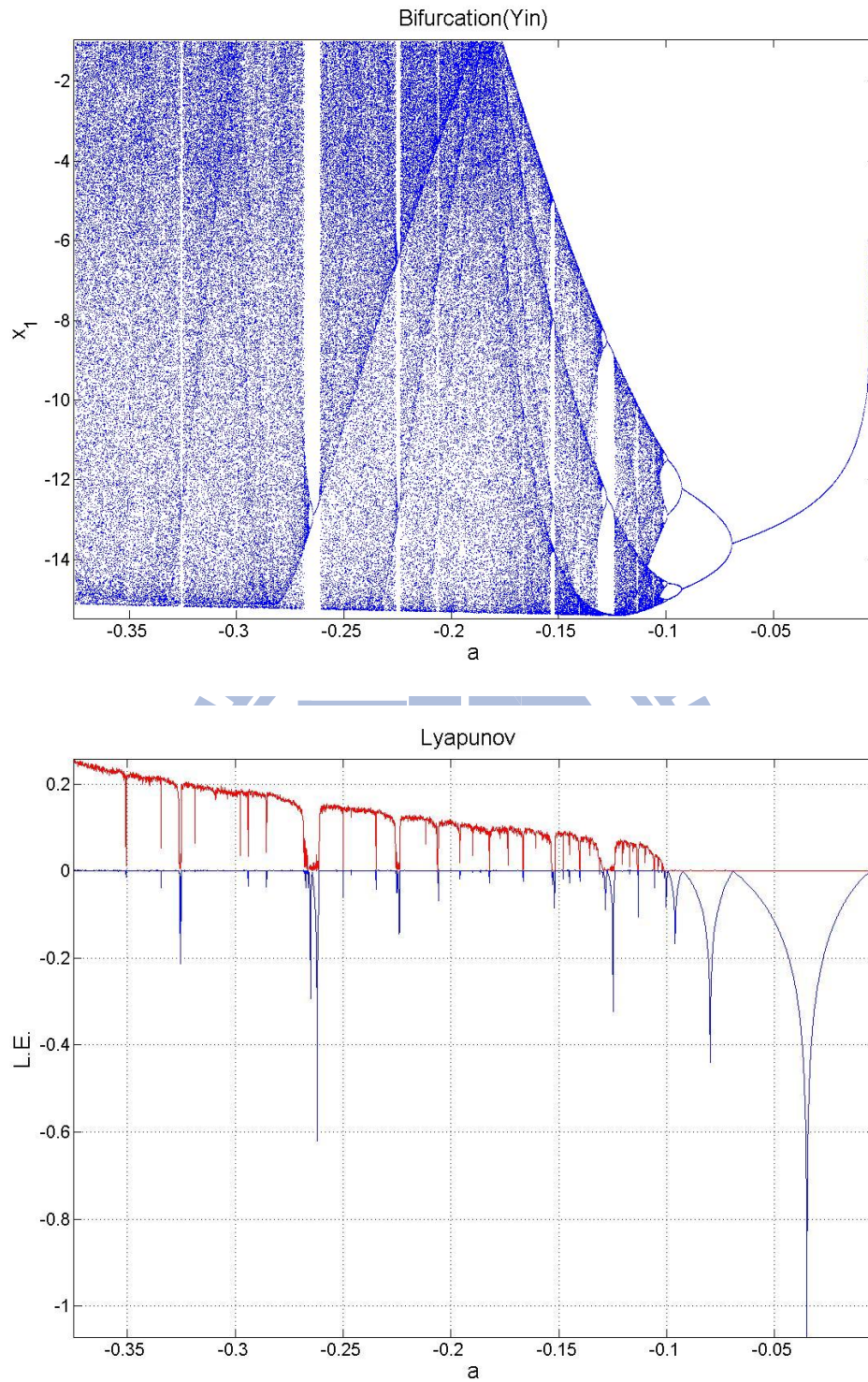


Fig. 2-6 Bifurcation diagram and Lyapunov exponents of chaotic Yin Rössler system with $b = -0.2$ and $c = -10$.

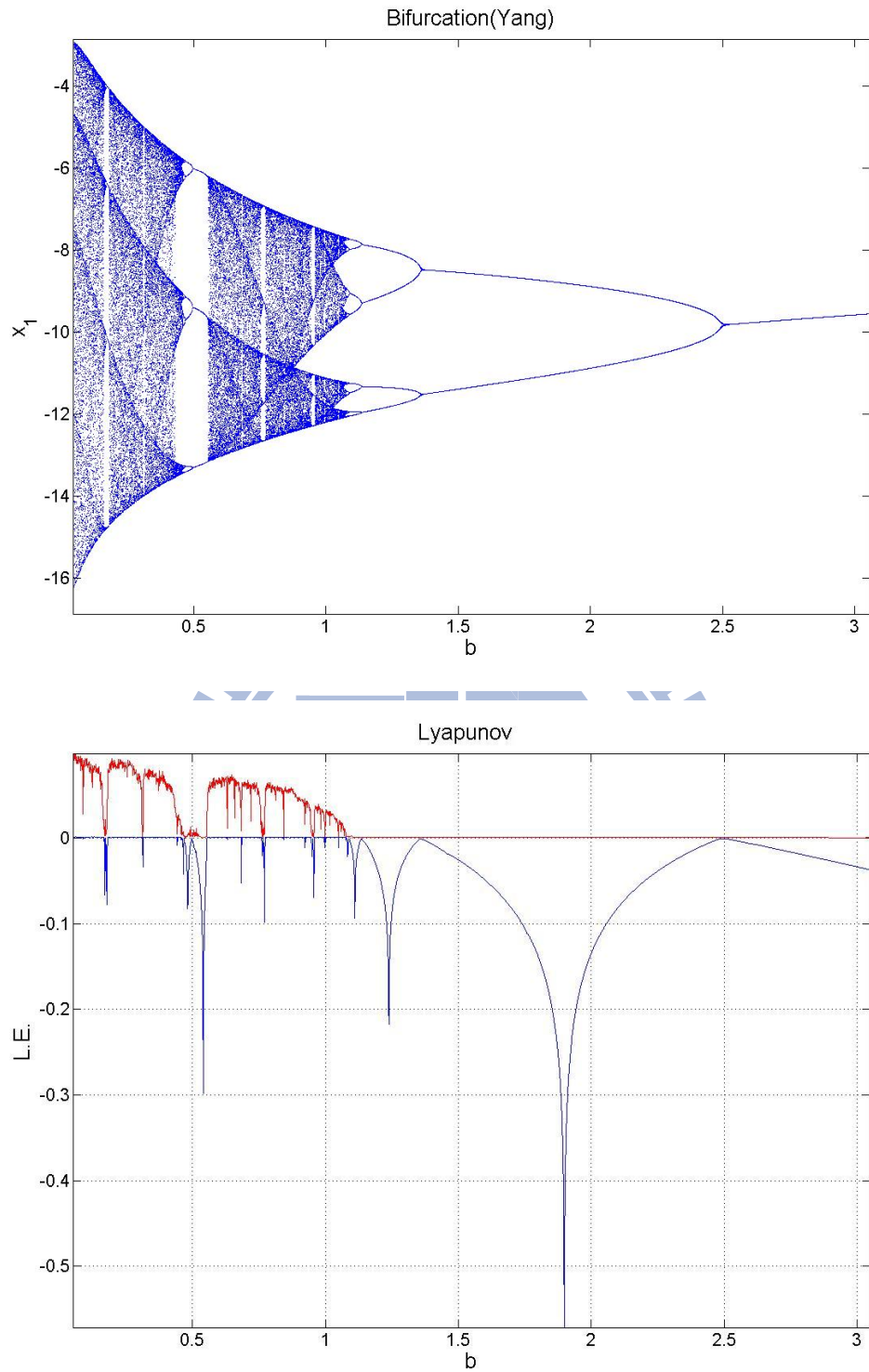


Fig. 2-7 Bifurcation diagram and Lyapunov exponents of chaotic Yang Rössler system with $a = 0.15$ and $c = 10$.

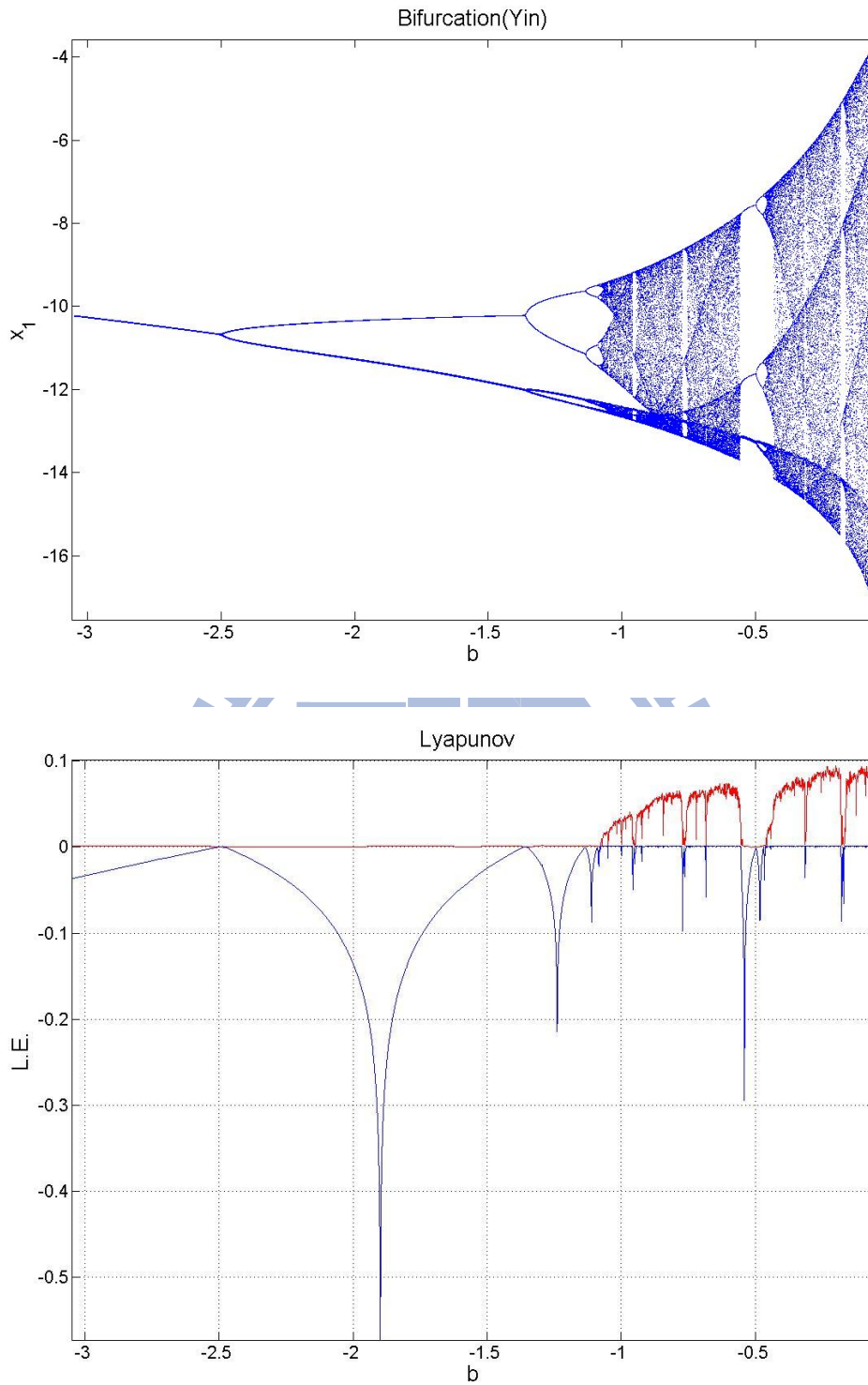


Fig. 2-8 Bifurcation diagram and Lyapunov exponents of chaotic Yin Rössler system with $a = -0.15$ and $c = -10$.

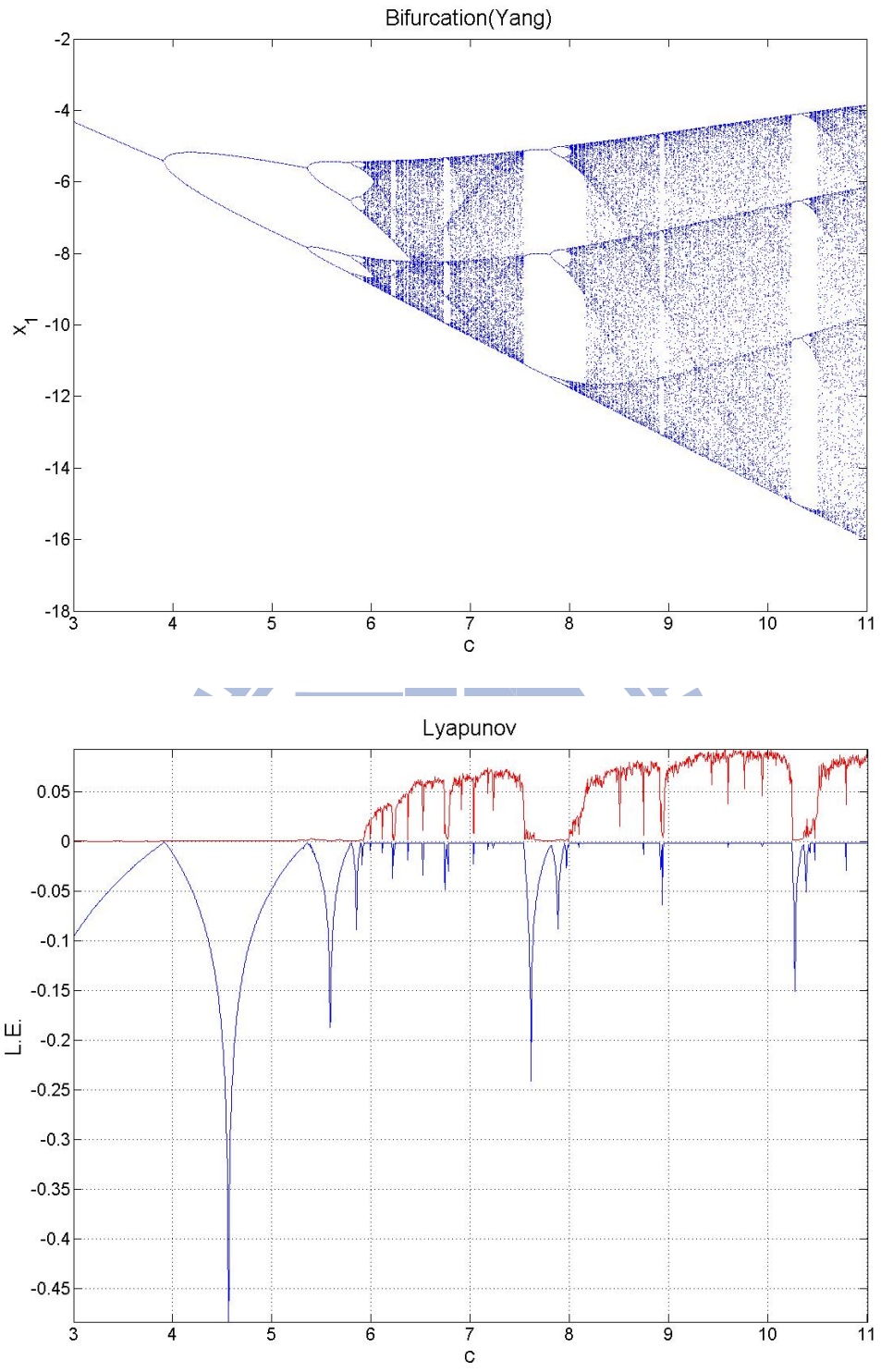


Fig. 2-9 Bifurcation diagram and Lyapunov exponents of chaotic Yang Rössler system with $a = 0.15$ and $b = 0.2$.

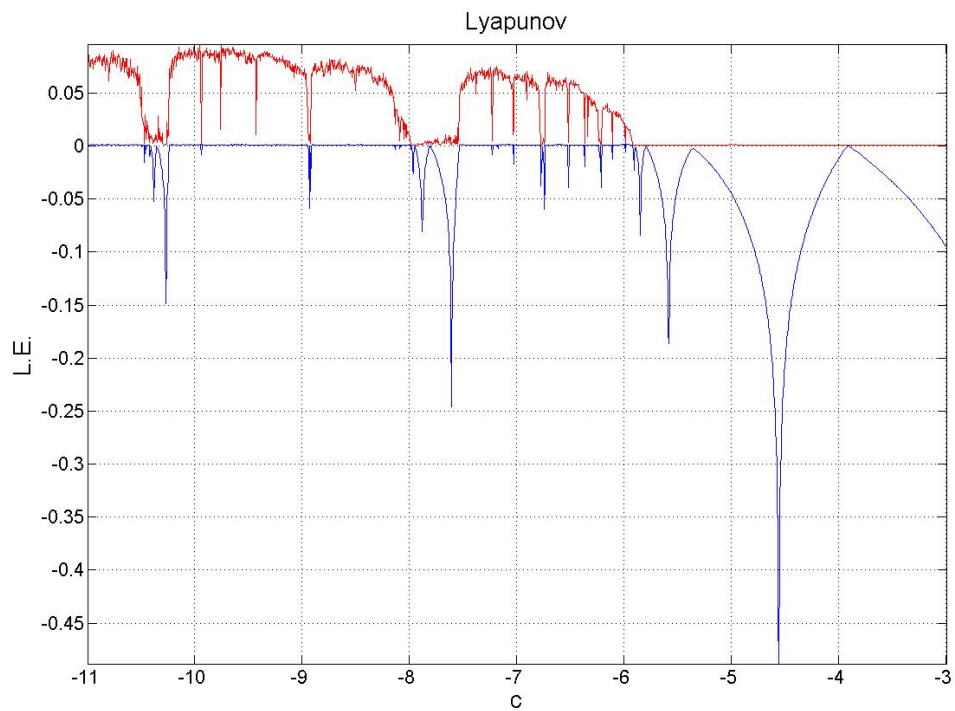
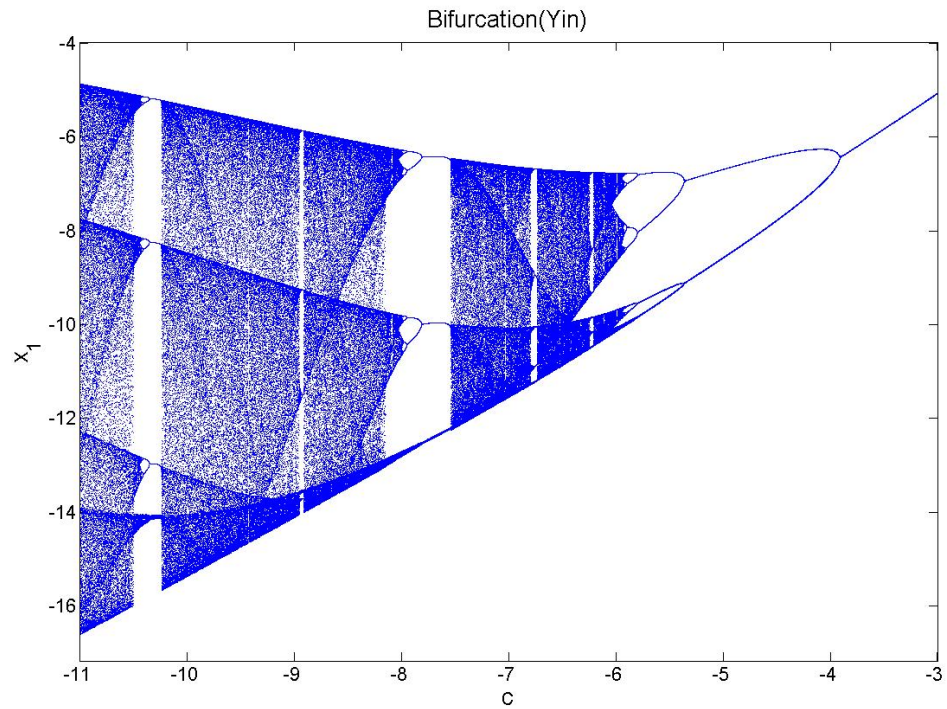


Fig. 2-10 Bifurcation diagram and Lyapunov exponents of chaotic Yin Rössler system with $a = -0.15$ and $b = -0.2$.

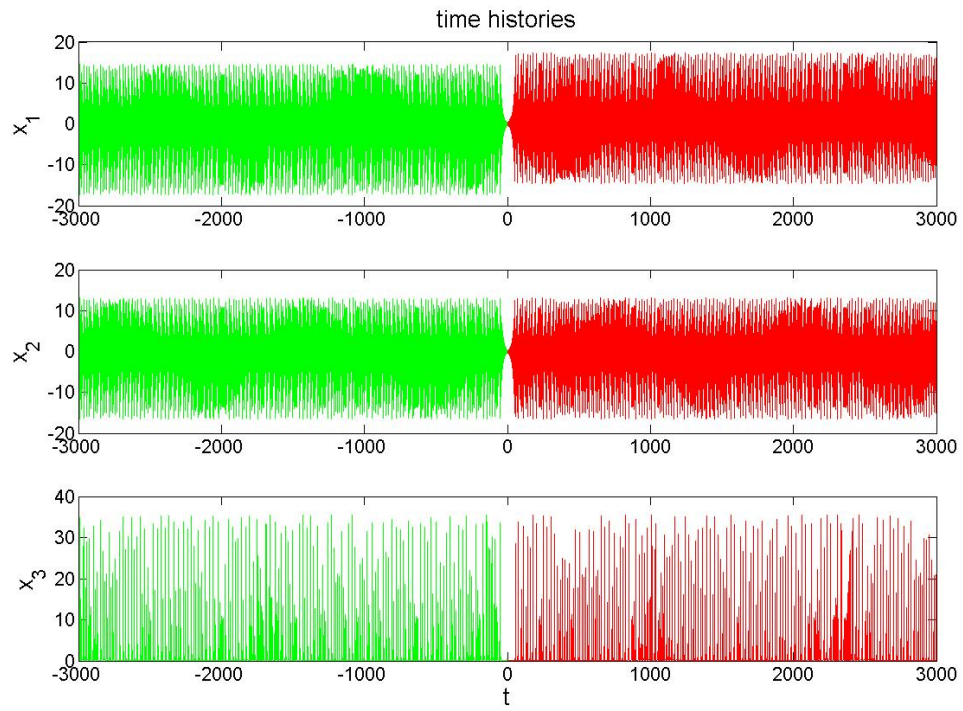
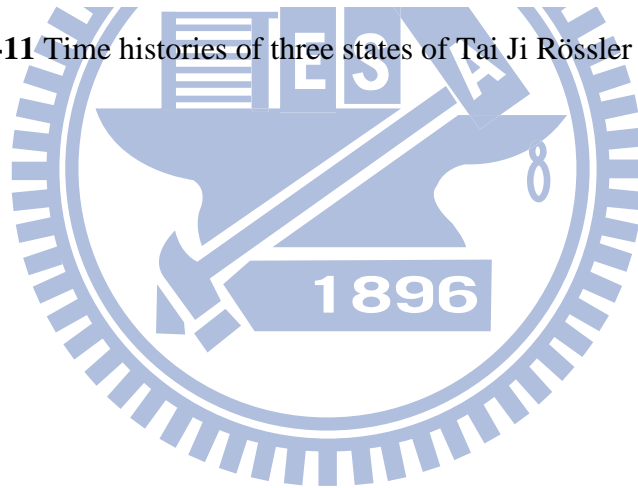


Fig. 2-11 Time histories of three states of Tai Ji Rössler system.



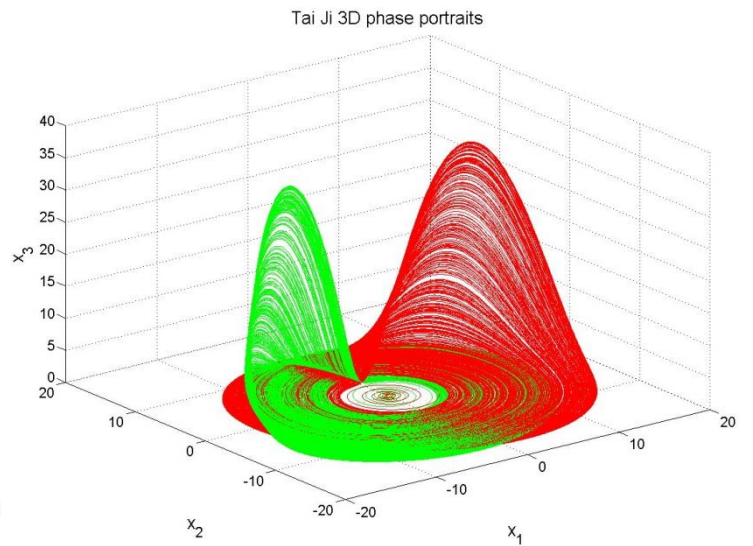
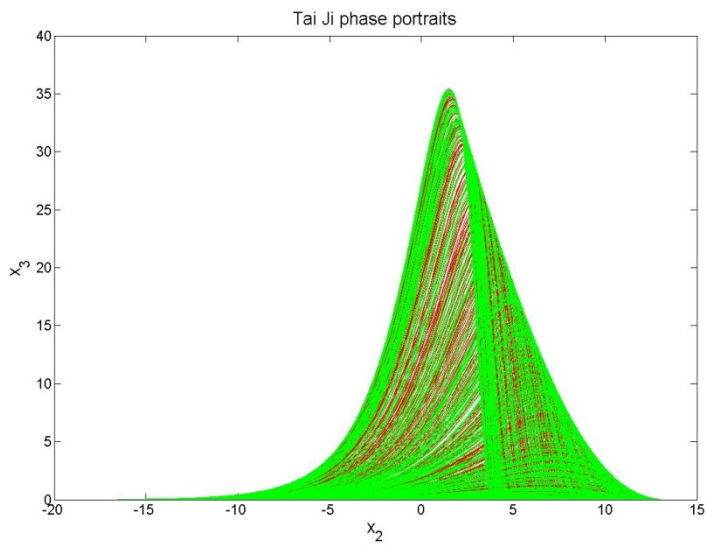
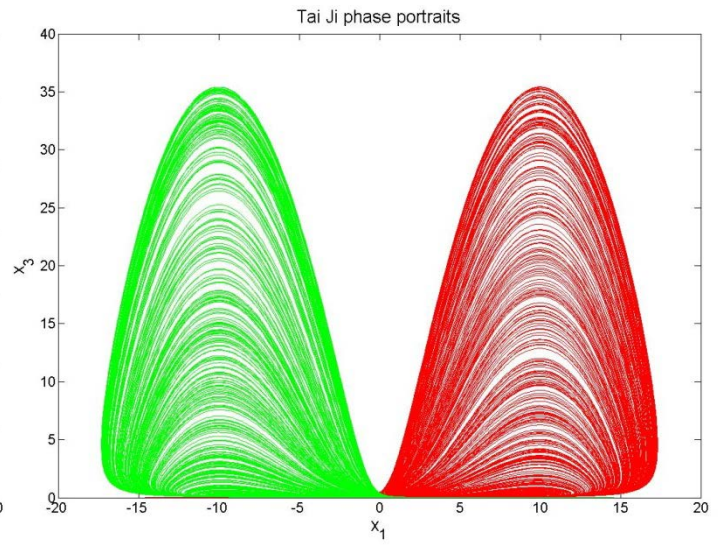
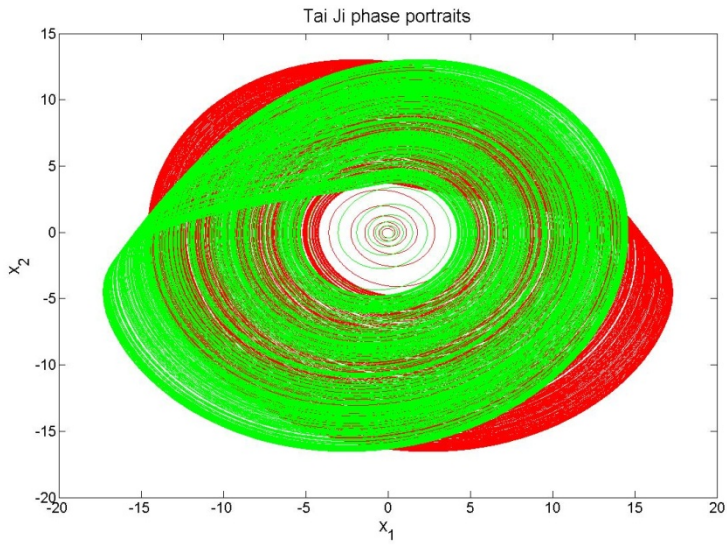


Fig. 2-12 Projections of phase portrait of chaotic Tai Ji Rössler systems.

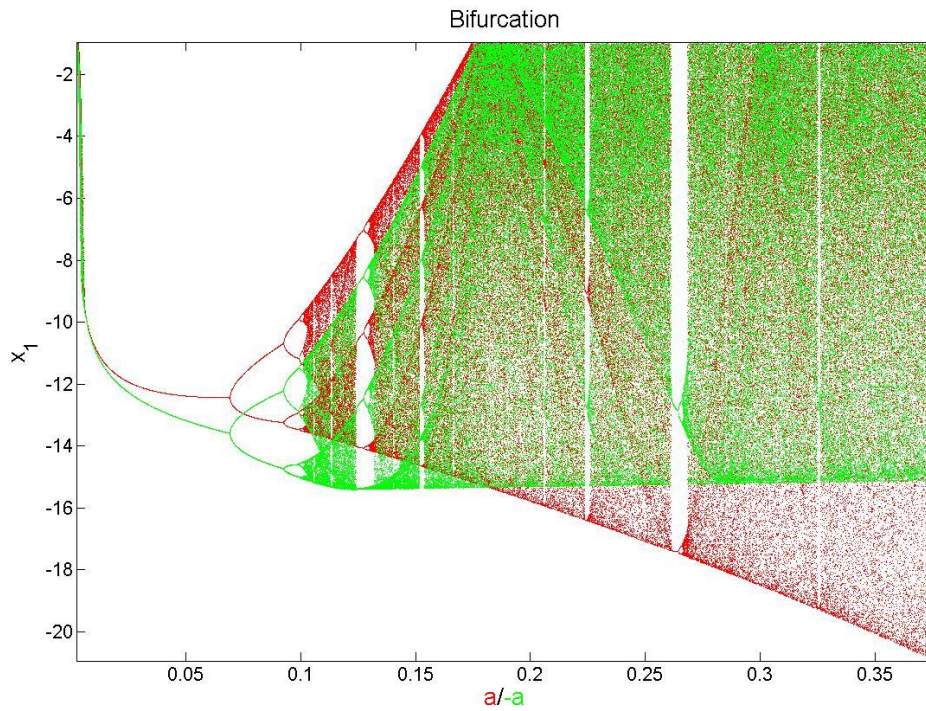


Fig. 2-13 Bifurcation diagram for the Yang, the red one, and Yin, the green one, Rössler systems.

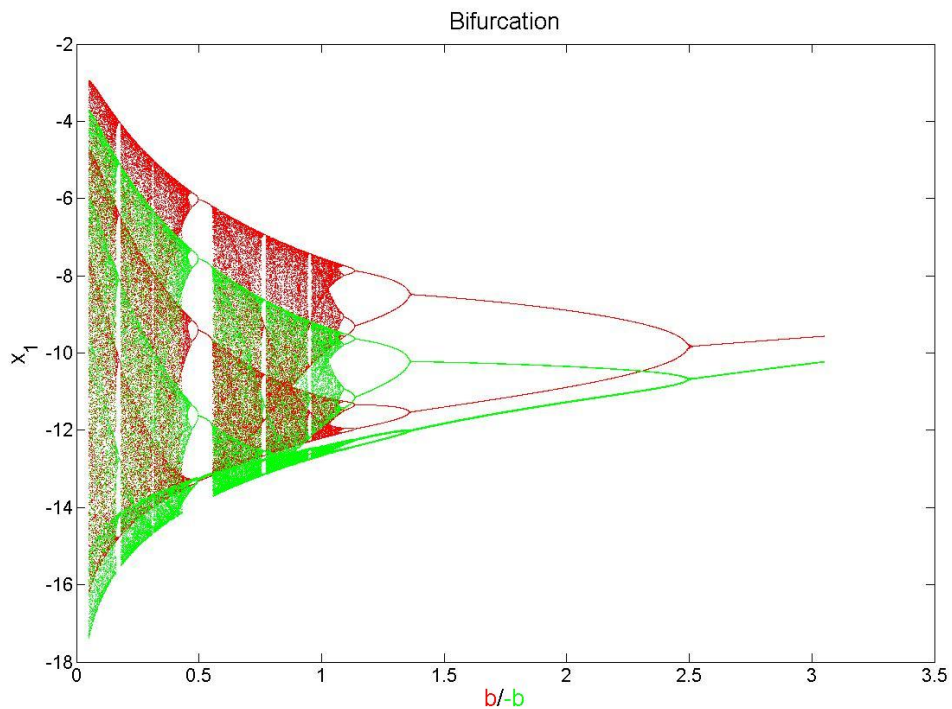


Fig. 2-14 Bifurcation diagram for the Yang, the red one, and Yin, the green one, Rössler systems.

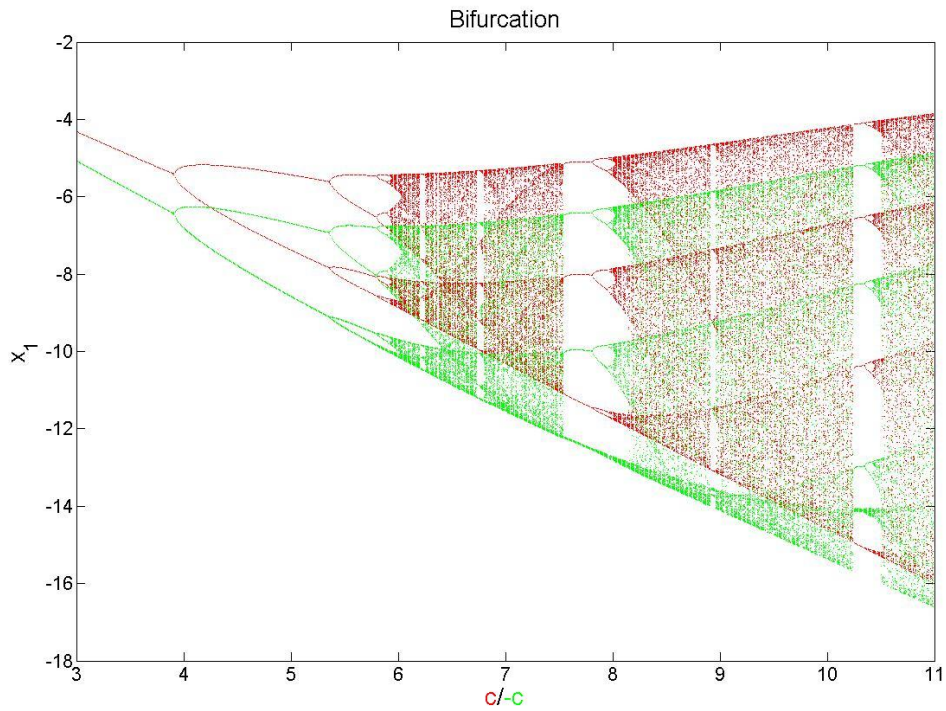


Fig. 2-15 Bifurcation diagram for the Yang, the red one, and Yin, the green one, Rössler systems.

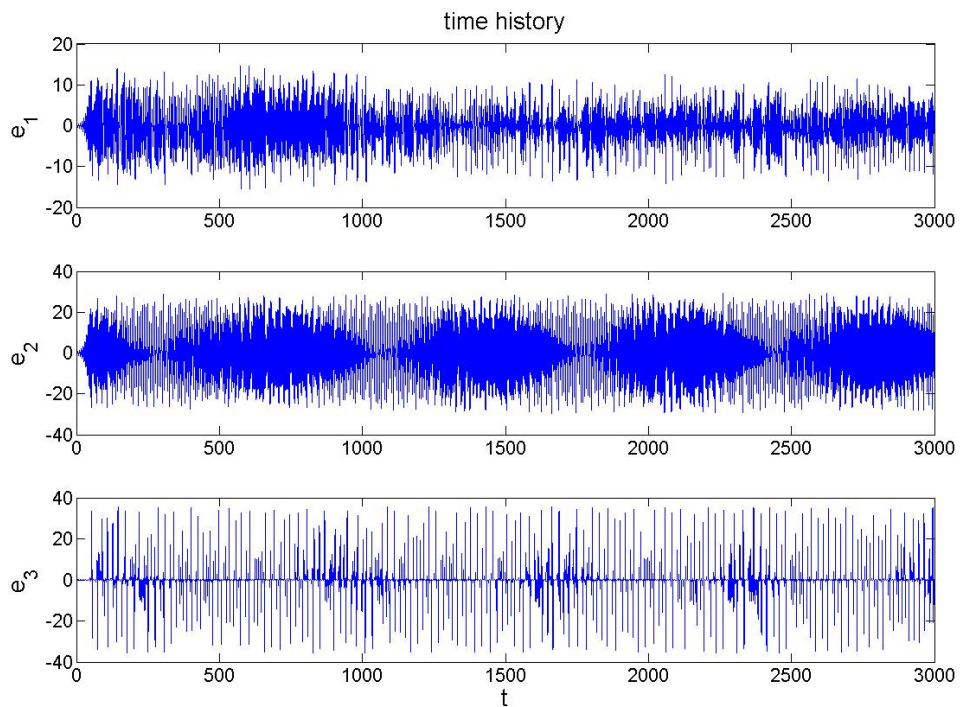


Fig. 2-16 Time histories of three states of error equation.

Chapter 3

Multiple Symplectic Derivative Synchronization of Ge-Ku-Van der Pol-Rössler System with Other Different Systems by Partial Region Stability Theory

3-1. Preliminary

When the symplectic derivative functions is extended to a more general form, $G(x, y, z, \dots, \dot{x}, \dot{y}, \dot{z}, \dots, \ddot{x}, \ddot{y}, \ddot{z}, \dots, t) = F(x, y, z, \dots, \dot{x}, \dot{y}, \dot{z}, \dots, \ddot{x}, \ddot{y}, \ddot{z}, \dots, t)$, the synchronization is called “multiple symplectic derivative synchronization”, where x, y, z, \dots are state vectors of Partner A and Partner B. $G(x, y, z, \dots, \dot{x}, \dot{y}, \dot{z}, \dots, \ddot{x}, \ddot{y}, \ddot{z}, \dots, t)$ and $F(x, y, z, \dots, \dot{x}, \dot{y}, \dot{z}, \dots, \ddot{x}, \ddot{y}, \ddot{z}, \dots, t)$ are given vector functions of $x, y, z, \dots, \dot{x}, \dot{y}, \dot{z}, \dots, \ddot{x}, \ddot{y}, \ddot{z}, \dots$, and time.

This chapter is presented as follows. In Section 2, method of synchronization by GYC partial region stability theory is shown. In Section 3, systems are synchronized by GYC partial region stability theory. In Section 4, synchronization by traditional Lyapunov function is shown. In Section 5, the comparison of synchronization ways is presented. In Section 6, summary is drawn.

3-2. Strategy of multiple symplectic derivative synchronization

There are two chaotic systems, partner system A and partner system B. The partner A is given by

$$\dot{x} = f(t, x) \tag{3-1}$$

The partner B is given by

$$\dot{y} = g(t, y) \quad (3-2)$$

In order that the error dynamics becomes always positive, the origin of y-coordinate system is translated to a constant vector.

Define $e = G - F + K$ as the error state vector, where $G = G(x, y, \dots, \dot{x}, \dot{y}, \dots, \ddot{x}, \ddot{y}, \dots, t)$ and $F = F(x, y, \dots, \dot{x}, \dot{y}, \dots, \ddot{x}, \ddot{y}, \dots, t)$ are two given functions, and K is a constant vector to keep the error dynamics always in first octant.

And then obtain the error vector derivative

$$\dot{e}_i = \dot{G}_i - \dot{F}_i - u_i \quad (3-3)$$

where u_i is a component of the control input vector u , $i = 1, 2, \dots, n$ keep the derivative of error dynamics \dot{e} always in seventh octant.

In this way, the error dynamics would satisfy the following Lyapunov function

$$V(e) = e_1 + e_2 + \dots + e_n > 0$$

and the derivative of the Lyapunov function

$$\dot{V}(e) = \dot{e}_1 + \dot{e}_2 + \dots + \dot{e}_n < 0$$

So the synchronization can be accomplished when $t \rightarrow \infty$, the limit of the error vector $e = [e_1, e_2, \dots, e_n]^T$ approaches to zero:

$$\lim_{t \rightarrow \infty} e = 0 \quad (3-4)$$

3-3. Synchronization by GYC partial region stability theory

Define

$$G(x, \dot{x}, \ddot{x}, y, \dot{y}, \ddot{y}, z, \dot{z}, \ddot{z}, t) = \begin{bmatrix} G_1 \\ G_2 \\ G_3 \\ G_4 \\ G_5 \\ G_6 \end{bmatrix}, \quad (3-5)$$

where

$$\begin{cases} G_1 = \sin x_1 + x_2 \sin x_3 + \cos t + \cos(\dot{x}_1) - \dot{x}_5 + a_2 x_5 + z_2 + \cos(\dot{z}_5 + z_5) + \sin(z_6 + 1) \\ \quad - \cos(x_2) \\ G_2 = x_4 + z_2 + a_2 x_5 - \dot{x}_5 + \dot{x}_4 - x_1 + x_6 - z_1 + \dot{z}_2 \\ G_3 = x_1 + y_5 - z_3 + \dot{x}_5 - a_2 x_5 + z_4 \sin(\dot{z}_2 + z_2) \\ G_4 = \ddot{x}_1 + y_3 \\ G_5 = x_2 + \sin t \\ G_6 = y_3 + \ddot{y}_6 \end{cases}$$

$$F(x, \dot{x}, \ddot{x}, y, \dot{y}, \ddot{y}, z, \dot{z}, \ddot{z}, t) = \begin{bmatrix} F_1 \\ F_2 \\ F_3 \\ F_4 \\ F_5 \\ F_6 \end{bmatrix}, \quad (3-6)$$

where

$$\begin{cases} F_1 = \cos z_4 + \sin(z_6 + 1) + \sin(100(\dot{x}_3 + gx_3 - h(1 - x_3^2)x_2)) + \dot{x}_1 \sin(x_3) + \cos t \\ F_2 = z_1 \sin x_1 - (\dot{z}_2 + z_2) \sin(100(\dot{x}_3 + gx_3 - h(1 - x_3^2)x_2)) \\ F_3 = x_4 + z_4 \sin z_1 + 100(\dot{x}_3 + gx_3 - h(1 - x_3^2)x_2) \\ F_4 = \ddot{x}_1 + \ddot{y}_1 \\ F_5 = \dot{x}_1 + z_6 + \sin t \\ F_6 = \dot{y}_2 + \ddot{y}_6 - z_5 \end{cases}$$

Our purpose is to achieve the multiple symplectic derivative synchronization

$$G(x, \dot{x}, \ddot{x}, y, \dot{y}, \ddot{y}, z, \dot{z}, \ddot{z}, t) = F(x, \dot{x}, \ddot{x}, y, \dot{y}, \ddot{y}, z, \dot{z}, \ddot{z}, t) - K.$$

Consider the system 1, combination of Ge-Ku-Van der Pol system and Rössler

System, described by

$$\begin{cases} \dot{x}_1 = x_2 \\ \dot{x}_2 = -a_1 x_2 - x_3(b_1(c_1 - x_1^2) + dx_3) \\ \dot{x}_3 = -gx_3 + h(1 - x_3^2)x_2 + lx_1 \\ \dot{x}_4 = -x_5 - x_6 + x_1 \\ \dot{x}_5 = x_4 + a_2 x_5 \\ \dot{x}_6 = b_2 + x_6(x_4 - c_2) \end{cases} \quad (3-7)$$

where $a_1=0.08$, $b_1=-0.35$, $c_1=100.56$, $d=-1000.02$, $g=0.61$, $h=0.08$, $l=0.01$, $a_2=0.15$,

$b_2=0.2$, $c_2=10$ and the initial conditions are $x_1(0) = 0.01$, $x_2(0) = 0.01$,

$x_3(0) = 0.01$, $x_4(0) = 0.3$, $x_5(0) = 0.1$, $x_6(0) = 0.5$. The chaotic attractor of the

combination of Ge-Ku-Van der Pol system and Rössler system is shown in Fig. 3-1.

The system 2, combination of Sprott 22 and Sprott A [26], described by

$$\begin{cases} \dot{y}_1 = y_2 \\ \dot{y}_2 = y_3 \\ \dot{y}_3 = -a_3 y_3 - y_2 - \sin y_1 \\ \dot{y}_4 = y_5 \\ \dot{y}_5 = -y_4 + y_5 y_6 + y_2 \\ \dot{y}_6 = 1 - y_5^2 \end{cases} \quad (3-8)$$

where $a_3=0.25$ and the initial conditions are $y_1(0) = 0.01$, $y_2(0) = 1$, $y_3(0) = 0.01$, $y_4(0) = 0.1$, $y_5(0) = 0.1$, $y_6(0) = 0.1$. The chaotic attractor of the combination of Sprott 22 and Sprott A is shown in Fig. 3-2.

The system 3, combination of Sprott B and Sprott C [26], described by

$$\begin{cases} \dot{z}_1 = z_2 z_3 \\ \dot{z}_2 = z_1 - z_2 \\ \dot{z}_3 = 1 - z_1 z_2 \\ \dot{z}_4 = z_5 z_6 + z_1 \\ \dot{z}_5 = z_4 - z_5 \\ \dot{z}_6 = 1 - z_4^2 \end{cases} \quad (3-9)$$

where the initial conditions are $z_1(0) = 0.01$, $z_2(0) = 0.01$, $z_3(0) = 0.01$, $z_4(0) = 0.02$, $z_5(0) = 0.1$, $z_6(0) = 0.05$. The chaotic attractor of the combination of Sprott B and Sprott C is shown in Fig. 3-3.

The state error is $e = G - F + K$ where $K = [3.5, 35, 5.5, 1.5, 5, 2]^T$ such that error dynamics always exists in first guardant as shown in Fig. 3-4 and Fig. 3-5.

$$\lim_{t \rightarrow \infty} e_i = G_i - F_i + K_i = 0, \quad (3-10)$$

where $i = 1, 2, \dots, 6$.

Our purpose is $\lim_{t \rightarrow \infty} e = 0$. We obtain the error dynamics:

$$\begin{cases} \dot{e}_1 = \dot{G}_1 - \dot{F}_1 - u_1 \\ \dot{e}_2 = \dot{G}_2 - \dot{F}_2 - u_2 \\ \dot{e}_3 = \dot{G}_3 - \dot{F}_3 - u_3 \\ \dot{e}_4 = \dot{G}_4 - \dot{F}_4 - u_4 \\ \dot{e}_5 = \dot{G}_5 - \dot{F}_5 - u_5 \\ \dot{e}_6 = \dot{G}_6 - \dot{F}_6 - u_6 \end{cases} \quad (3-11)$$

By partial region stability theory, we can choose a Lyapunov function in the form

of a positive definite function in first quadrant:

$$V(e) = e_1 + e_2 + e_3 + e_4 + e_5 + e_6 \quad (3-12)$$

Its time derivative is

$$\begin{aligned} \dot{V}(e) = & (\dot{G}_1 - \dot{F}_1 - u_1) + (\dot{G}_2 - \dot{F}_2 - u_2) + (\dot{G}_3 - \dot{F}_3 - u_3) + \\ & (\dot{G}_4 - \dot{F}_4 - u_4) + (\dot{G}_5 - \dot{F}_5 - u_5) + (\dot{G}_6 - \dot{F}_6 - u_6) \end{aligned} \quad (3-13)$$

Choose the controller u as

$$u = \begin{bmatrix} u_1 \\ u_2 \\ u_3 \\ u_4 \\ u_5 \\ u_6 \end{bmatrix} = \begin{bmatrix} e_1 - \dot{x}_2 \sin(x_2) \\ e_2 - \dot{x}_6 \\ e_3 + \ddot{y}_4 \\ e_4 + \ddot{y}_1 \\ e_5 - \dot{x}_2 \\ e_6 - \dot{y}_3 \end{bmatrix} \quad (3-14)$$

We obtain

$$\dot{V}(e) = -e_1 - e_2 - e_3 - e_4 - e_5 - e_6 < 0 \quad (3-15)$$

which is negative definite function in first quadrant. Error states versus time and their time histories are shown in Fig. 3-6 and Fig. 3-7.

3-4. Synchronization by traditional method

If the traditional Lyapunov function is used, it means that

$$V(e) = e_1^2 + e_2^2 + e_3^2 + e_4^2 + e_5^2 + e_6^2 \quad (3-16)$$

It's time derivative is

$$\dot{V}(e) = 2(e_1\dot{e}_1 + e_2\dot{e}_2 + e_3\dot{e}_3 + e_4\dot{e}_4 + e_5\dot{e}_5 + e_6\dot{e}_6) \quad (3-17)$$

We want to find u of (3-11) such that \dot{V} satisfies

$$\dot{V}(e) = -(e_1^2 + e_2^2 + e_3^2 + e_4^2 + e_5^2 + e_6^2) < 0 \quad (3-18)$$

Choose

$$u = \begin{bmatrix} u_1 \\ u_2 \\ u_3 \\ u_4 \\ u_5 \\ u_6 \end{bmatrix} = \begin{bmatrix} 0.5e_1 - \dot{x}_2 \sin(x_2) \\ 0.5e_2 - \dot{x}_6 \\ 0.5e_3 + \ddot{y}_4 \\ 0.5e_4 + \ddot{y}_1 \\ 0.5e_5 - \dot{x}_2 \\ 0.5e_6 - \dot{y}_3 \end{bmatrix}$$

Introduce u into Eq.(3-11) where $i = 1, 2, \dots, 6$, (3-17) becomes

$$\dot{V}(e) = -(e_1^2 + e_2^2 + e_3^2 + e_4^2 + e_5^2 + e_6^2)$$

which is negative definite function in all quadrants. And error states versus time and time histories are shown in Fig. 3-8 and Fig. 3-9.

3-5. Comparison between new strategy and traditional method

From the previous sections, we know that the controllers u of the new strategy and of the traditional method are different. Tables and Figures (Fig. 3-10 and Fig. 3-11) for comparing the efficiency of convergence are given as follows. The superiority of new strategy is obvious. The error states of new strategy are much smaller and decay more quickly than that of traditional method.

Table 3-1 the value of error dynamics at second 614 ~ 624 for traditionl
method.

t	e_1	e_2	e_3	e_4	e_5	e_6
614	0.0035	0.0673	0.0050	0.0093	0.0082	0.0019
615	0.0022	0.0408	0.0030	0.0120	0.2267	0.0168
616	0.0013	0.0247	0.0018	0.0044	0.0834	0.0062
617	0.0008	0.0150	0.0011	0.0016	0.0307	0.0023
618	0.0005	0.0091	0.0007	0.0006	0.0113	0.0008
619	0.0003	0.0055	0.0004	0.0002	0.0042	0.0003
620	0.0002	0.0033	0.0002	0.0001	0.0015	0.0001
621	0.0001	0.0020	0.0002	0.0000	0.0006	0.0000
622	0.0001	0.0012	0.0001	0.0000	0.0002	0.0000
623	0.0000	0.0007	0.0001	0.0000	0.0001	0.0000
624	0.0000	0.0005	0.0000	0.0000	0.0000	0.0000

Table 3-2 the value ($\times 10^{-4}$) of error dynamics at second 614 ~ 624 for new strategy.

t	e_1	e_2	e_3	e_4	e_5	e_6
614	0.0325	0.6164	0.0456	0.0855	0.0748	0.0177
615	0.0120	0.2267	0.0168	0.0315	0.0275	0.0065
616	0.0044	0.0834	0.0062	0.0116	0.0101	0.0024
617	0.0016	0.0307	0.0023	0.0043	0.0037	0.0009
618	0.0006	0.0113	0.0008	0.0016	0.0014	0.0003
619	0.0002	0.0042	0.0003	0.0006	0.0005	0.0001
620	0.0001	0.0015	0.0001	0.0002	0.0002	0.0000
621	0.0000	0.0006	0.0000	0.0001	0.0001	0.0000
622	0.0000	0.0002	0.0000	0.0000	0.0000	0.0000
623	0.0000	0.0001	0.0000	0.0000	0.0000	0.0000
624	0.0000	0.0000	0.0000	0.0000	0.0000	0.0000

3-6. Summary

In this chapter, a new synchronization is presented. We not only use the variables but also their derivatives in two given synchronization functions. New strategy to achieve chaos control by GYC partial region stability is used. Finally, Tables and Figures are given to prove that the new strategy do synchronize system more quickly.

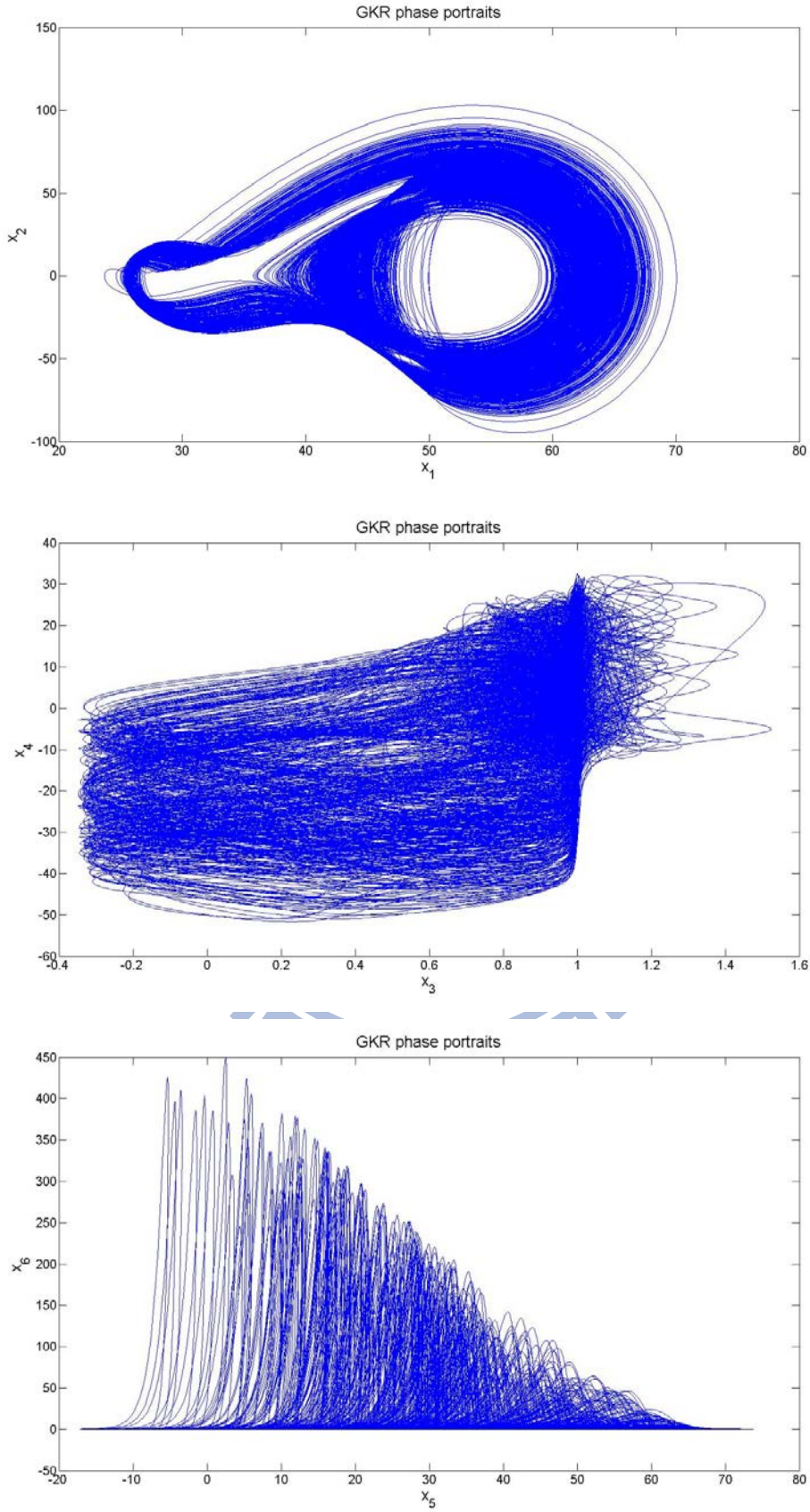


Fig. 3-1 Phase portrait of system 1.

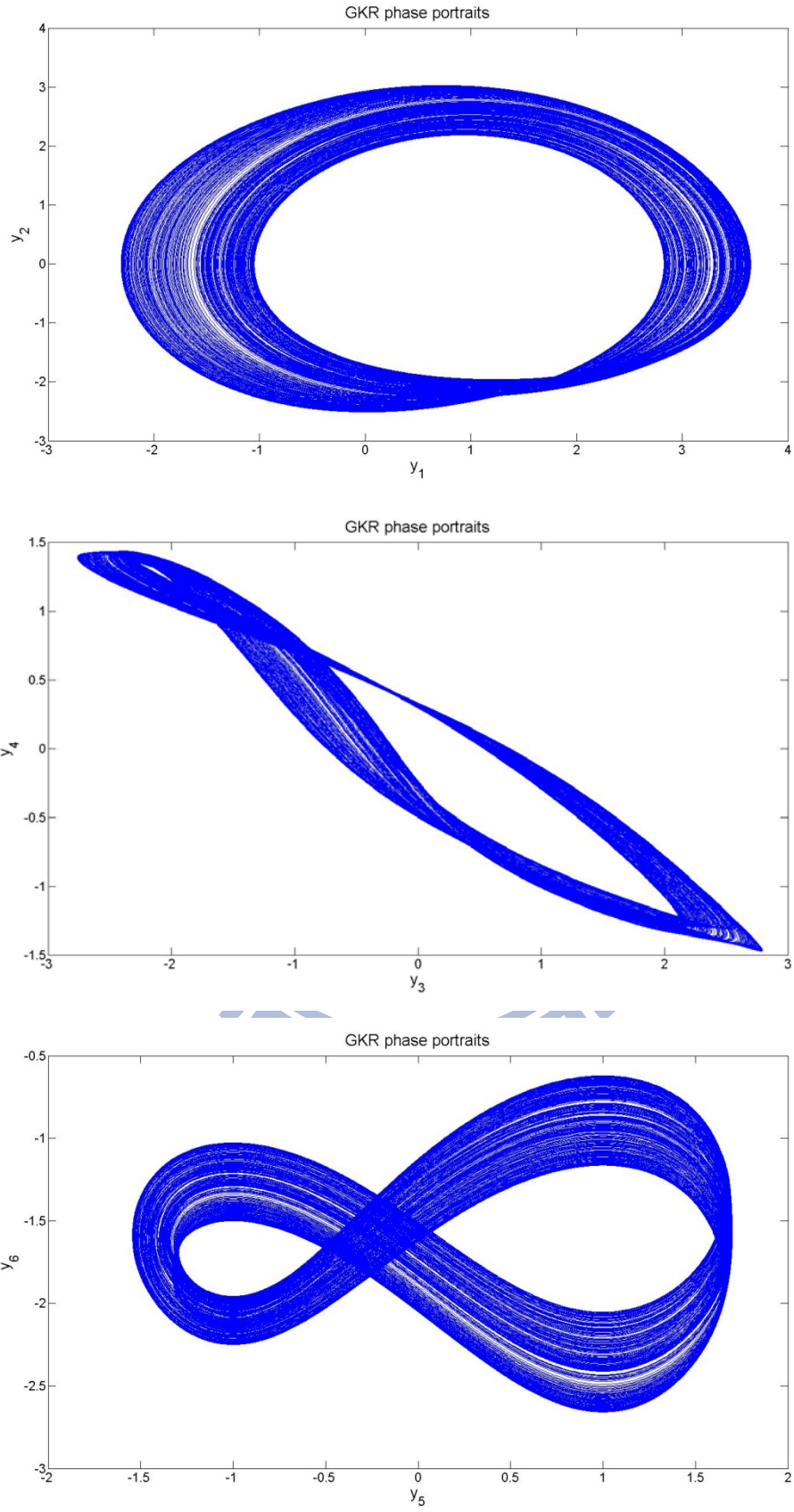


Fig. 3-2 Phase portrait of system 2.

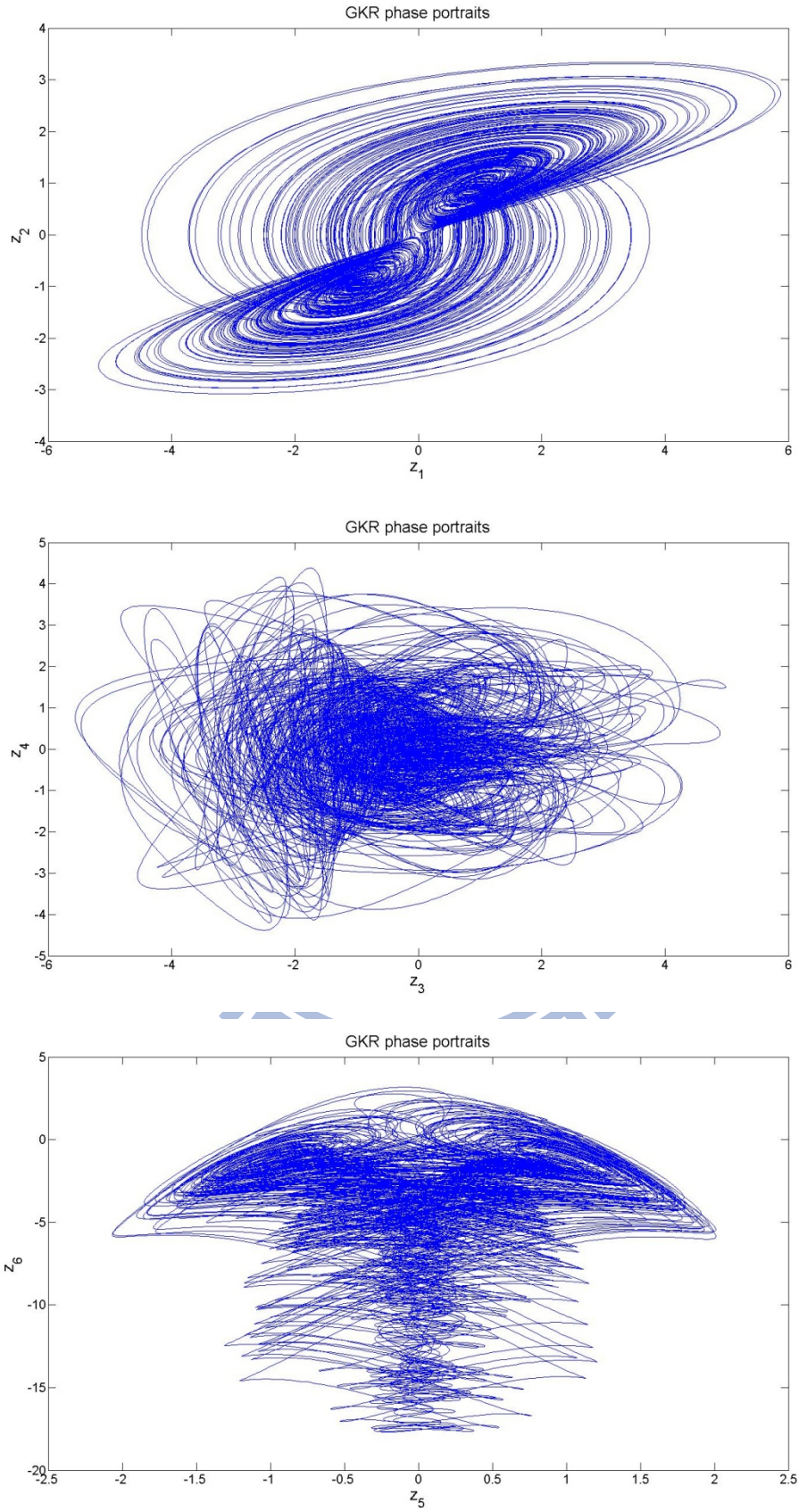


Fig. 3-3 Phase portrait of system 3.

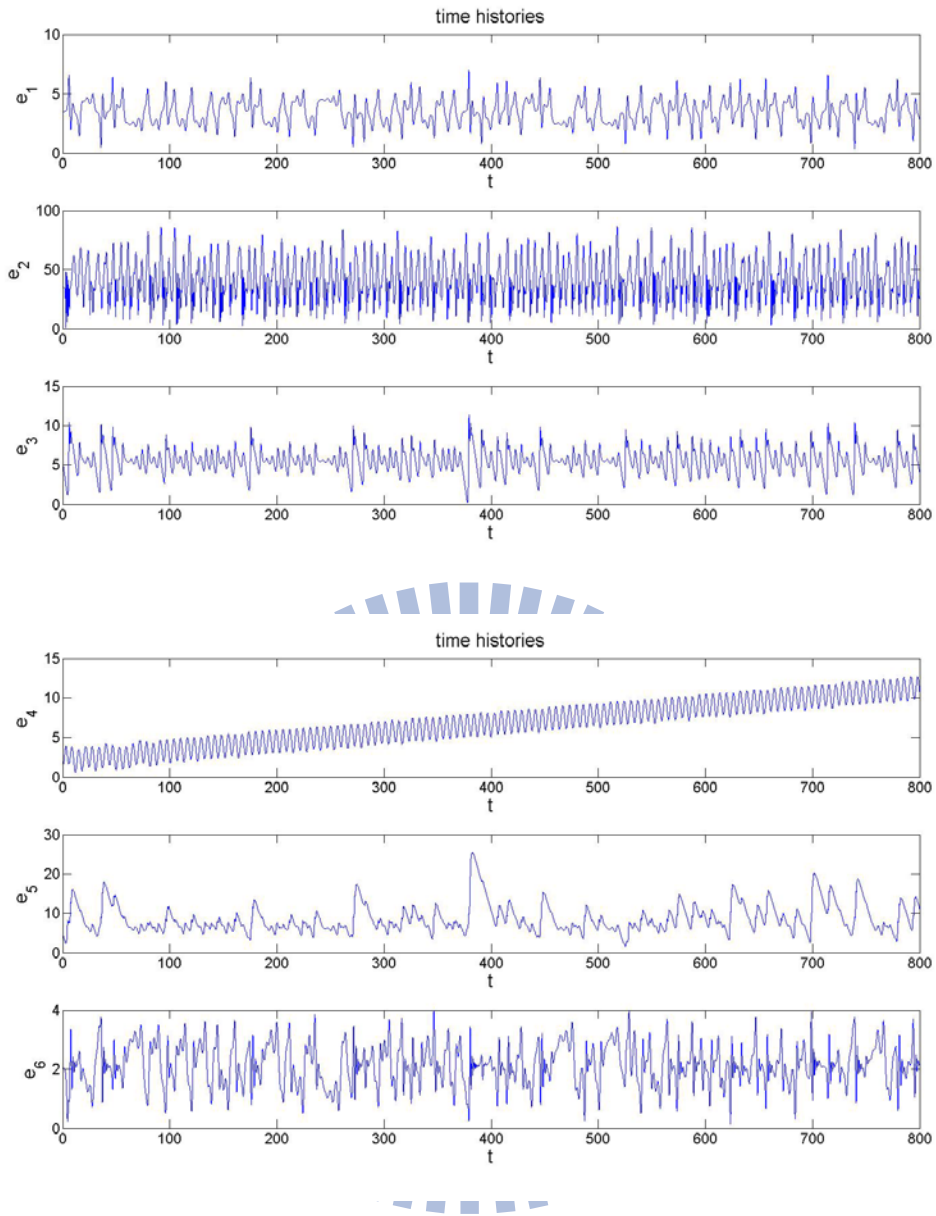


Fig. 3-4 Time histories of error function before synchronization.

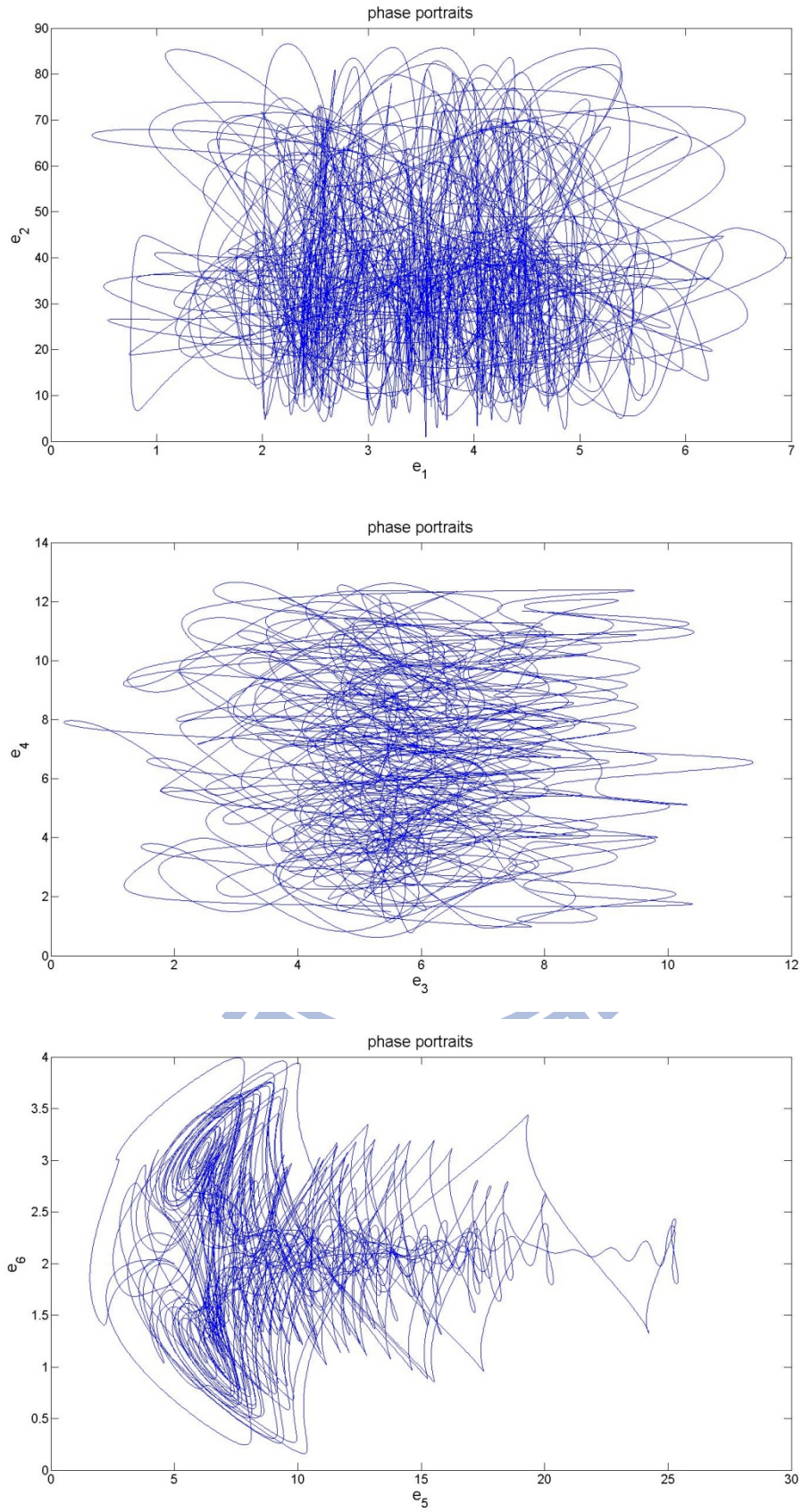


Fig. 3-5 Phase portrait of error function before synchronization.

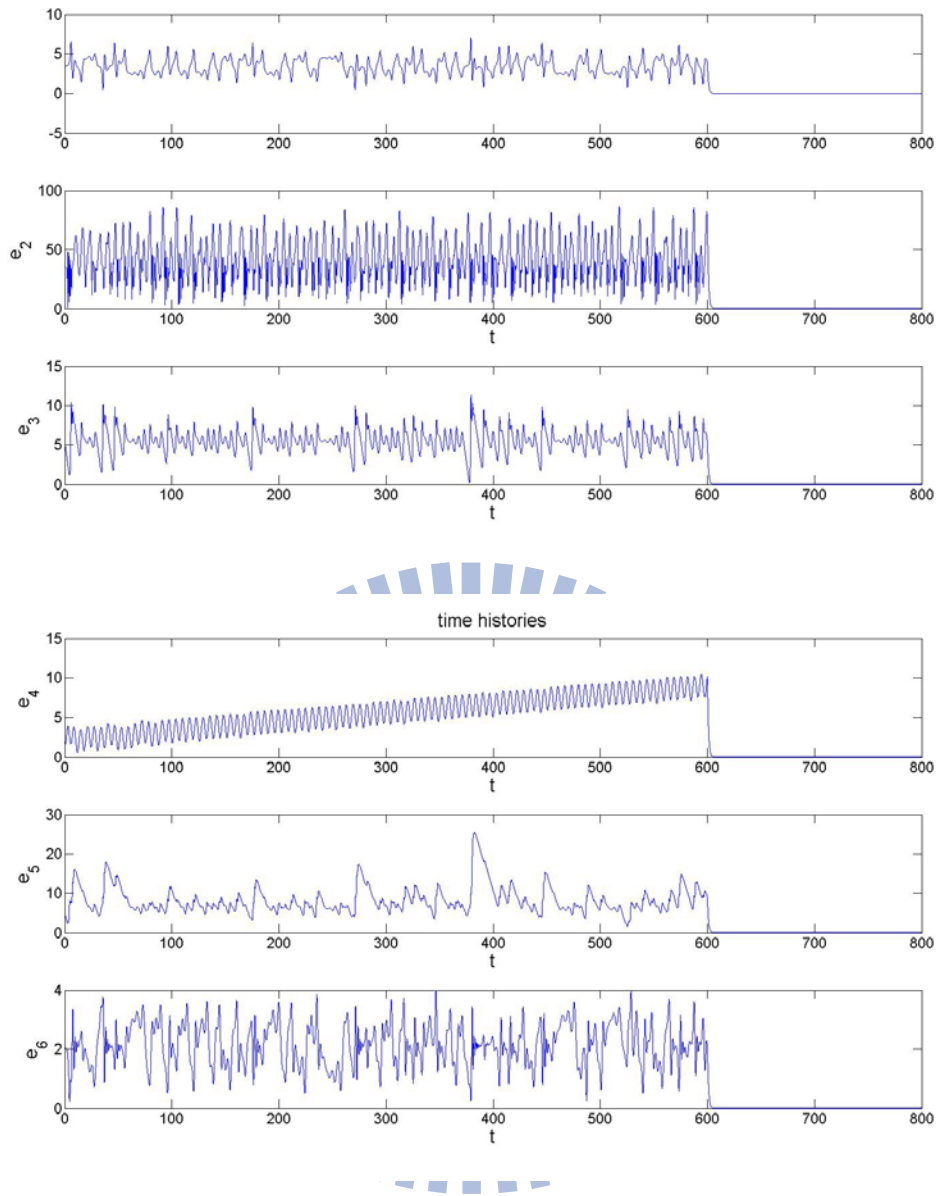


Fig. 3-6 Time histories of error function after synchronization for new strategy.

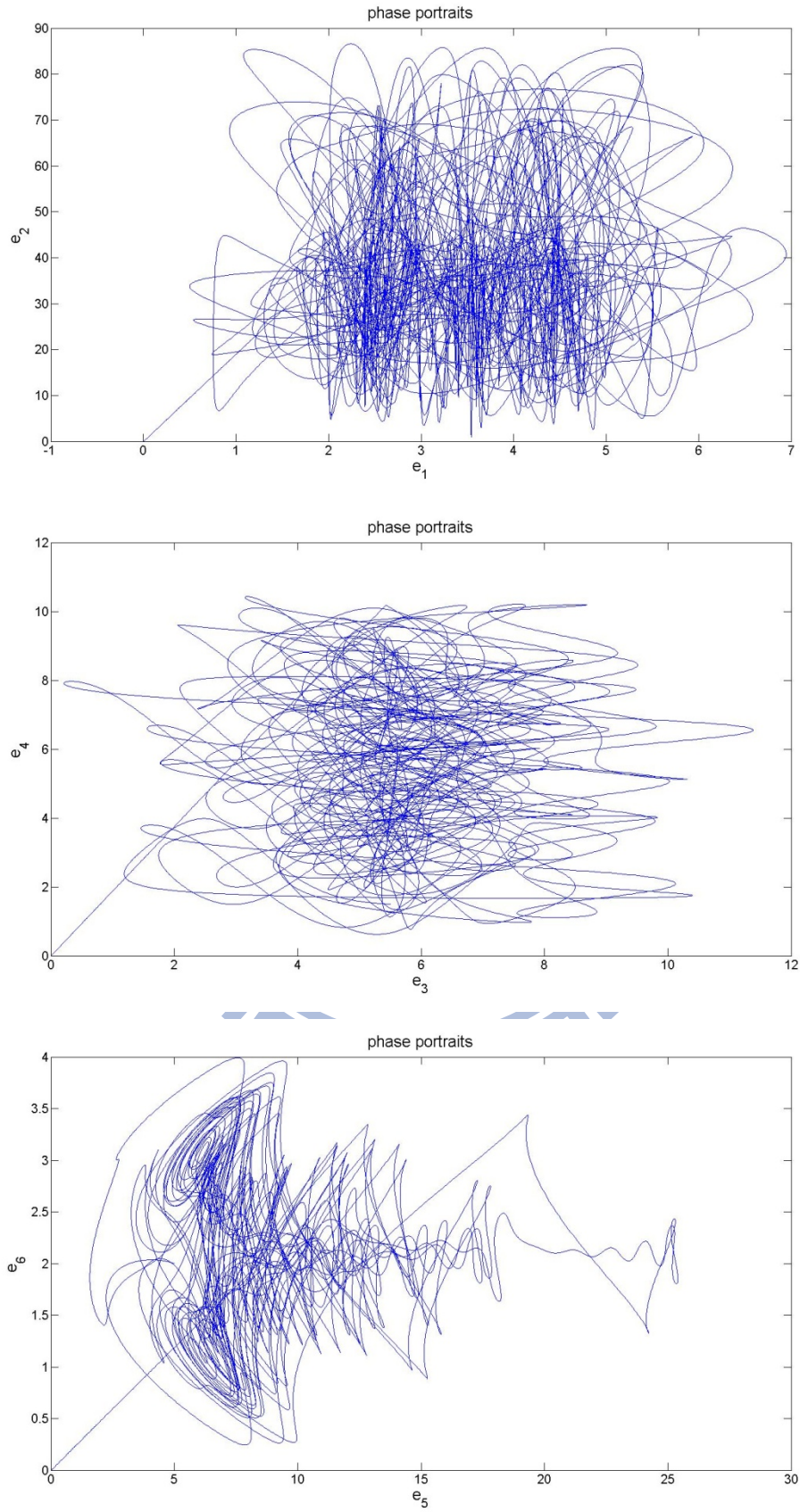


Fig. 3-7 Phase portrait of error function after synchronization for new strategy.

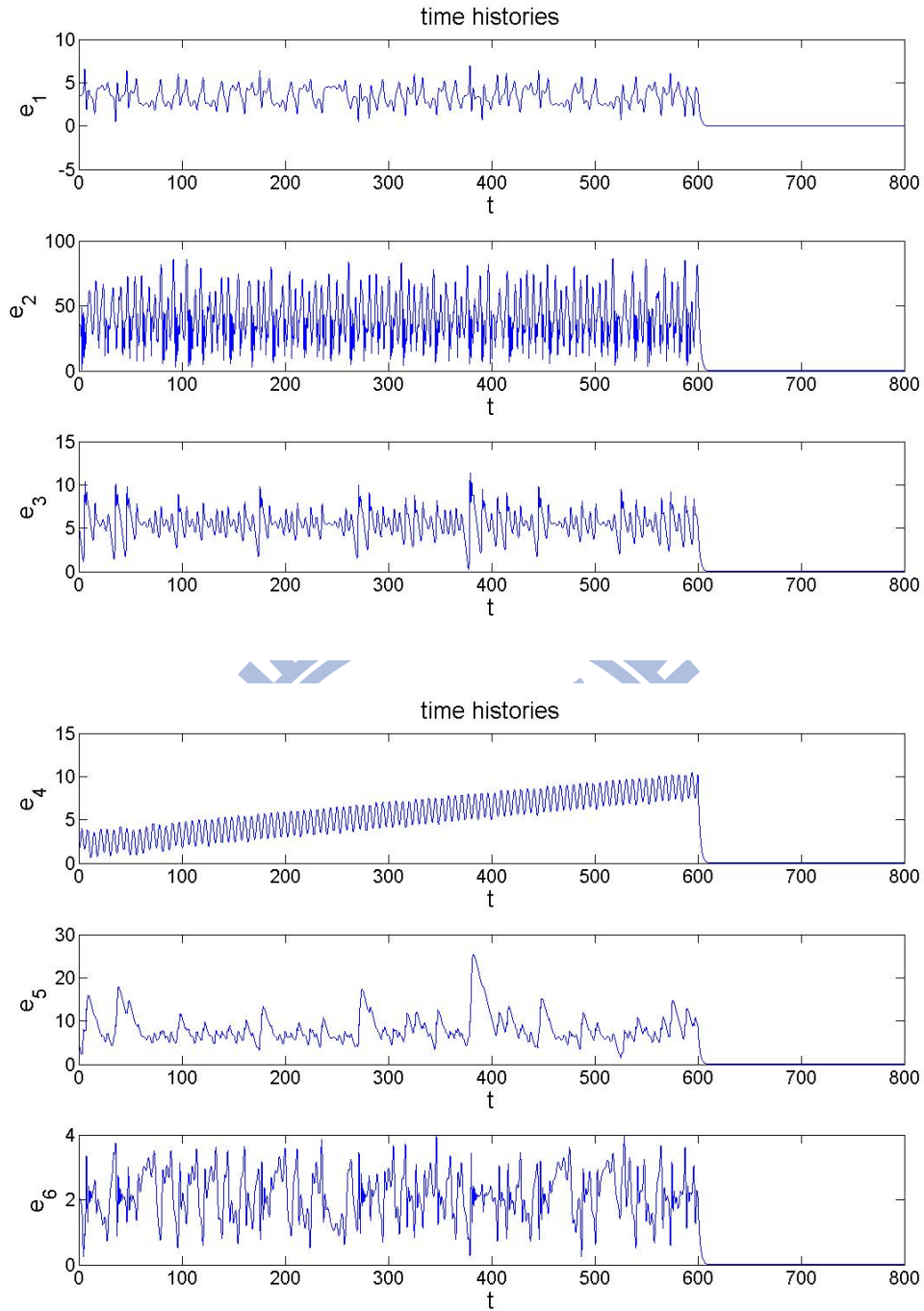


Fig. 3-8 Time histories of error function after synchronization for traditional method.

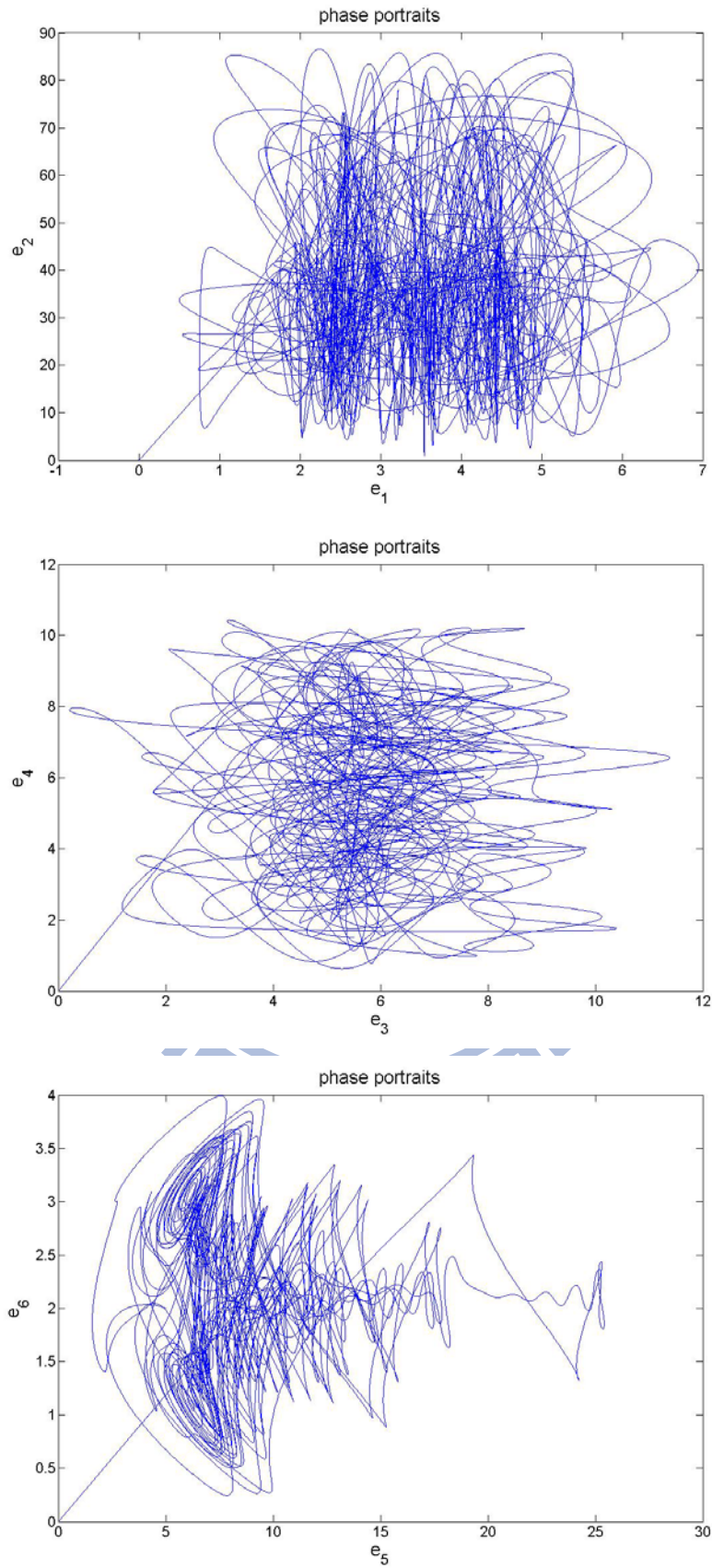


Fig. 3-9 Phase portrait of error function after synchronization for traditional

method.

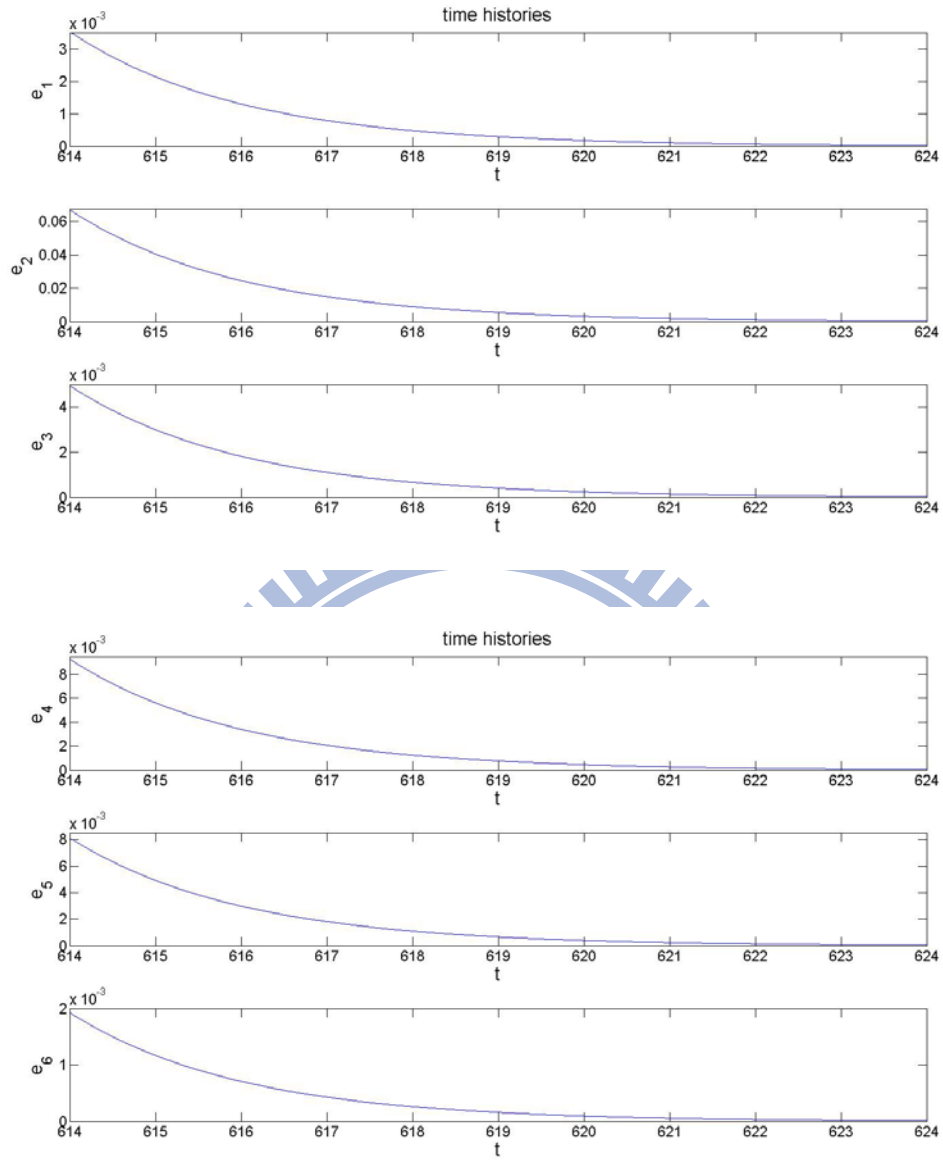


Fig. 3-10 Time histories of error function (3-11) after synchronization for traditional method.

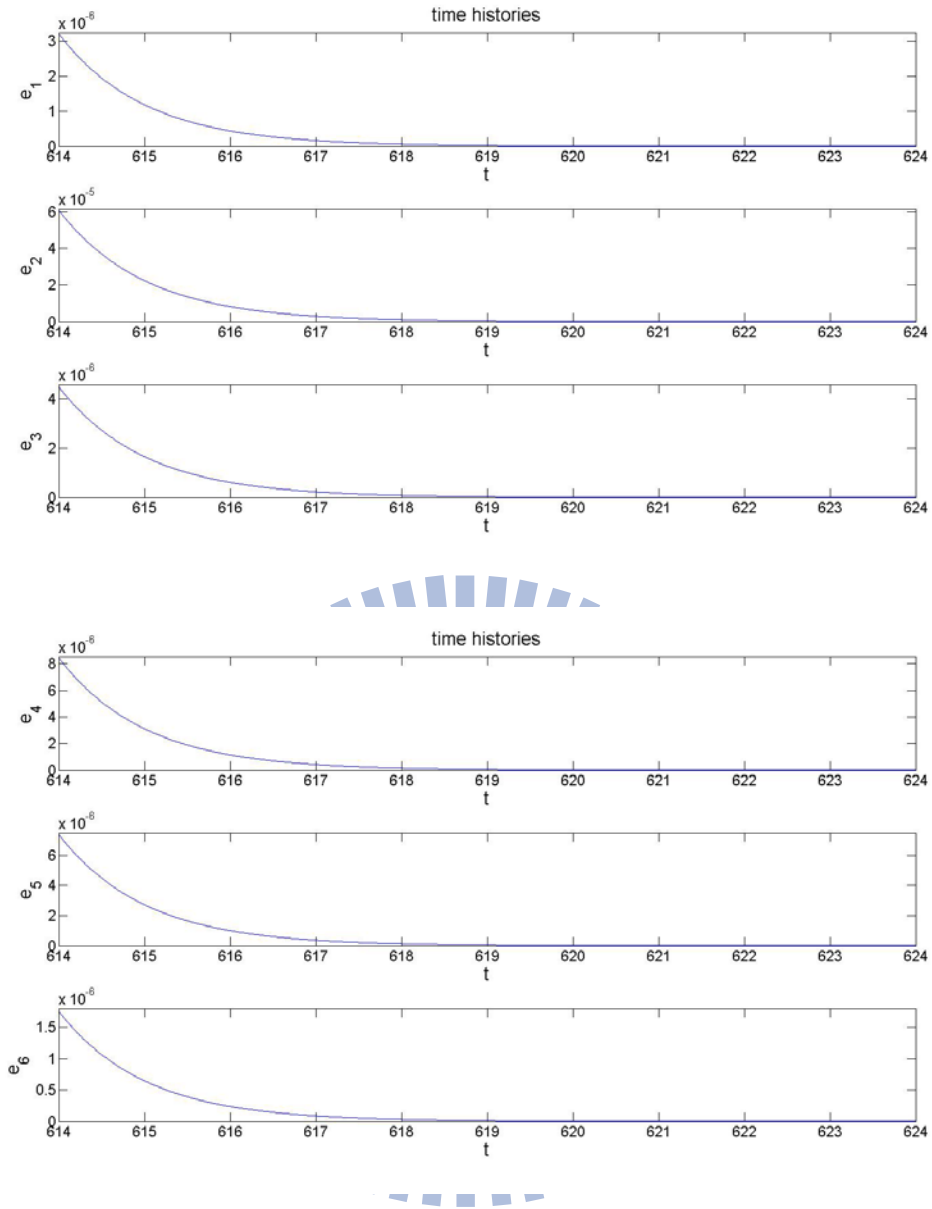


Fig. 3-11 Time histories of error function (3-11) after synchronization for new strategy.

Chapter 4

Multiple Symplectic Derivative Synchronization of Rössler System and Sprott A System with Variable Time Scales by Partial Region Stability Theory

4-1. Preliminary

In this chapter, a new kind of synchronization by two different chaos systems with different time scales is presented. It means that the double symplectic derivative synchronization with variable time scale is $G(x, y, \dot{x}, \dot{y}, \ddot{x}, \ddot{y}, t, \tau) = F(x, y, \dot{x}, \dot{y}, \ddot{x}, \ddot{y}, t, \tau)$, where τ is a variable time scale, $\tau = \tau(t)$.

This chapter is presented as follows. In Section 2, systems are synchronized in the different time variable by GYC partial region stability theory. In Section 3, the traditional method is used. In Section 4, the comparison of synchronization ways is presented. In Section 5, summary is drawn.

4-2. Synchronization of different time on other octant

Define

$$G(x, \dot{x}, y, \dot{y}, t, \tau) = \begin{bmatrix} \sin x_1 + y_3 - \dot{x}_1 - x_3 - \dot{y}_2 \\ x_3 - \dot{y}_1 - \dot{x}_1 \\ \dot{y}_1 + x_2 + \cos x_2 \end{bmatrix} \quad (4-1)$$

$$F(x, \dot{x}, y, \dot{y}, t, \tau) = \begin{bmatrix} x_2 + y_1 + \sin(\dot{x}_2 - ax_2) \\ \dot{x}_1 - y_2 + x_3 \\ \cos x_2 + y_2 \end{bmatrix} \quad (4-2)$$

Our purpose is to achieve the multiple symplectic derivative synchronization

$$G(x, \dot{x}, y, \dot{y}, t, \tau) = F(x, \dot{x}, y, \dot{y}, t, \tau) - K.$$

Consider the Rössler System is described by

$$\begin{cases} \dot{x}_1 = -x_2 - x_3 \\ \dot{x}_2 = x_1 + ax_2 \\ \dot{x}_3 = b + x_3(x_1 - c) \end{cases} \quad (4-3)$$

where $a = 0.15$, $b = 0.2$, $c = 10$ and the initial condition are $x_1(0) = 0.3$, $x_2(0) = 0.1$, $x_3(0) = 0.5$. The chaotic attractor of Rössler system is shown in Fig. 4-1 and Fig. 4-2.

The Sprott A [18] is described by

$$\begin{cases} \frac{\partial y_1}{\partial \tau} = y_2 \\ \frac{\partial y_2}{\partial \tau} = -y_1 + y_2 y_3 \\ \frac{\partial y_3}{\partial \tau} = 1 - y_2^2 \end{cases} \quad (4-4)$$

where the initial condition are $y_1(0) = 0.1$, $y_2(0) = 0.1$, $y_3(0) = 0.1$ and τ is a function of t shown as:

$$\tau(t) = t + \cos t$$

The chaotic attractor of Sprott A is shown in Fig. 4-3 and Fig. 4-4.

The state error is $e = G - F + K$ where $K = [-4, 22, -20]^T$ such that error dynamics always exists in sixth octant as shown in Fig. 4-5 and Fig. 4-6, where the octants are defined as Table 4-1 and Fig. 4-7:

Table 4-1 The sign symbols of eight octants.

octant	sign symbols	octant	sign symbols
first	(+, +, +)	fifth	(+, +, -)
second	(-, +, +)	sixth	(-, +, -)
third	(-, -, +)	seventh	(-, -, -)
forth	(+, -, +)	eighth	(+, -, -)

Our purpose is $\lim_{t \rightarrow \infty} e = 0$. We obtain (3-3) for $i = 1, 2, 3$:

$$\begin{cases} \dot{e}_1 = \dot{G}_1 - \dot{F}_1 - u_1 \\ \dot{e}_2 = \dot{G}_2 - \dot{F}_2 - u_2 \\ \dot{e}_3 = \dot{G}_3 - \dot{F}_3 - u_3 \end{cases} \quad (4-5)$$

By partial region stability theory, we can choose a Lyapunov function in the form of a positive definite function in sixth octant by Table 4-1.

$$V(e) = -e_1 + e_2 - e_3 \quad (4-6)$$

Its time derivative is

$$\dot{V}(e) = -(\dot{G}_1 - \dot{F}_1 - u_1) + (\dot{G}_2 - \dot{F}_2 - u_2) - (\dot{G}_3 - \dot{F}_3 - u_3) \quad (4-7)$$

Choose

$$u = \begin{bmatrix} u_1 \\ u_2 \\ u_3 \end{bmatrix} = \begin{bmatrix} e_1 + 1 - y_2^2 \\ e_2 - y_1 + y_2 y_3 \\ e_3 + x_1 + ax_2 \end{bmatrix} \quad (4-8)$$

such that

$$\dot{V}(e) = e_1 - e_2 + e_3 < 0 \quad (4-9)$$

which is negative definite function in sixth octant. Error states versus time and time histories are shown in Fig. 4-8 and Fig. 4-9.

4-3. Synchronization by traditional method

If the traditional Lyapunov function is used, it means that

$$V(e) = e_1^2 + e_2^2 + e_3^2 \quad (4-10)$$

Its time derivative is

$$\dot{V}(e) = 2(e_1 \dot{e}_1 + e_2 \dot{e}_2 + e_3 \dot{e}_3) \quad (4-11)$$

We want to find u of Eq. (4-11) such that \dot{V} satisfies

$$\dot{V}(e) = -e_1^2 - e_2^2 - e_3^2$$

Choose

$$\mathbf{u} = \begin{bmatrix} u_1 \\ u_2 \\ u_3 \end{bmatrix} = \begin{bmatrix} 0.5e_1 + 1 - y_2^2 \\ 0.5e_2 - y_1 + y_2 y_3 \\ 0.5e_3 + x_1 + ax_2 \end{bmatrix}$$

Introduce \mathbf{u} into Eq. (4-5) where $i = 1, 2, 3$, Eq. (4-11) becomes

$$\dot{V}(\mathbf{e}) = -(e_1^2 + e_2^2 + e_3^2)$$

which is negative definite function in all octants. And error states versus time and time histories are shown in Fig. 4-10 and Fig. 4-11.

4-4. Comparison between new strategy and traditional method

From the previous sections, we know that the controllers \mathbf{u} of the new strategy and of the traditional method are different. Tables, Table 4-2 and Table 4-3, and figures, Fig. 4-12 and Fig. 4-13, for comparing the efficiency of convergence are given as follows. The superiority of new strategy is obvious. The error states of new strategy are much smaller and decay far more quickly than that of traditional method.

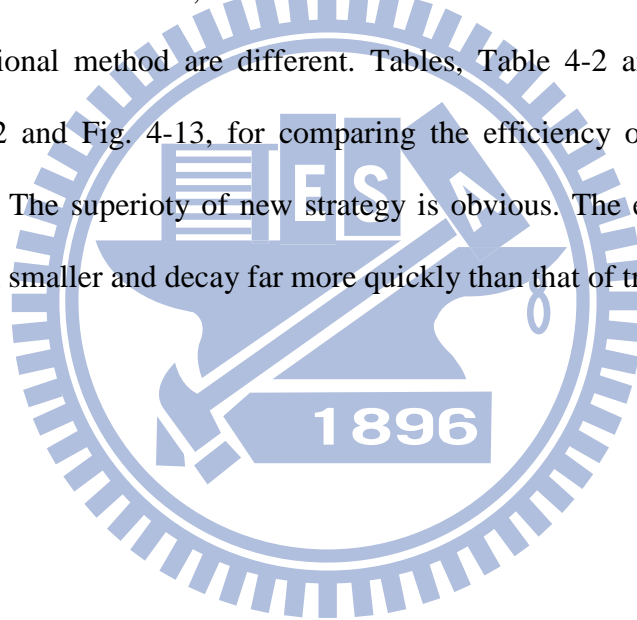


Table 4-2 The value of errors at second 610 ~ 620 for traditionl method.

t	e_1	e_2	e_3
610	-0.0415	0.1442	-0.1402
611	-0.0252	0.0875	-0.0850
612	-0.0153	0.0531	-0.0516
613	-0.0093	0.0322	-0.0313
614	-0.0056	0.0195	-0.0190
615	-0.0034	0.0118	-0.0115
616	-0.0021	0.0072	-0.0070
617	-0.0013	0.0044	-0.0042
618	-0.0008	0.0026	-0.0026
619	-0.0005	0.0016	-0.0016
620	-0.0003	0.0010	-0.0009

Table 4-3 The value ($\times 10^{-2}$) of errors at second 610 ~ 620 for new strategy.

t	e_1	e_2	e_3
610	-0.02811	0.09766	-0.09494
611	-0.01034	0.03593	-0.03493
612	-0.00380	0.01322	-0.01285
613	-0.00140	0.00486	-0.00473
614	-0.00051	0.00179	-0.00174
615	-0.00019	0.00066	-0.00064
616	-0.00007	0.00024	-0.00024
617	-0.00003	0.00009	-0.00009
618	-0.00001	0.00003	-0.00003
619	-0.00000	0.00001	-0.00001
620	-0.00000	0.00000	-0.00000

4-5. Summary

In this chapter, a new multiple symplectic derivative synchronization with variable time scales is presented. Time scales of two partners are different, which for partner A is t and for partner B is τ . Also new strategy to achieve chaos control by GYC partial region stability is used and Tables and Figures are given to prove that the new strategy do synchronize system far more quickly.

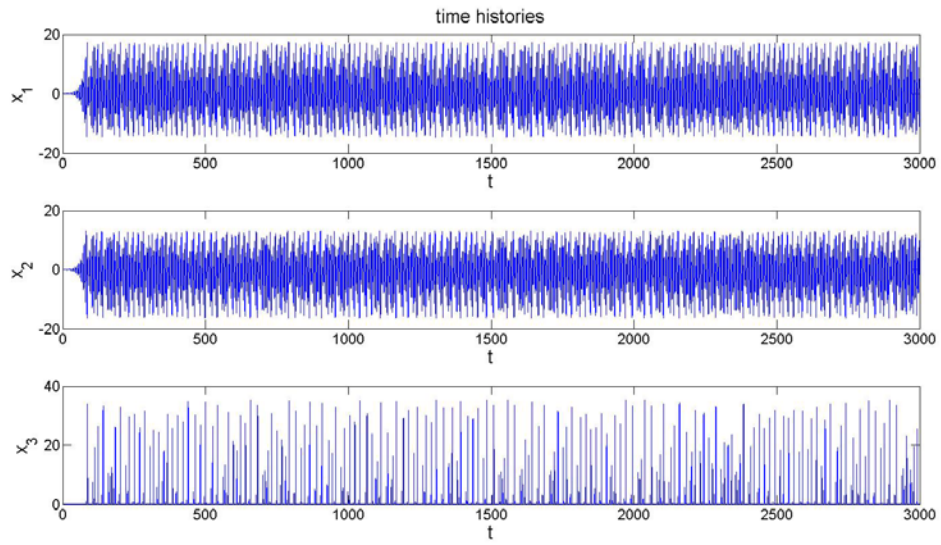
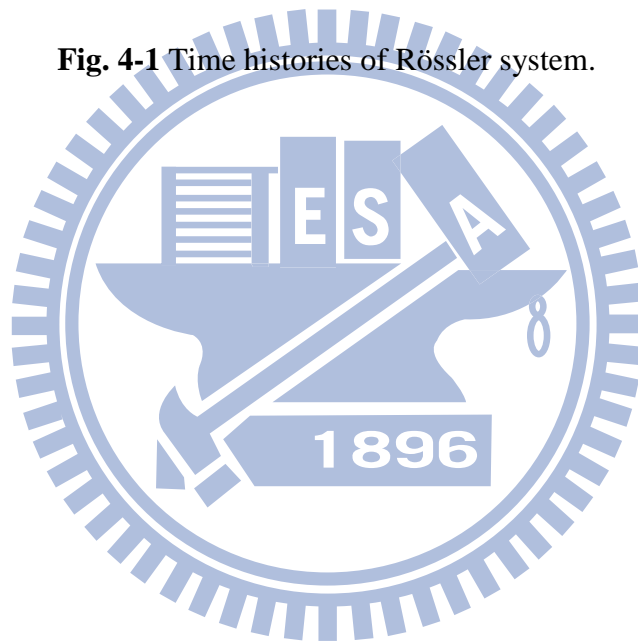
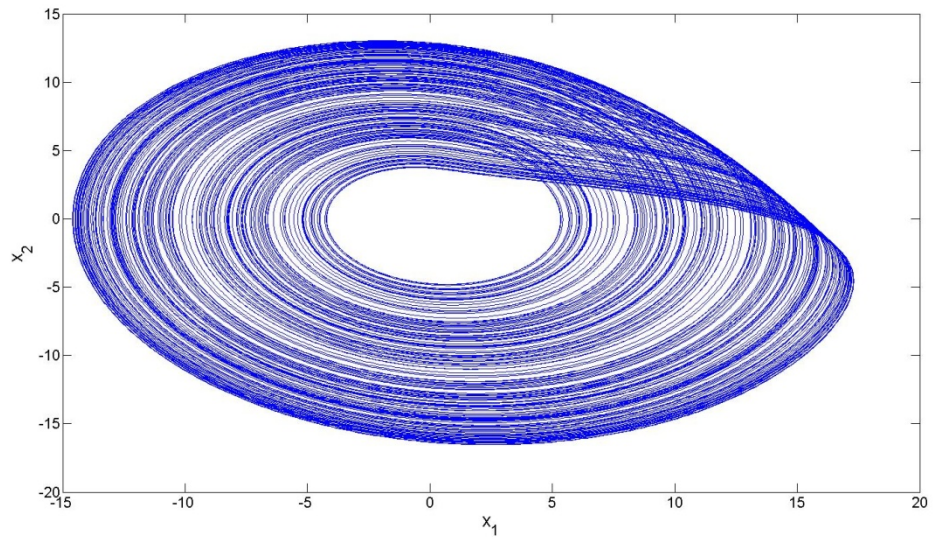


Fig. 4-1 Time histories of Rössler system.





Phase portraits

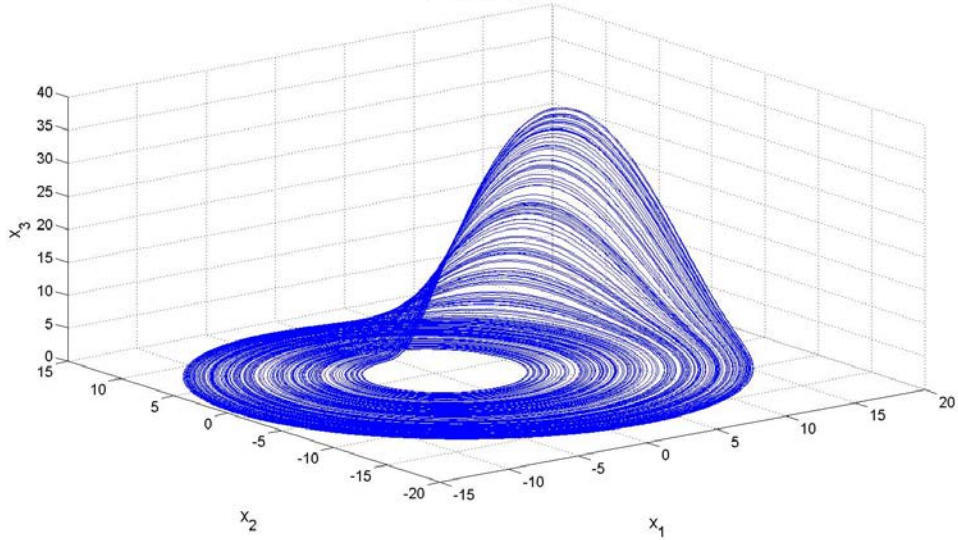


Fig. 4-2 Phase portraits of Rössler system.

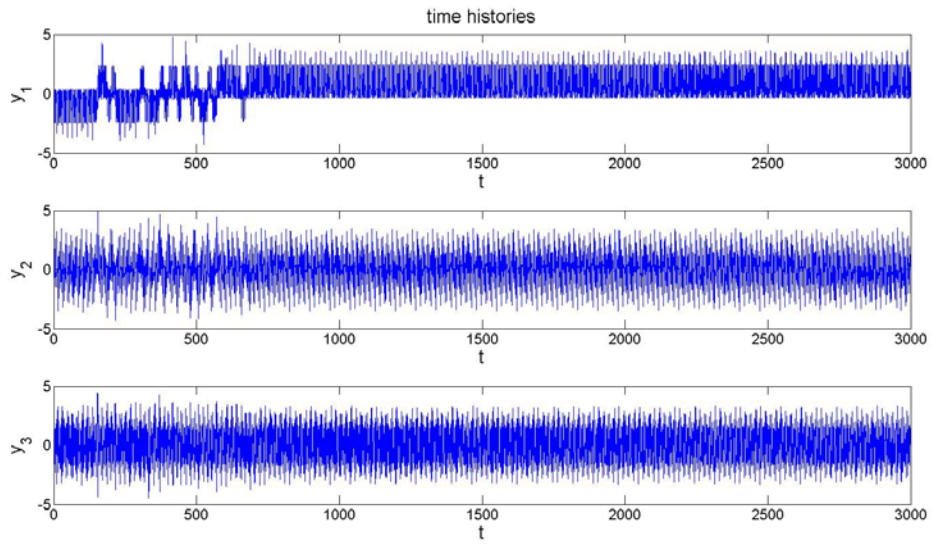
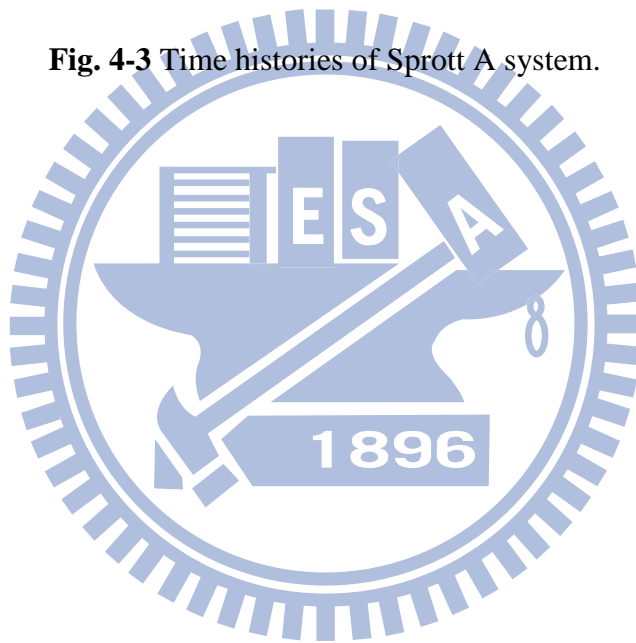


Fig. 4-3 Time histories of Sprott A system.



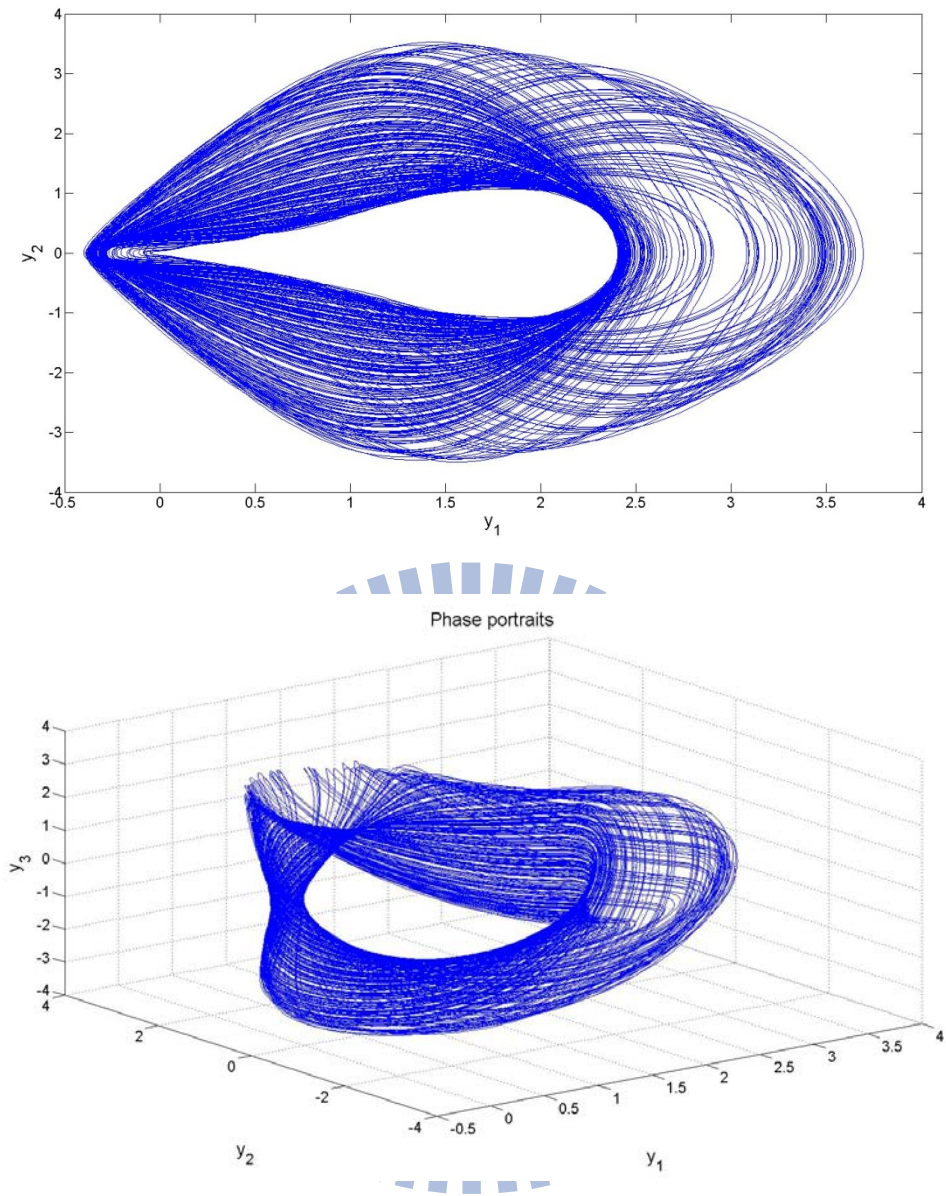


Fig. 4-4 Phase portraits of Sprott A system.

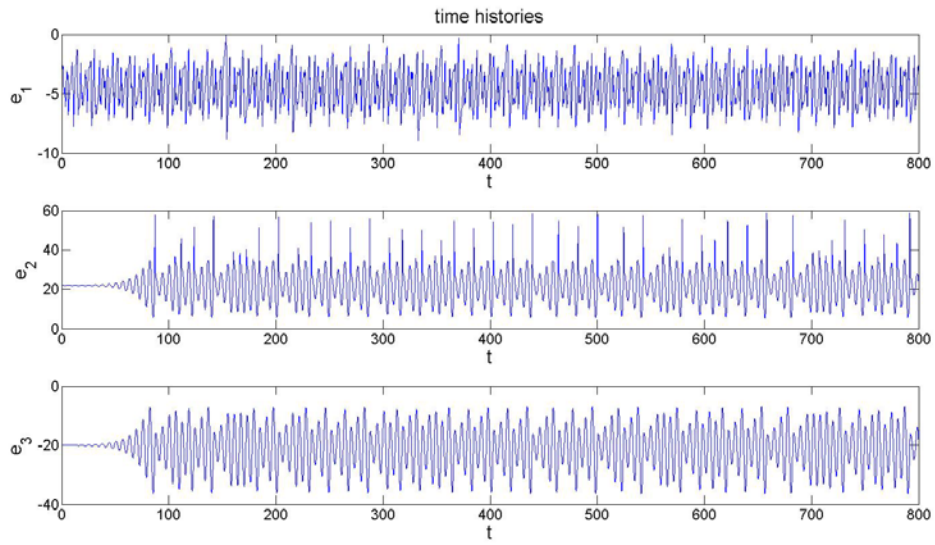


Fig. 4-5 Time histories of error function before synchronization for new strategy.



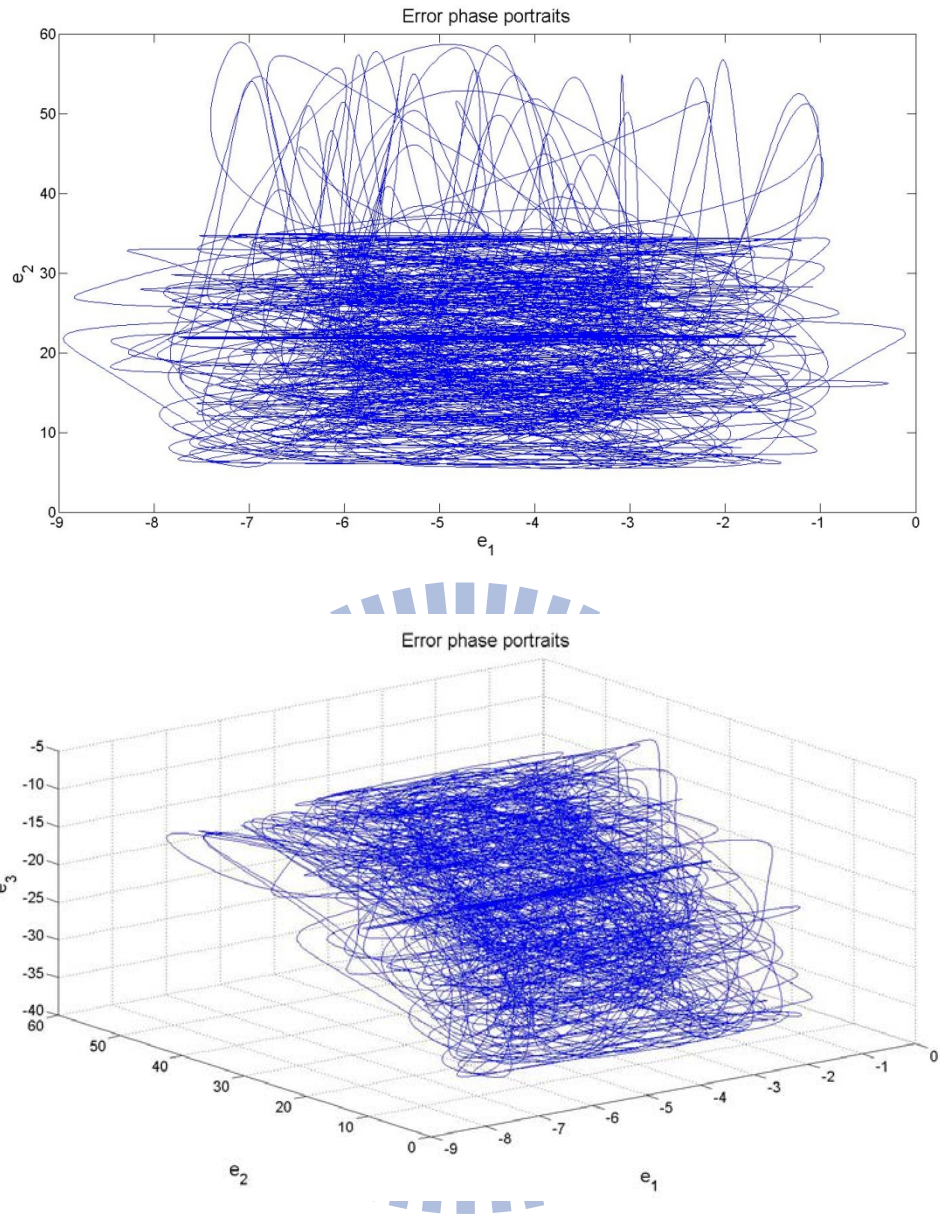


Fig. 4-6 Phase portraits of error function before synchronization for new strategy.

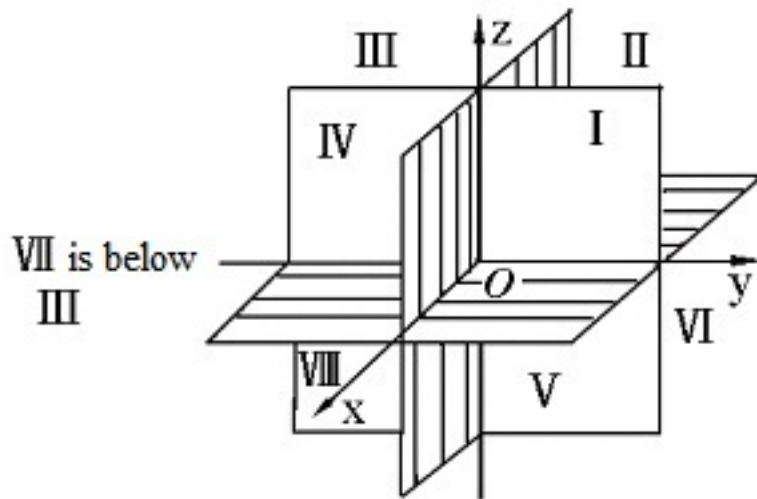


Fig. 4-7 Relative positions of eight octants.

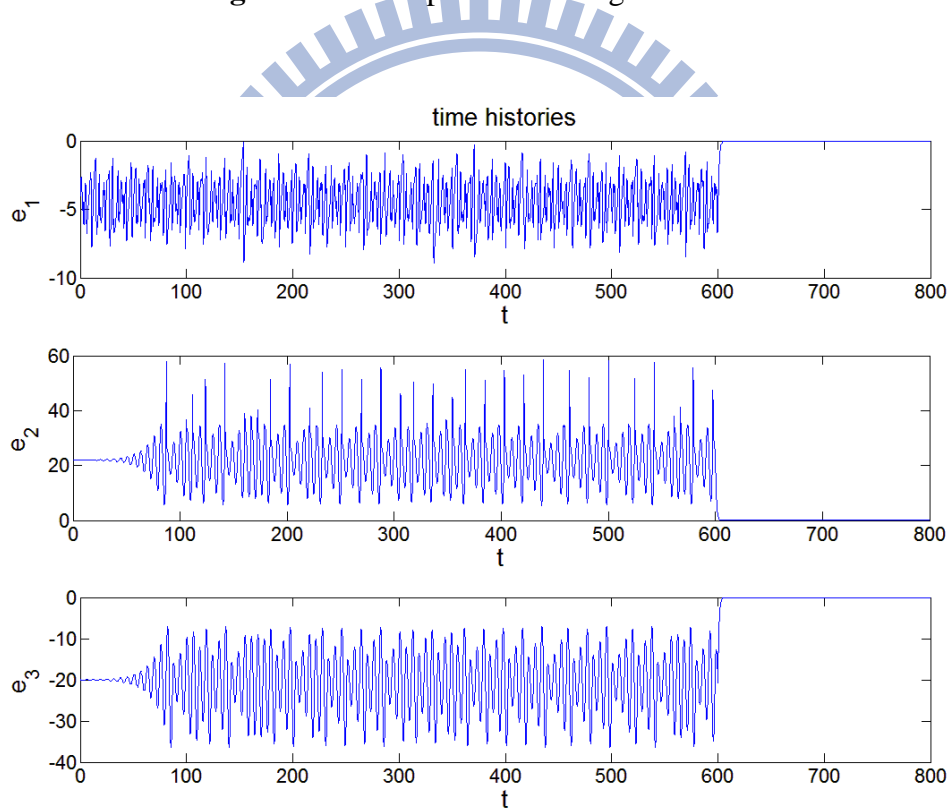
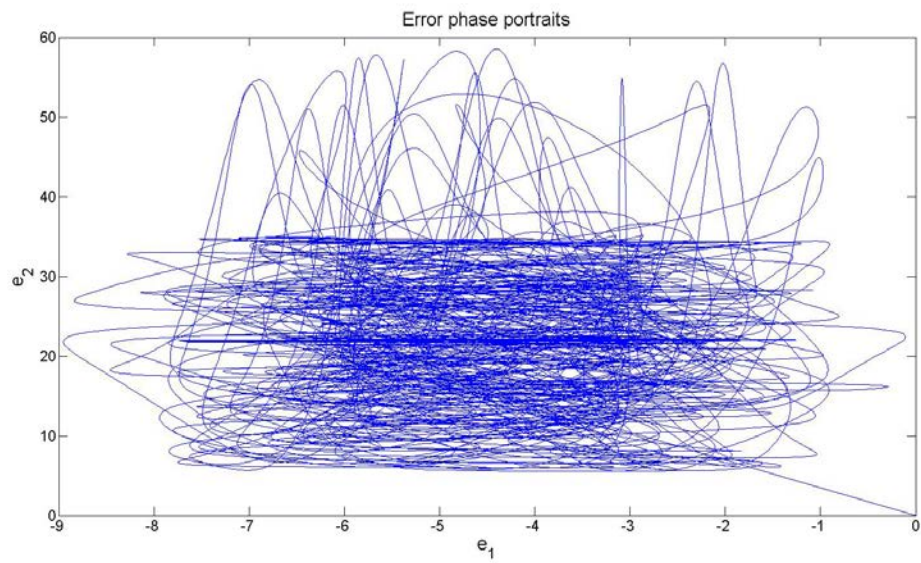


Fig. 4-8 Time histories of error function after synchronization for new strategy.



Error phase portraits

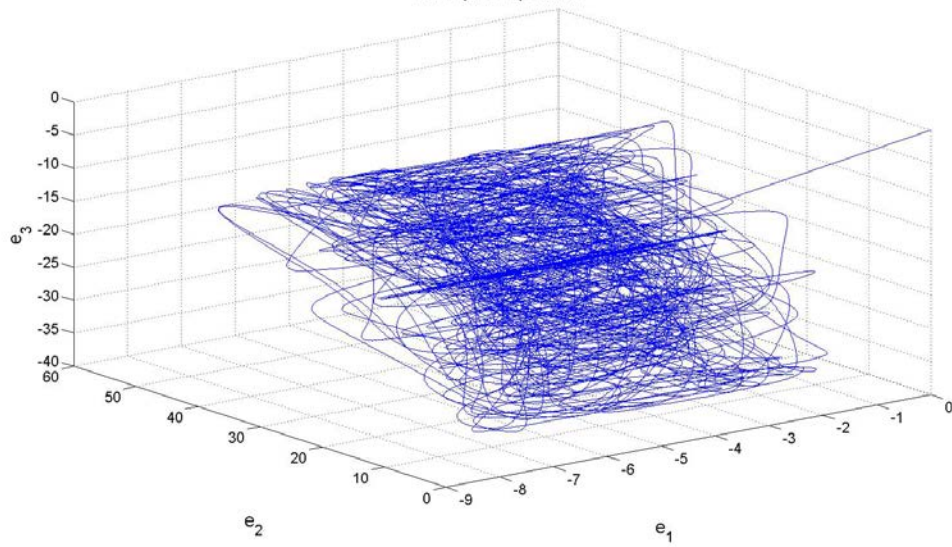


Fig. 4-9 Phase portrait of error function after synchronization for new strategy.

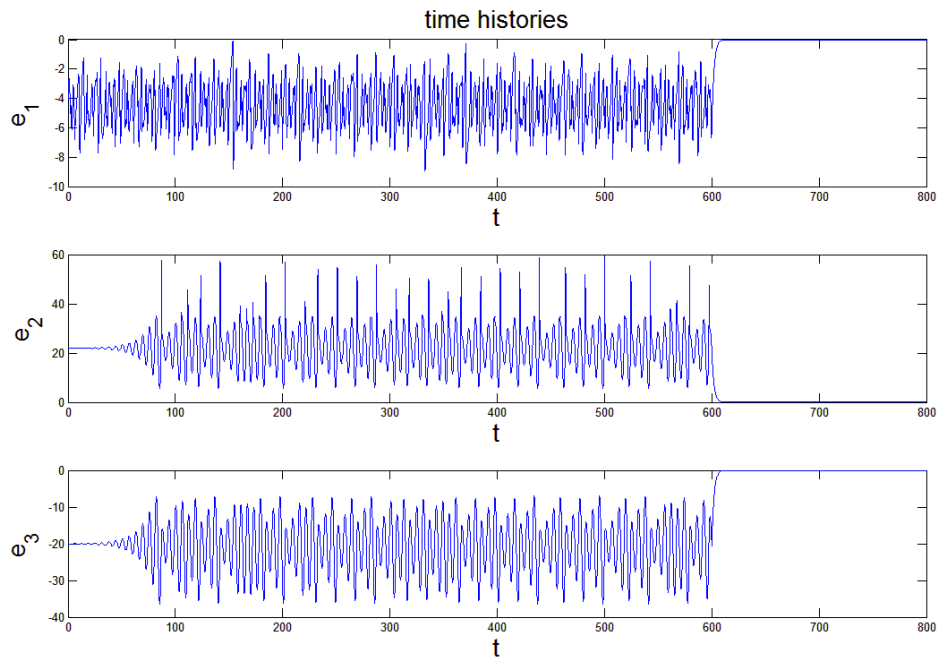
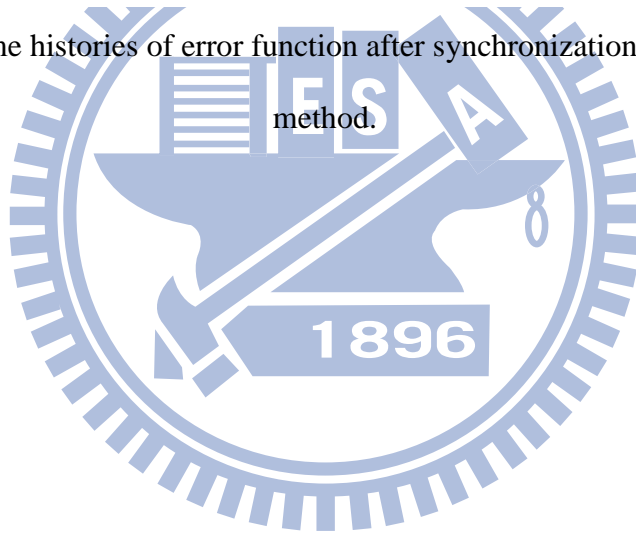
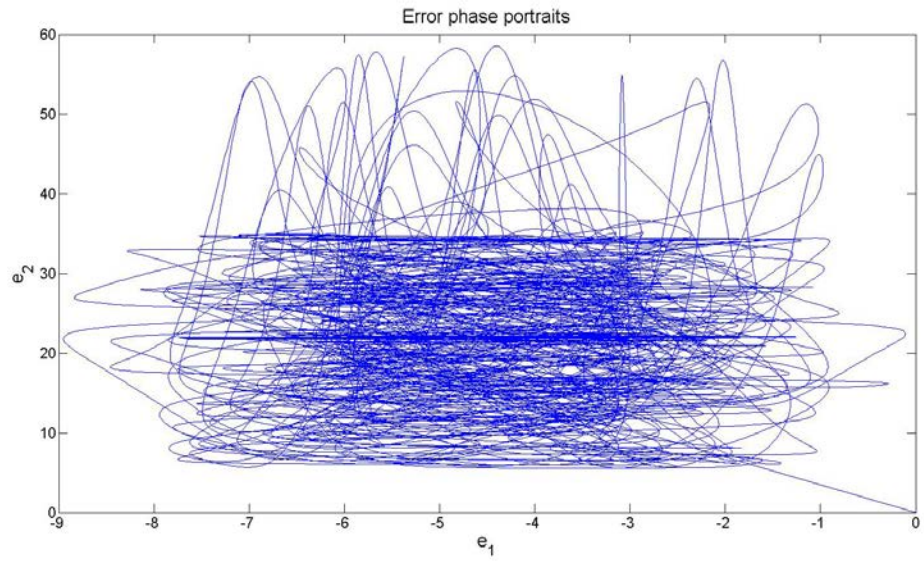


Fig. 4-10 Time histories of error function after synchronization for traditional method.





Error phase portraits

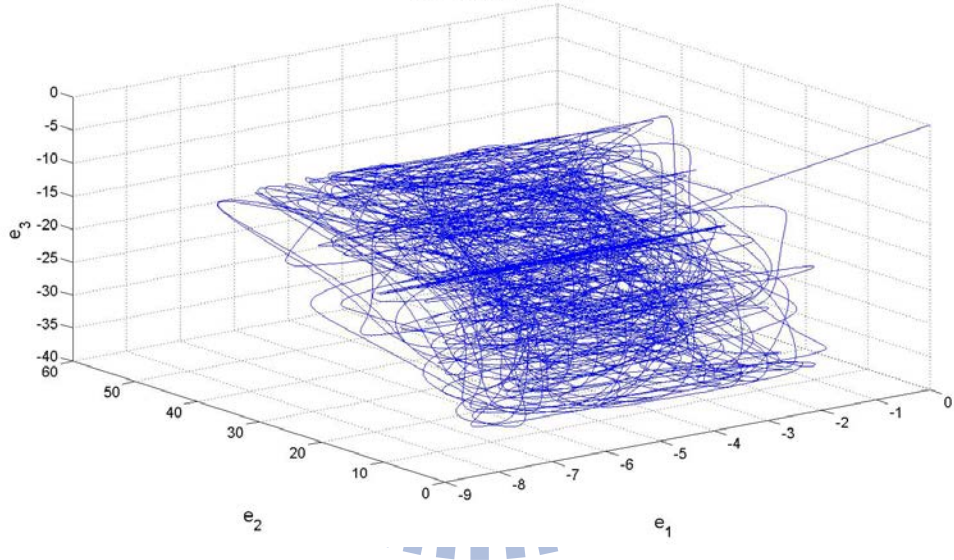


Fig. 4-11 Phase portrait of error function after synchronization for traditional method.

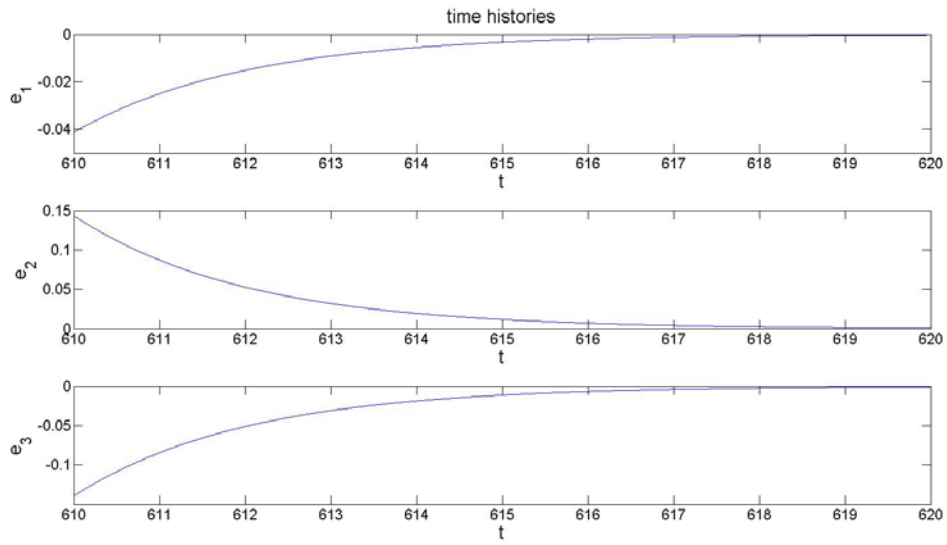


Fig. 4-12 Time histories of error function after synchronization for traditional method.

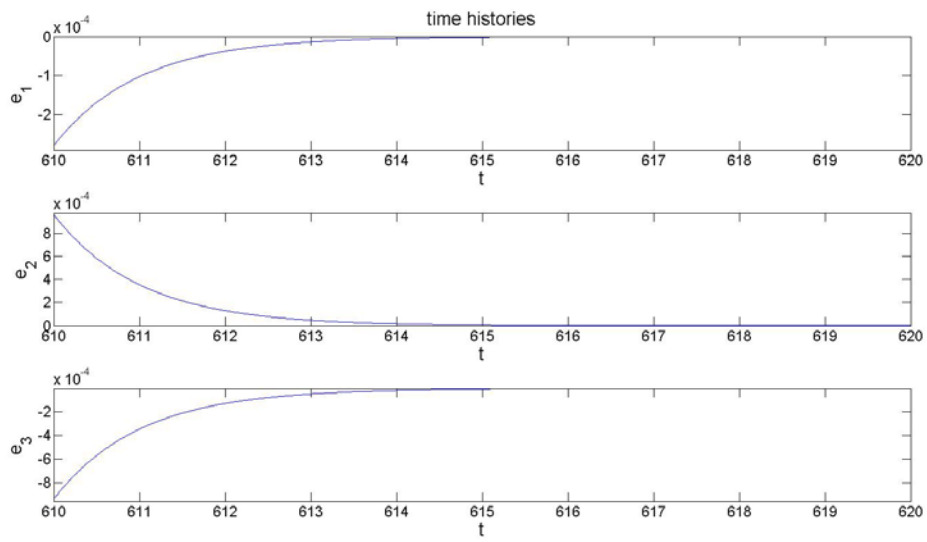


Fig. 4-13 Time histories of error function after synchronization for new strategy.

Chapter 5

Kan trigram and Li trigram Multiple Symplectic Derivative Synchronization by Partial Region Stability Theory

5-1. Preliminary

The eight trigrams, shown in Fig. 5-1, is a part of Chinese philosophy, and they have their own direction, figure, and representation. trigram has three parts, upper, central, and low. The three parts of Kan trigram and Li trigram both represent three different chaos systems separately, and they are used to complete a two times multiple symplectic derivative synchronization by GYC partial region stability theory.

This chapter is presented as follows. In Section 2, systems used in this chapter are shown and the Yang (normal) and Yin (historical) systems for Rössler System, Sprott 22 system, and Sprott C system are synchronized. In Section 3, the Kan trigram multiple symplectic derivative synchronization is presented by GYC partial region stability theory. In Section 4, the Li trigram multiple symplectic derivative synchronization is proposed. In Section 5, summary is drawn.

5-2. Synchronization of Yang and Yin systems

The Yang Rössler system is

$$\begin{cases} \dot{x}_1 = -x_2 - x_3 \\ \dot{x}_2 = x_1 + a_{11}x_2 \\ \dot{x}_3 = b_{11} + x_3(x_1 - c_{11}) \end{cases} \quad (5-1)$$

and the Yin Rössler system is

$$\begin{cases} \dot{x}_4 = x_5 + x_6 \\ \dot{x}_5 = -x_4 - a_{12}x_5 \\ \dot{x}_6 = -b_{12} - x_6(x_4 - c_{12}) \end{cases} \quad (5-2)$$

where $a_{11}=0.15$, $b_{11}=0.2$, $c_{11}=10$, $a_{12}=-0.15$, $b_{12}=-0.2$, $c_{12}=-10$ and the initial condition are $x_{10}= 0.3$, $x_{20}= 0.1$, $x_{30}=0.5$, $x_{40}= 0.3$, $x_{50}= 0.1$, $x_{60}=0.5$. The chaotic attractor of Tai Ji Rössler system, the combination of Yang and Yin systems, is shown in Fig. 5-2 and Fig. 5-3.

Set the Yin Rössler system be

$$\begin{cases} \dot{x}_4 = x_5 + x_6 & + k(x_1 - x_4) \\ \dot{x}_5 = -x_4 - a_{12}x_5 & + k(x_2 - x_5) \\ \dot{x}_6 = -b_{12} - x_6(x_4 - c_{12}) & + k(x_3 - x_6) \end{cases} \quad (5-3)$$

where x_1 , x_2 , and x_3 are states of Eq. (5-1), k is a positive constant, 100.

The states of linear feedback synchronization for Yang Rössler system and Yin Rössler system are shown in Fig. 5-4.

The Yang Sprott 22 system is

$$\begin{cases} \dot{y}_1 = y_2 \\ \dot{y}_2 = y_3 \\ \dot{y}_3 = -a_{21}y_3 - y_2 - \sin y_1 \end{cases} \quad (5-4)$$

and the Yin Sprott 22 system is

$$\begin{cases} \dot{y}_4 = -y_5 \\ \dot{y}_5 = -y_6 \\ \dot{y}_6 = a_{22}y_6 + y_5 + \sin y_4 \end{cases} \quad (5-5)$$

where $a_{21}=0.25$, $a_{22}=-0.25$ and the initial condition are $y_{10}= 0.3$, $y_{20}= 0.1$, $y_{30}=0.5$, $y_{40}= 0.3$, $y_{50}= 0.1$, $y_{60}=0.5$. The chaotic attractor of Tai Ji Sprott 22 system, the combination of Yang and Yin systems, is shown in Fig. 5-5 and Fig. 5-6.

There are four types of linear feedback synchronizations of Sprott 22 system for Li trigram synchronization.

(5-1) Set the Yang Sprott 22 system be

$$\begin{cases} \dot{y}_{11} = y_{12} & + k(x_1 - y_{11}) \\ \dot{y}_{12} = y_{13} & + k(x_2 - y_{12}) \\ \dot{y}_{13} = -a_{21}y_{13} - y_{12} - \sin y_{11} + k(x_3 - y_{13}) \end{cases} \quad (5-6)$$

where x_1 , x_2 , and x_3 are states of Eq. (5-1), k is a positive constant, 100.

(5-2) Set the Yang Sprott 22 system be

$$\begin{cases} \dot{y}_{21} = y_{22} & + k(x_4 - y_{21}) \\ \dot{y}_{22} = y_{23} & + k(x_5 - y_{22}) \\ \dot{y}_{23} = -a_{21}y_{23} - y_{22} - \sin y_{21} + k(x_6 - y_{23}) \end{cases} \quad (5-7)$$

where x_4 , x_5 , and x_6 are states of Eq. (5-2), k is a positive constant, 100.

(5-3) Set the Yin Sprott 22 system be

$$\begin{cases} \dot{y}_{14} = -y_{15} & + k(z_1 - y_{14}) \\ \dot{y}_{15} = -y_{16} & + k(z_2 - y_{15}) \\ \dot{y}_{16} = a_{22}y_{16} + y_{15} + \sin y_{14} + k(z_3 - y_{16}) \end{cases} \quad (5-8)$$

where z_1 , z_2 , and z_3 are states of Eq (5-10), k is a positive constant, 100.

(5-4) Set the Yin Sprott 22 system be

$$\begin{cases} \dot{y}_{24} = -y_{25} & + k(z_4 - y_{24}) \\ \dot{y}_{25} = -y_{26} & + k(z_5 - y_{25}) \\ \dot{y}_{26} = a_{22}y_{26} + y_{25} + \sin y_{24} + k(z_6 - y_{26}) \end{cases} \quad (5-9)$$

where z_4 , z_5 , and z_6 are states of Eq. (5-11), k is a positive constant, 100.

The four types of states of linear feedback synchronization for Sprott 22 system are shown in Figs. 7~10.

The Yang Sprott C system is

$$\begin{cases} \dot{z}_1 = z_2 z_3 \\ \dot{z}_2 = z_1 - a_{31} z_2 \\ \dot{z}_3 = b_{31} - c_{31} z_1^2 \end{cases} \quad (5-10)$$

and the Yin Sprott C system is

$$\begin{cases} \dot{z}_4 = -z_5 z_6 \\ \dot{z}_5 = -z_4 + a_{32} z_5 \\ \dot{z}_6 = -b_{32} + c_{32} z_4^2 \end{cases} \quad (5-11)$$

where $a_{31}=1$, $b_{31}=1$, $c_{31}=1$, $a_{32}=-1$, $b_{32}=-1$, $c_{32}=-1$ and the initial condition

are $z_{10}=0.3$, $z_{20}=0.1$, $z_{30}=0.5$, $z_{40}=0.3$, $z_{50}=0.1$, $z_{60}=0.5$. The chaotic attractor of Tai Ji Sprott C system, the combination of Yang and Yin systems, is shown in Fig. 5-11 and Fig. 5-12.

Set the Yang Sprott C system be

$$\begin{cases} \dot{z}_1 = z_2 z_3 + k(z_4 - z_1) \\ \dot{z}_2 = z_1 - a_{31} z_2 + k(z_5 - z_2) \\ \dot{z}_3 = b_{31} - c_{31} z_1^2 + k(z_6 - z_3) \end{cases} \quad (5-12)$$

where z_4 , z_5 , and z_6 are states of Eq. (5-11), k is a positive constant, 100.

The states of linear feedback synchronization for Yang Sprott C system and Yin Sprott C system are shown in Fig. 5-13.

5-3. Kan trigram synchronization

At first, Eq. (5-3) which Eq. (5-2) is synchronized with Eq. (5-1) is complete.

Define

$$G_1(x, \dot{x}, y, \dot{y}, z, \dot{z}, t) = \begin{bmatrix} y_1 + \cos y_2 - \dot{x}_4 \\ y_2 + \sin y_3 + \dot{x}_5 \\ y_3 + \sin y_2 - \dot{x}_4 - \dot{x}_5 \end{bmatrix}, \quad (5-13)$$

$$F_1(x, \dot{x}, y, \dot{y}, z, \dot{z}, t) = \begin{bmatrix} \dot{x}_5 + y_1 + \cos \dot{y}_1 + x_6 \\ x_4 + \dot{y}_1 + \sin \dot{y}_2 \\ x_6 + \dot{y}_2 \end{bmatrix}, \quad (5-14)$$

Our purpose is to achieve the multiple symplectic derivative synchronization

$$G_1(x, \dot{x}, y, \dot{y}, z, \dot{z}, t) = F_1(x, \dot{x}, y, \dot{y}, z, \dot{z}, t) - K.$$

The state error is $e = G - F + K$ where $K = [68, 29, 38]^T$ such that error dynamics always exists in first quadrant.

$$e_{1i} = G_{1i} - F_{1i} + K_i \quad i = 1, 2, 3.$$

Our purpose is $\lim_{t \rightarrow \infty} e = 0$. We obtain the error dynamics:

$$\dot{e}_{1i} = \dot{G}_{1i} - \dot{F}_{1i} - u_{1i} \quad i = 1, 2, 3.$$

By partial region stability theory, we can choose a Lyapunov function in the form

of a positive definite function in first quadrant:

$$V_1(e_1) = e_{11} + e_{12} + e_{13} \quad (5-15)$$

Its time derivative is

$$\dot{V}_1(e_1) = (\dot{G}_{11} - \dot{F}_{11} - u_{11}) + (\dot{G}_{12} - \dot{F}_{12} - u_{12}) + (\dot{G}_{13} - \dot{F}_{13} - u_{13})$$

Choose the controller u_1 as

$$u_1 = \begin{bmatrix} u_{11} \\ u_{12} \\ u_{13} \end{bmatrix} = \begin{bmatrix} e_{11} + y_2 \\ e_{12} - 0.15\dot{x}_5 \\ e_{13} + y_2 \cos y_1 \end{bmatrix} \quad (5-16)$$

We obtain

$$\dot{V}_1(e_1) = -e_{11} - e_{12} - e_{13} < 0 \quad (5-17)$$

which is negative definite function in first quadrant. Error states versus time and their time histories are shown in Fig. 5-14 and Fig. 5-15.

And then, Eq. (5-12) which Eq. (5-10) is synchronized with Eq. (5-11) is complete.

Define

$$G_2(x, \dot{x}, y, \dot{y}, z, \dot{z}, t) = \begin{bmatrix} z_1 + z_2 - \dot{y}_5 \\ z_2 + \dot{z}_2 + \cos y_4 \\ z_3 + y_4 + \cos y_5 \end{bmatrix}, \quad (5-18)$$

$$F_2(x, \dot{x}, y, \dot{y}, z, \dot{z}, t) = \begin{bmatrix} y_6 + \cos y_4 - \dot{z}_2 \\ -y_5 + \cos y_5 - z_1 \\ -\dot{z}_1/z_2 + \cos y_6 \end{bmatrix}, \quad (5-19)$$

Our purpose is to achieve the multiple symplectic derivative synchronization

$$G_2(x, \dot{x}, y, \dot{y}, z, \dot{z}, t) = F_2(x, \dot{x}, y, \dot{y}, z, \dot{z}, t) - K.$$

The state error is $e = G - F + K$ where $K = [68, 29, 38]^T$ such that error dynamics always exists in first quadrant.

$$e_{2i} = G_{2i} - F_{2i} + K_i \quad i = 1, 2, 3.$$

Our purpose is $\lim_{t \rightarrow \infty} e = 0$. We obtain the error dynamics:

$$\dot{e}_{2i} = \dot{G}_{2i} - \dot{F}_{2i} - u_{2i} \quad i = 1, 2, 3.$$

By partial region stability theory, we can choose a Lyapunov function in the form of a positive definite function in first quadrant:

$$V_2(e_2) = e_{21} + e_{22} + e_{23} \quad (5-20)$$

Its time derivative is

$$\dot{V}_2(e_2) = (\dot{G}_{21} - \dot{F}_{21} - u_{21}) + (\dot{G}_{22} - \dot{F}_{22} - u_{22}) + (\dot{G}_{23} - \dot{F}_{23} - u_{23})$$

Choose the controller u as

$$u_2 = \begin{bmatrix} u_{21} \\ u_{22} \\ u_{23} \end{bmatrix} = \begin{bmatrix} e_{21} - y_5 \sin y_4 \\ e_{22} - y_6 \\ e_{23} - y_5 \end{bmatrix} \quad (5-21)$$

We obtain

$$\dot{V}_2(e_2) = -e_{21} - e_{22} - e_{23} < 0 \quad (5-22)$$

which is negative definite function in first quadrant. Error states versus time and their time histories are shown in Fig. 5-16 and Fig. 5-17.

At last, e_1 and e_2 are the components of error states e . Error states versus time and their time histories are shown in Fig. 5-18 and Fig. 5-19.

5-4. Li trigram synchronization

At first, Eq. (5-6) which Eq. (5-4) is synchronized with Eq. (5-1) and Eq. (5-8) which Eq. (5-5) is synchronized with Eq. (5-10) are complete.

Define

$$G_1(x, \dot{x}, y, \dot{y}, z, \dot{z}, t) = \begin{bmatrix} y_{14} + y_{15}y_{16} - y_{11}\dot{y}_{11} - y_{11}y_{13} \\ y_{15} + y_{16}y_{14} - y_{12}\dot{y}_{11} \\ y_{16} + y_{14}y_{15} + y_{15}\dot{y}_{15} + \dot{y}_{13} \end{bmatrix}, \quad (5-23)$$

$$F_1(x, \dot{x}, y, \dot{y}, z, \dot{z}, t) = \begin{bmatrix} y_{11}y_{12} + \dot{y}_{14} + \dot{y}_{15} \\ y_{12}y_{13} - \dot{y}_{15} + \dot{y}_{15}y_{16} + y_{15}y_{16} \\ y_{11}y_{13} + y_{15}^2 + y_{15}\dot{y}_{15} \end{bmatrix}, \quad (5-24)$$

Our purpose is to achieve the multiple symplectic derivative synchronization

$$G_1(x, \dot{x}, y, \dot{y}, z, \dot{z}, t) = F_1(x, \dot{x}, y, \dot{y}, z, \dot{z}, t) - K.$$

The state error is $e = G - F + K$ where $K = [2, 11, 108]^T$ such that error dynamics always exists in first quadrant.

$$e_{1i} = G_{1i} - F_{1i} + K_i \quad i = 1, 2, 3.$$

Our purpose is $\lim_{t \rightarrow \infty} e = 0$. We obtain the error dynamics:

$$\dot{e}_{1i} = \dot{G}_{1i} - \dot{F}_{1i} - u_{1i} \quad i = 1, 2, 3.$$

By partial region stability theory, we can choose a Lyapunov function in the form of a positive definite function in first quadrant:

$$V_1(\mathbf{e}_1) = e_{11} + e_{12} + e_{13} \quad (5-25)$$

Its time derivative is

$$\dot{V}_1(\mathbf{e}_1) = (\dot{G}_{11} - \dot{F}_{11} - u_{11}) + (\dot{G}_{12} - \dot{F}_{12} - u_{12}) + (\dot{G}_{13} - \dot{F}_{13} - u_{13})$$

Choose the controller u_1 as

$$u_1 = \begin{bmatrix} u_{11} \\ u_{12} \\ u_{13} \end{bmatrix} = \begin{bmatrix} e_{11} + \dot{y}_{15} \\ e_{12} + 2y_{12}\dot{y}_{12} \\ e_{13} - 10\dot{y}_{13} \end{bmatrix} \quad (5-26)$$

We obtain

$$\dot{V}_1(\mathbf{e}_1) = -e_{11} - e_{12} - e_{13} < 0 \quad (5-27)$$

which is negative definite function in first quadrant. Error states versus time and their time histories are shown in Fig. 5-20 and Fig. 5-21.

And then, Eq. (5-7) which Eq. (5-4) is synchronized with Eq. (5-2) and Eq. (5-9) which Eq. (5-5) is synchronized with Eq. (5-11) are complete.

Define

$$G_2(x, \dot{x}, y, \dot{y}, z, \dot{z}, t) = \begin{bmatrix} y_{24} - y_{23} + y_{21}\dot{y}_{21} - y_{21}y_{23} \\ y_{25} - y_{25} + \dot{y}_{21}y_{23} - y_{22}^2 \\ y_{26} - y_{21} - 10y_{23} - \dot{y}_{23} \end{bmatrix}, \quad (5-28)$$

$$F_2(x, \dot{x}, y, \dot{y}, z, \dot{z}, t) = \begin{bmatrix} y_{21}y_{22} - \dot{y}_{25} - \dot{y}_{21} + y_{22} \\ y_{22}y_{23} - \dot{y}_{25} - \dot{y}_{21} + y_{23} \\ y_{21}y_{23} - \dot{y}_{24}/y_{25} + \dot{y}_{22} \end{bmatrix}, \quad (5-29)$$

Our purpose is to achieve the multiple symplectic derivative synchronization

$$G_2(x, \dot{x}, y, \dot{y}, z, \dot{z}, t) = F_2(x, \dot{x}, y, \dot{y}, z, \dot{z}, t) - K.$$

The state error is $e = G - F + K$ where $K = [2,11,108]^T$ such that error dynamics always exists in first quadrant.

$$e_{2i} = G_{2i} - F_{2i} + K_i \quad i = 1, 2, 3.$$

Our purpose is $\lim_{t \rightarrow \infty} e = 0$. We obtain the error dynamics:

$$\dot{e}_{2i} = \dot{G}_{2i} - \dot{F}_{2i} - u_{2i} \quad i = 1, 2, 3.$$

By partial region stability theory, we can choose a Lyapunov function in the form of a positive definite function in first quadrant:

$$V_2(\mathbf{e}_2) = e_{21} + e_{22} + e_{23} \quad (5-30)$$

Its time derivative is

$$\dot{V}_2(\mathbf{e}_2) = (\dot{G}_{21} - \dot{F}_{21} - u_{21}) + (\dot{G}_{22} - \dot{F}_{22} - u_{22}) + (\dot{G}_{23} - \dot{F}_{23} - u_{23})$$

Choose the controller u as

$$u_2 = \begin{bmatrix} u_{21} \\ u_{22} \\ u_{23} \end{bmatrix} = \begin{bmatrix} e_{21} - \dot{y}_{25} \\ e_{22} - \dot{y}_{24} \\ e_{23} - 0.15\dot{y}_{22} \end{bmatrix} \quad (5-31)$$

We obtain

$$\dot{V}_2(\mathbf{e}_2) = -e_{21} - e_{22} - e_{23} < 0 \quad (5-32)$$

which is negative definite function in first quadrant. Error states versus time and their time histories are shown in Fig. 5-22 and Fig. 5-23.

At last, \mathbf{e}_1 and \mathbf{e}_2 are the components of error states e . Error states versus time and their time histories are shown in Fig. 5-24 and Fig. 5-25.

5-5. Summary

The figures of Kan and Li trigrams are used to complete a different kind of synchronization. The error dynamics have three stages. Firstly, in 0 ~ 100 sec. no control is applied. And then, the synchronization of Yang and Yin system appears in second 101 ~ 200. Finally, after second 201, error dynamics achieve synchronization. It seems very complex, but it is full compliance with the eight trigram.





Fig. 5-1 Relation of the eight trigrams.

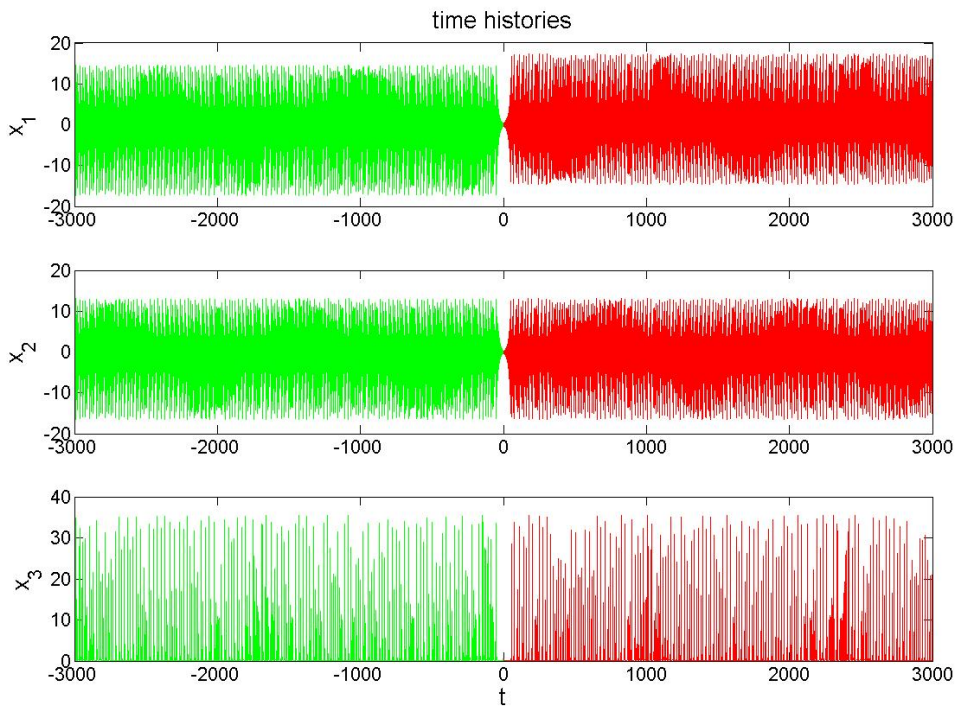


Fig. 5-2 Time histories of Tai Ji Rössler system.

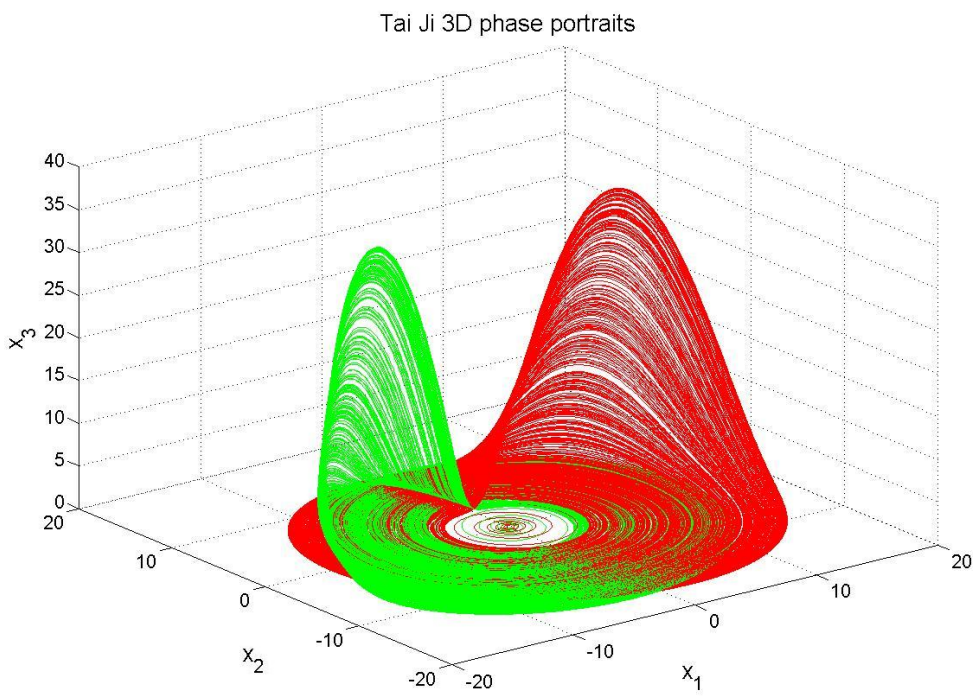
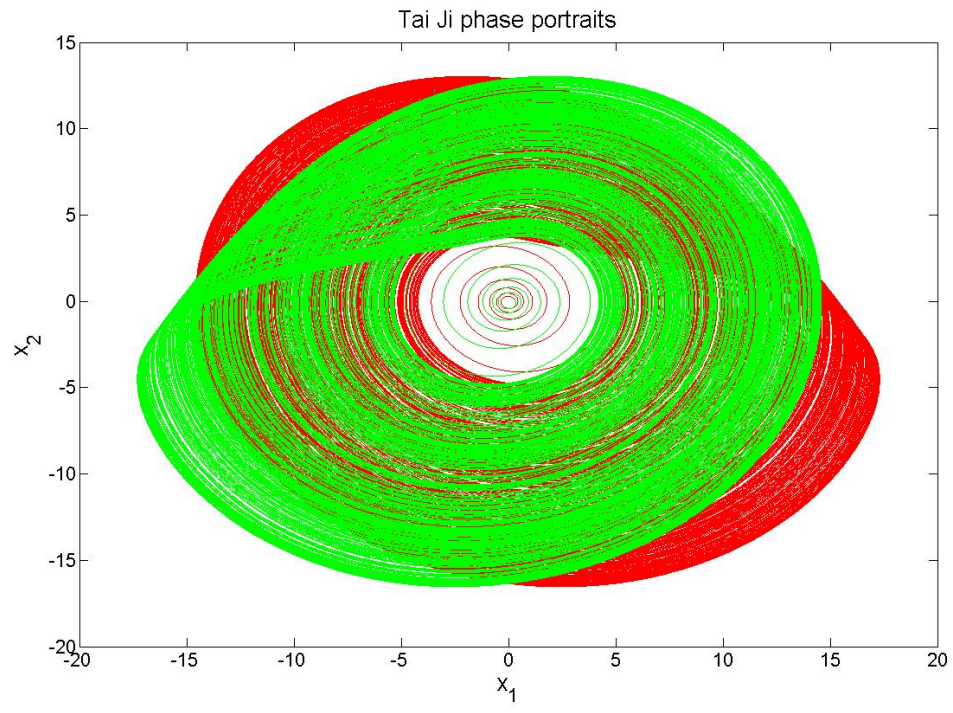


Fig. 5-3 Phase portraits of Rössler system.

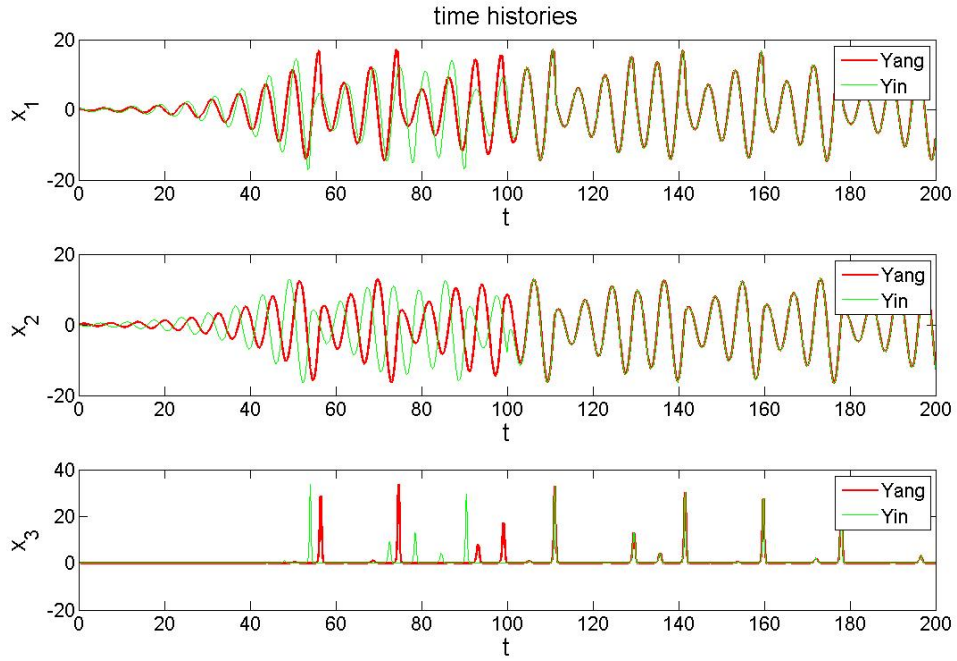


Fig. 5-4 Synchronization for Yin Rössler system and Yang Rössler system.

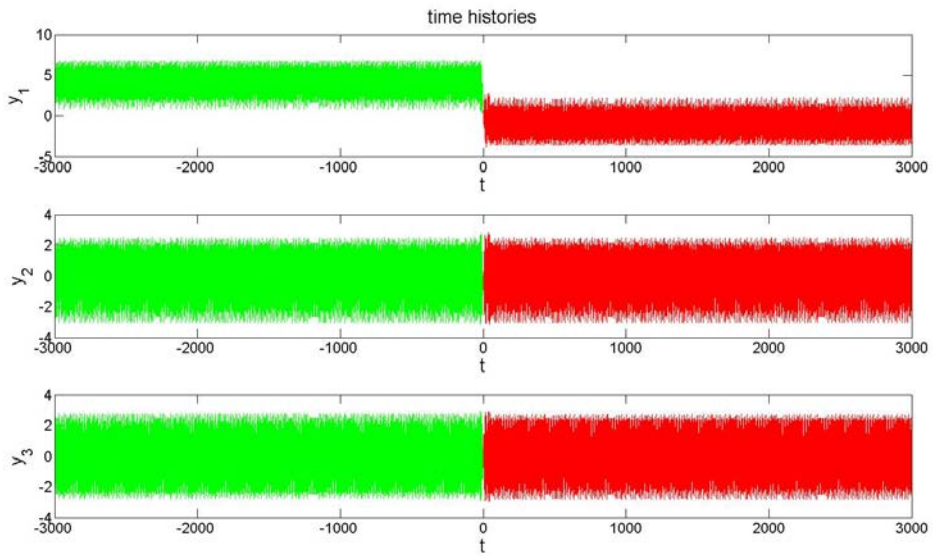


Fig. 5-5 Time histories of Tai Ji Sprott 22 system.

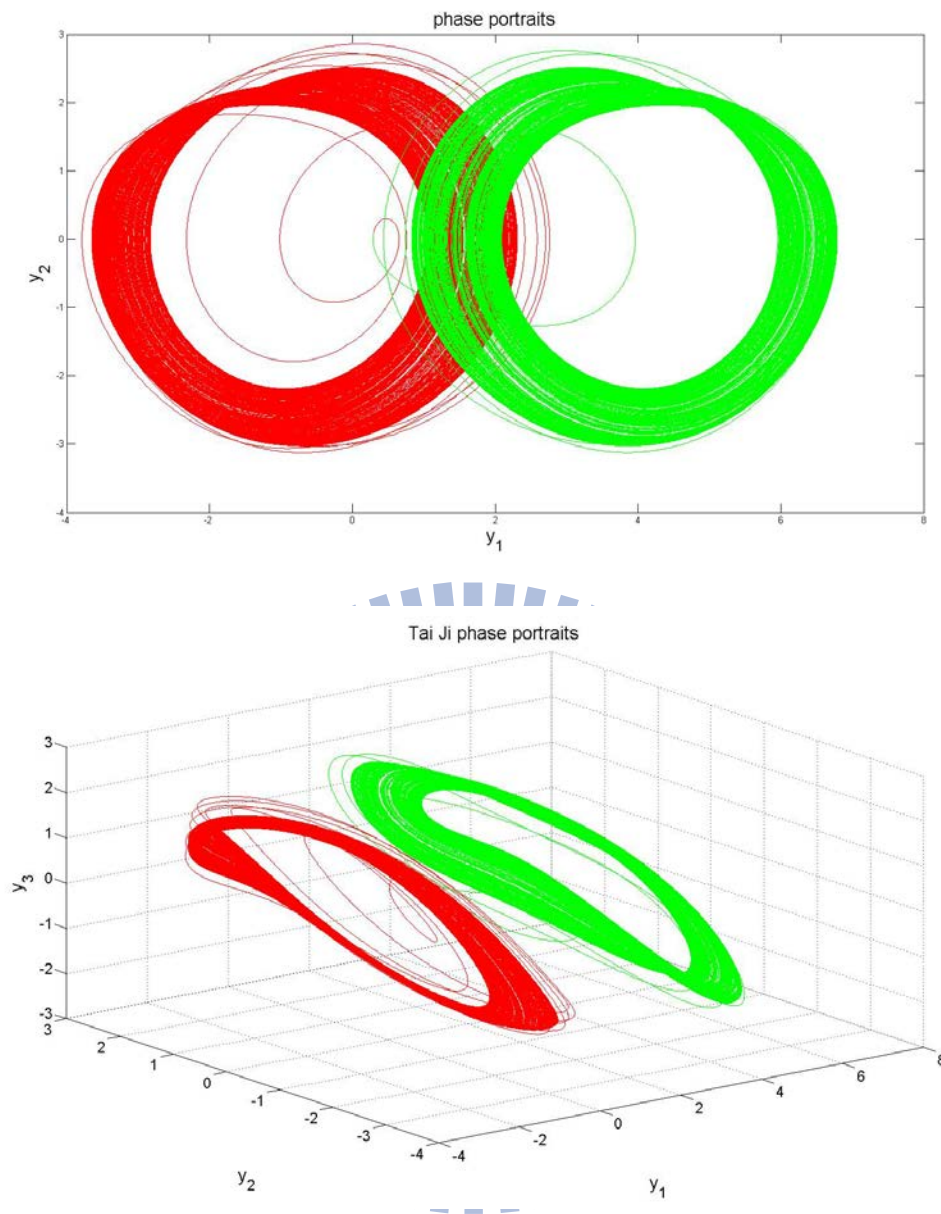


Fig. 5-6 Phase portraits of Tai Ji Sprott 22 system.

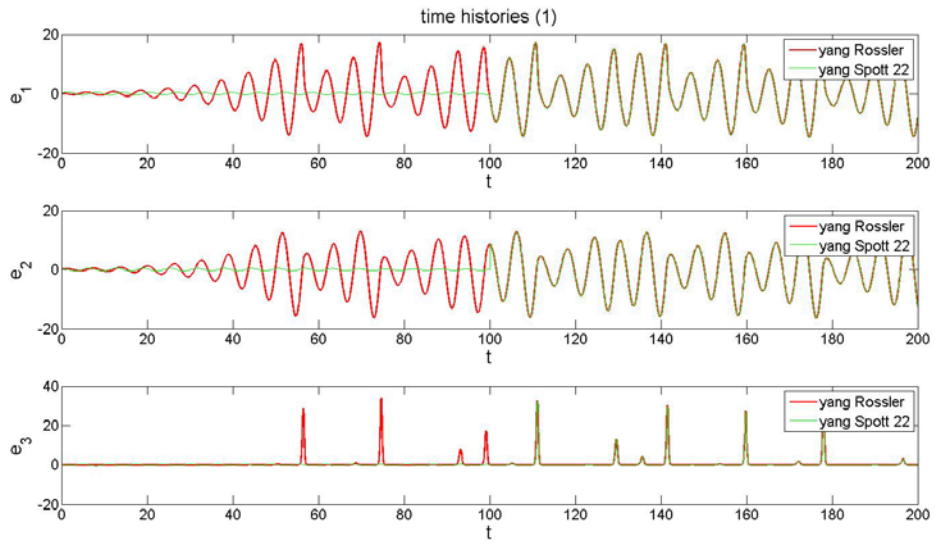


Fig. 5-7 Synchronization for Yang Spott 22 system and Yang Rössler system.

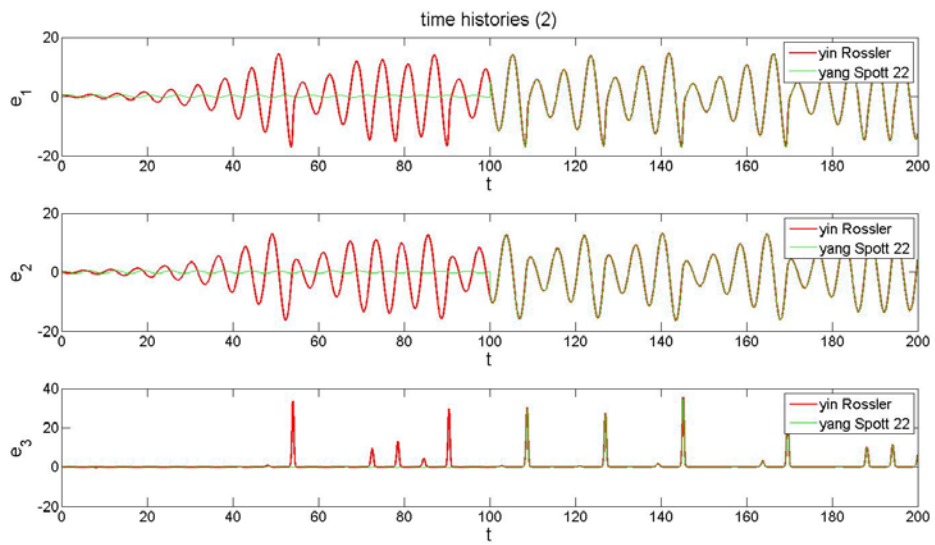


Fig. 5-8 Synchronization for Yang Spott 22 system and Yin Rössler system.

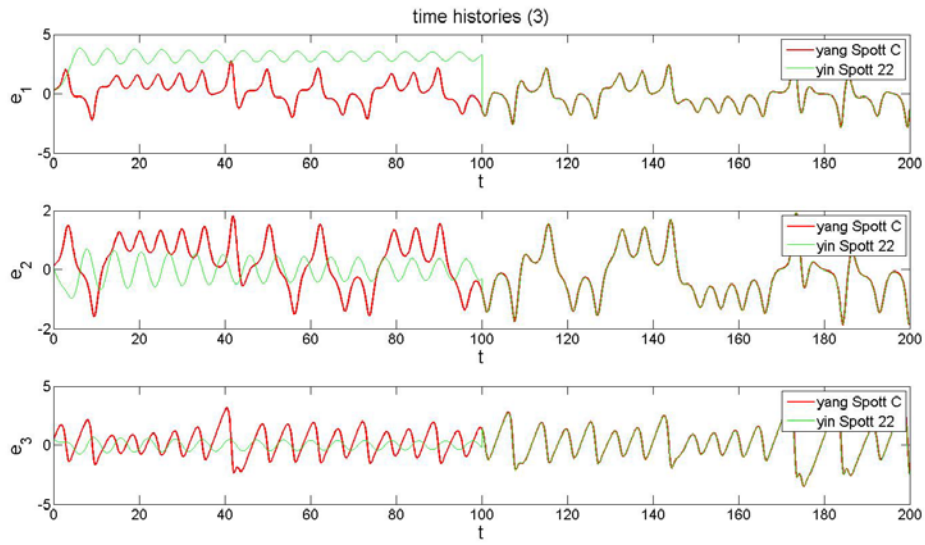


Fig. 5-9 Synchronization for Yin Sprott 22 system and Yang Sprott C system.

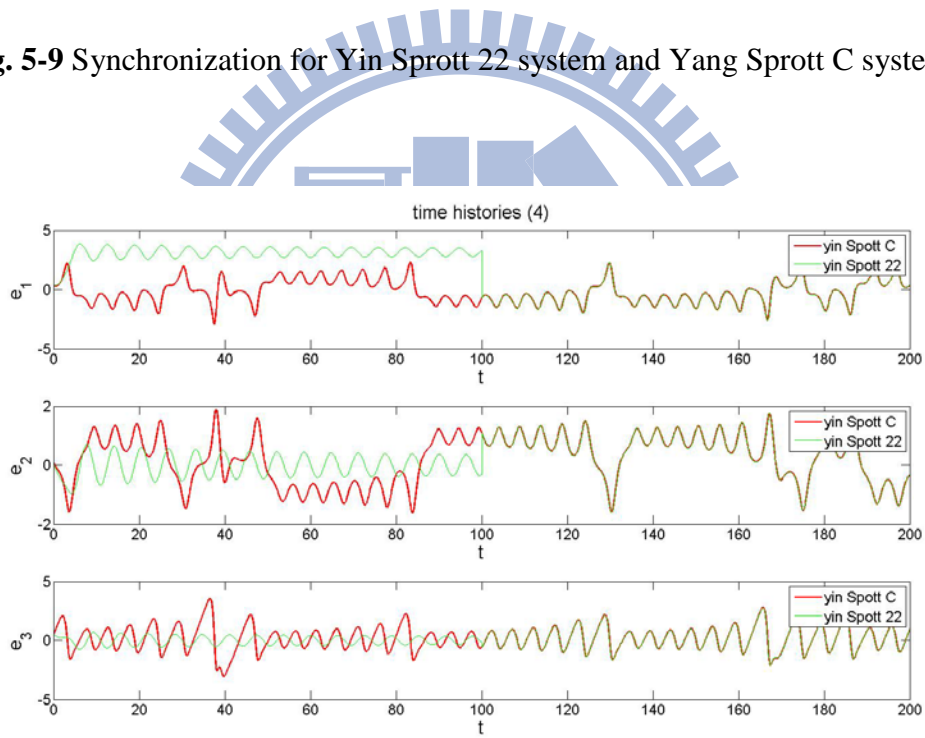


Fig. 5-10 Synchronization for Yin Sprott 22 system and Yin Sprott C system.

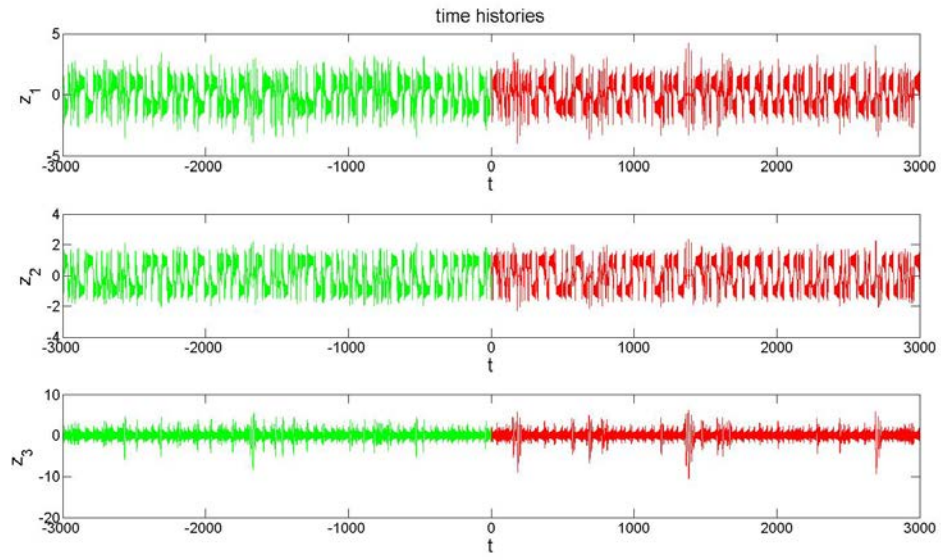
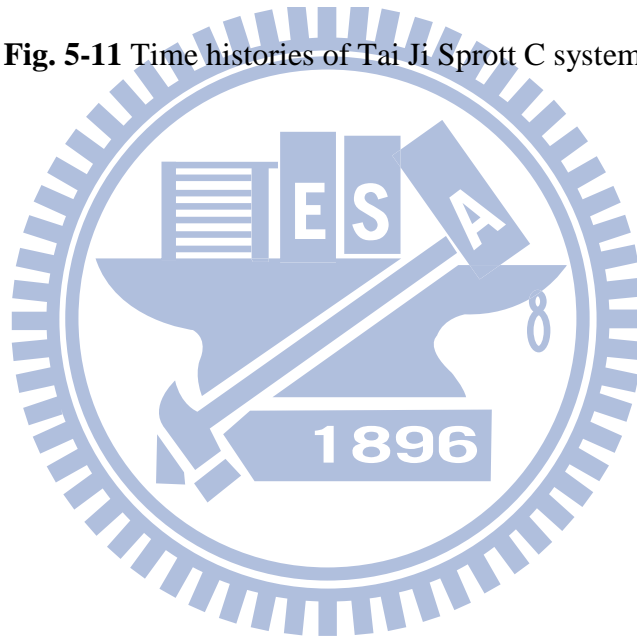


Fig. 5-11 Time histories of Tai Ji Sprott C system.



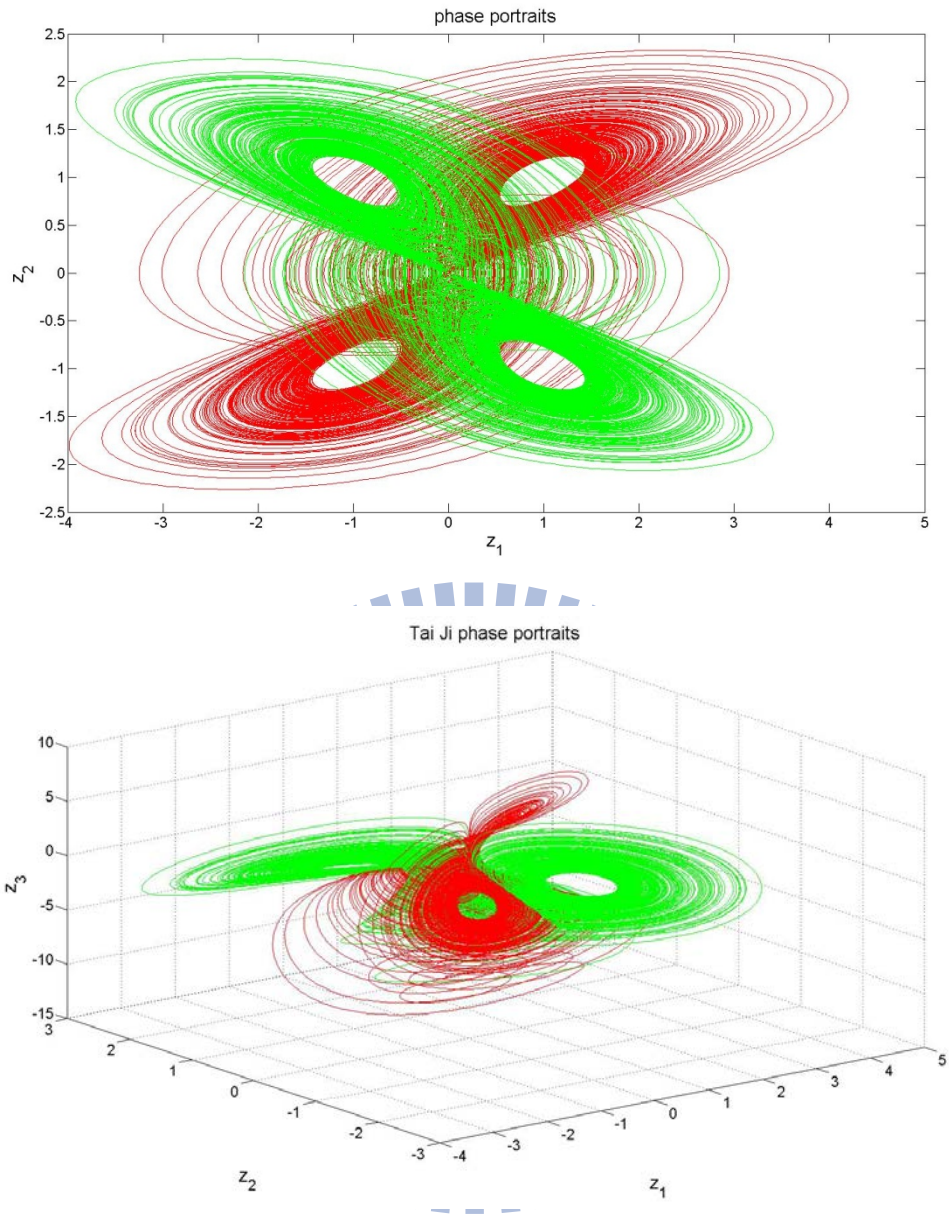


Fig. 5-12 Phase portraits of Tai Ji Sprott C system.

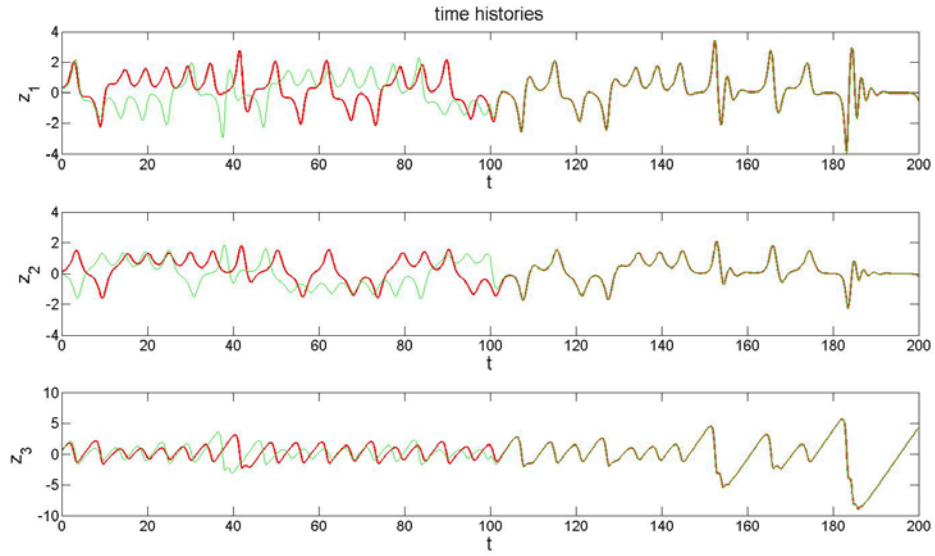


Fig. 5-13 Synchronization for Yang Sprott C system and Yin Sprott C system.

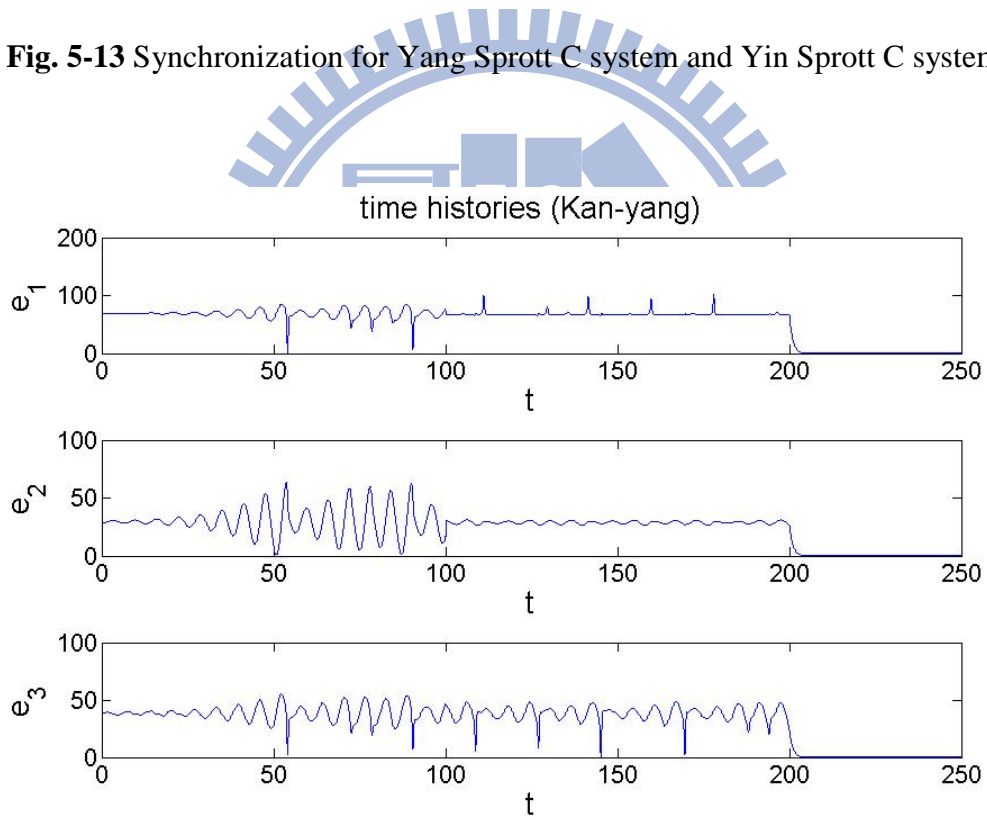


Fig. 5-14 Time histories of Yang error function for Kan trigram.

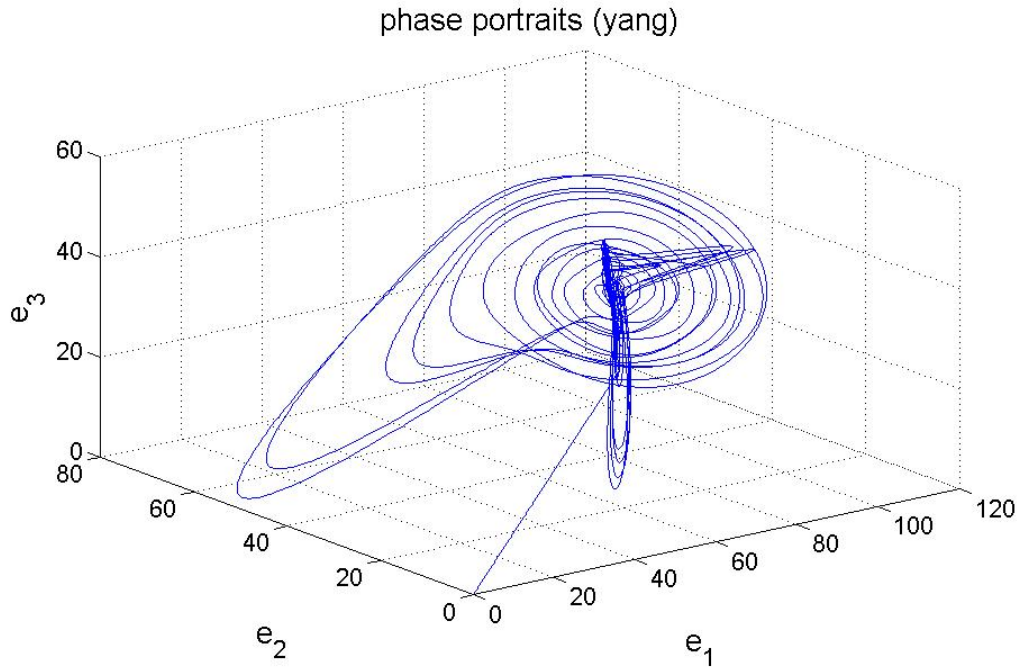


Fig. 5-15 Phase portraits of Yang error function for Kan trigram.

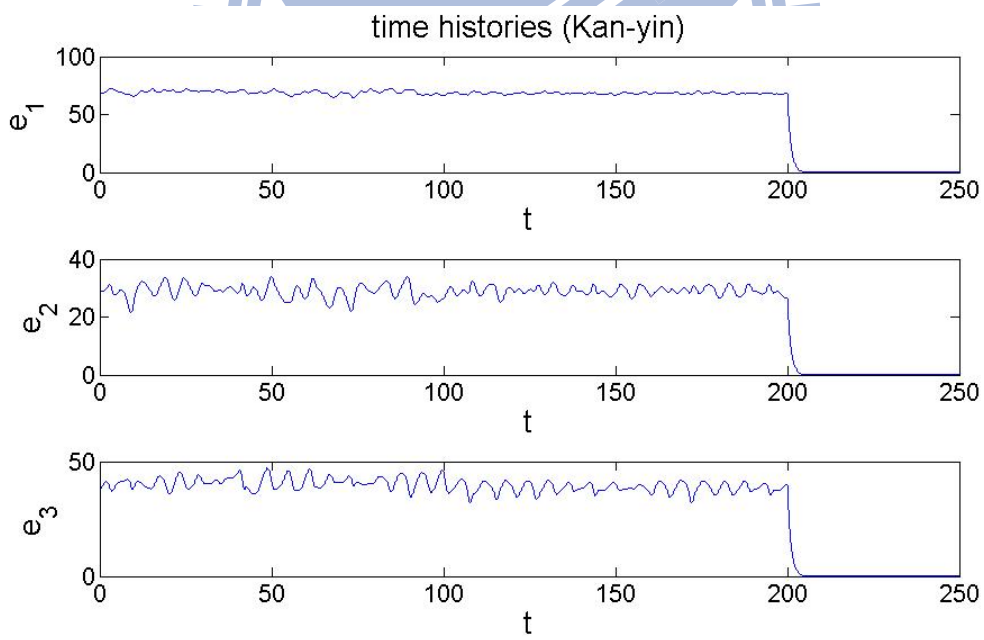


Fig. 5-16 Time histories of Yin error function for Kan trigram.

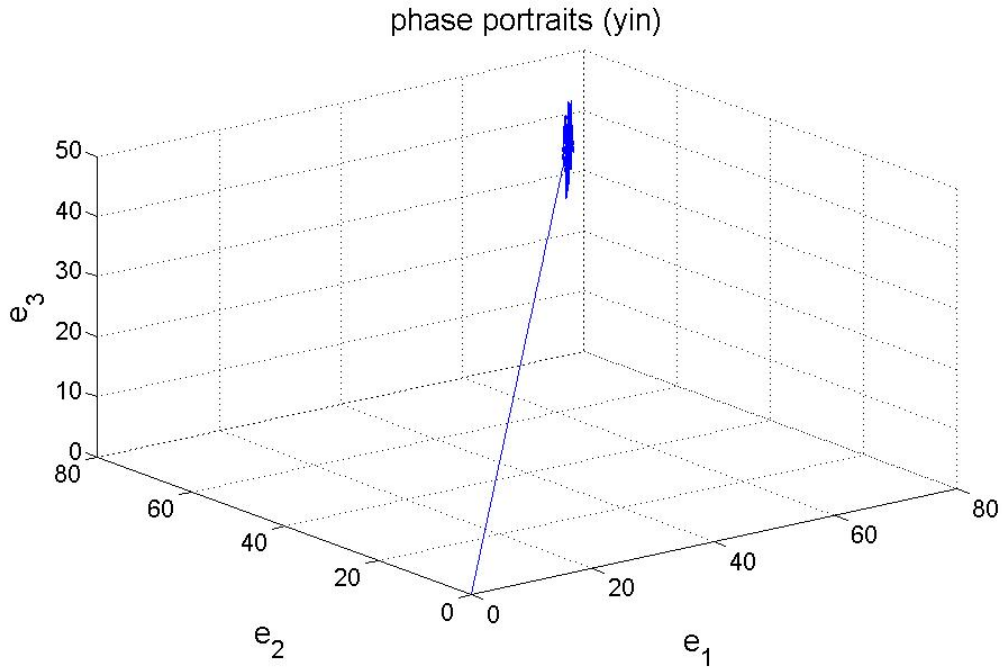


Fig. 5-17 Phase portraits of Yin error function for Kan trigram.

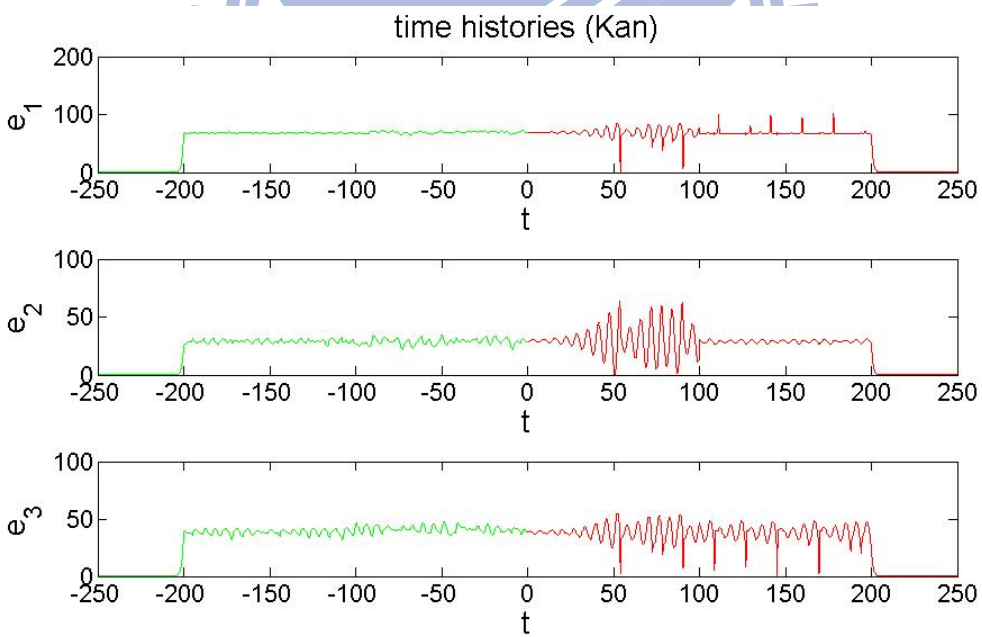


Fig. 5-18 Time histories of error function e for Kan trigram.

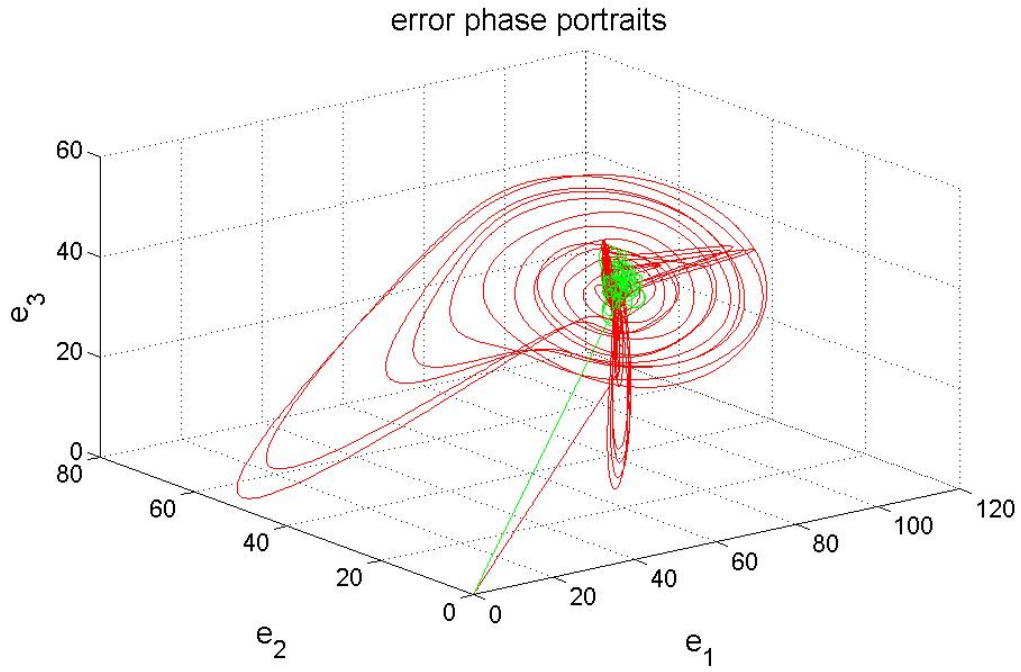


Fig. 5-19 Phase portraits of error function e for Kan trigram.

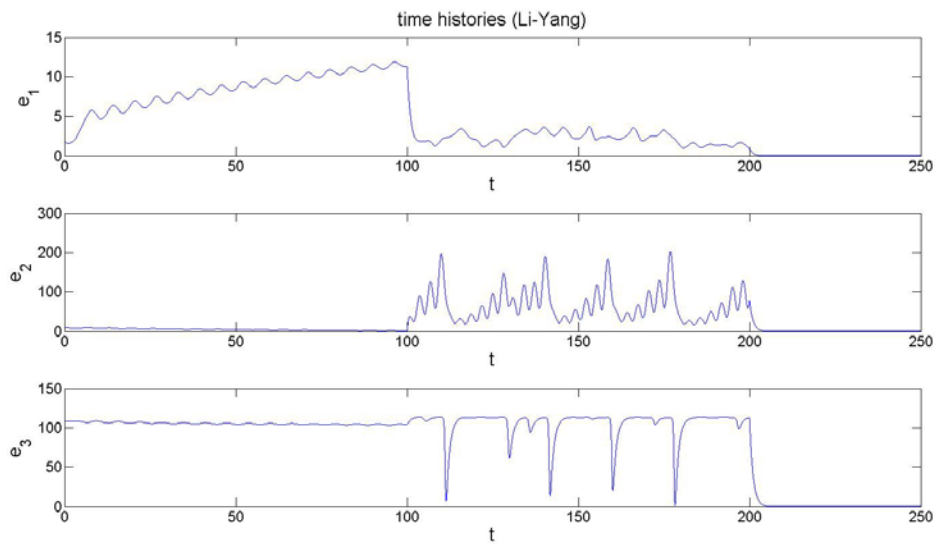


Fig. 5-20 Time histories of Yang error function for Li trigram.

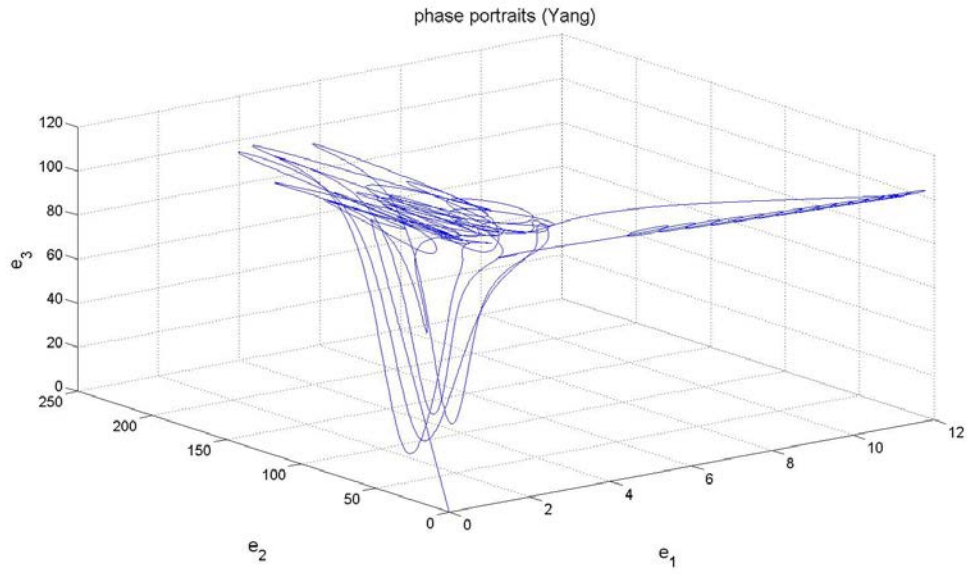


Fig. 5-21 Phase portraits of Yang error function for Li trigram.

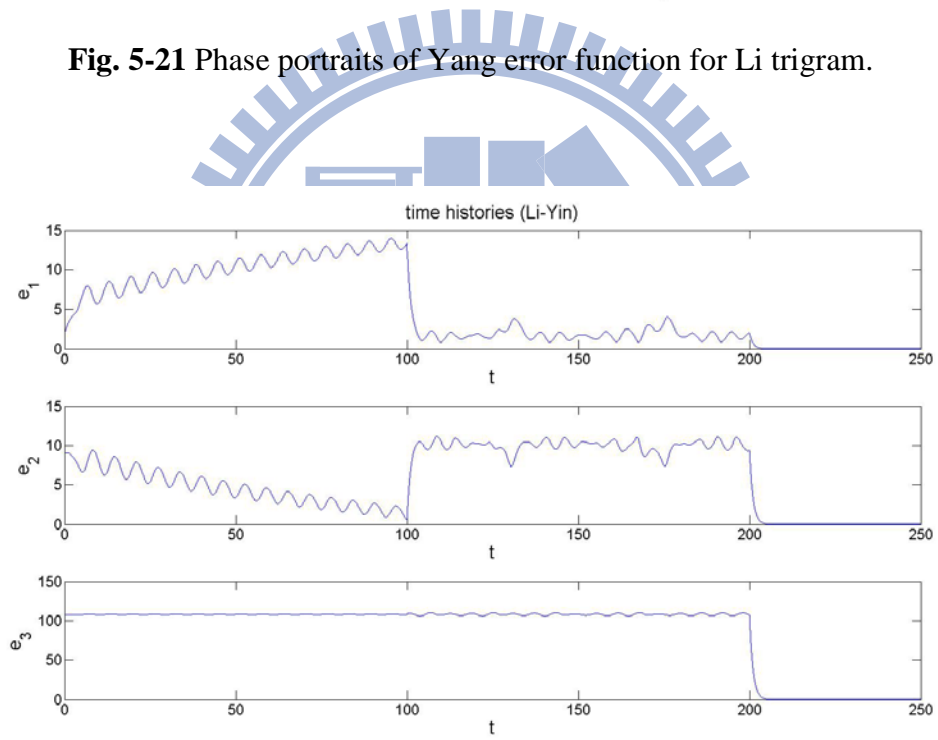


Fig. 5-22 Time histories of Yin error function for Li trigram.

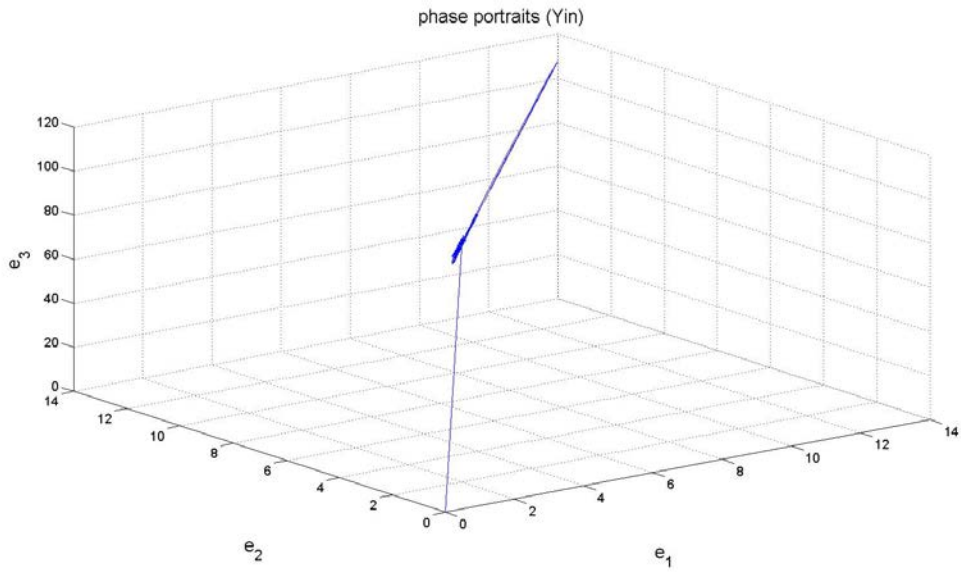


Fig. 5-23 Phase portraits of Yin error function for Li trigram.

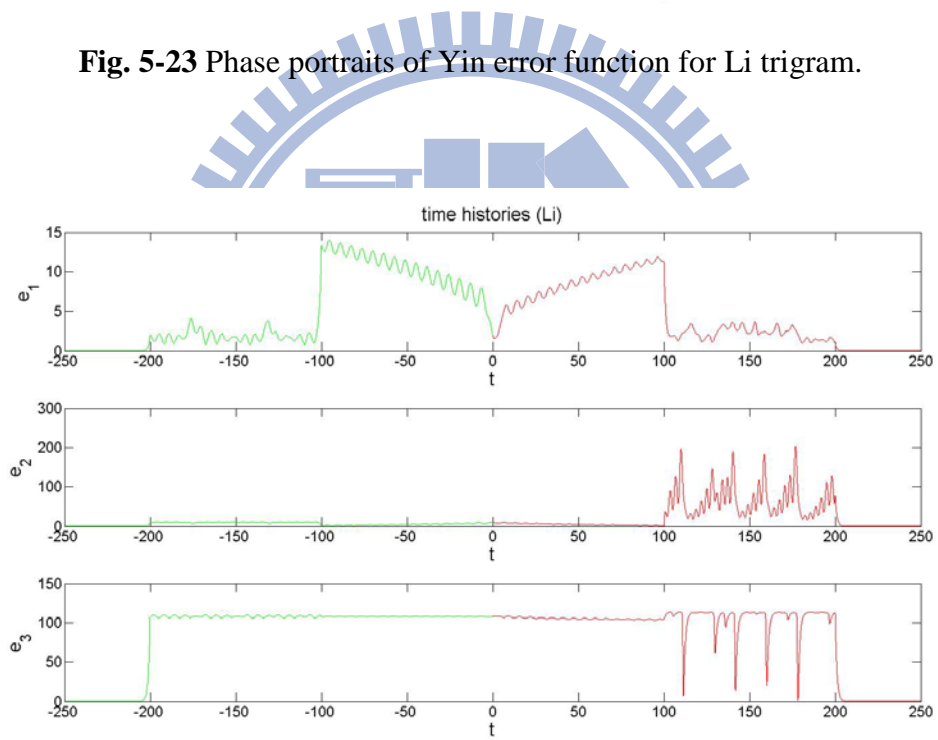


Fig. 5-24 Time histories of error function e for Li trigram.

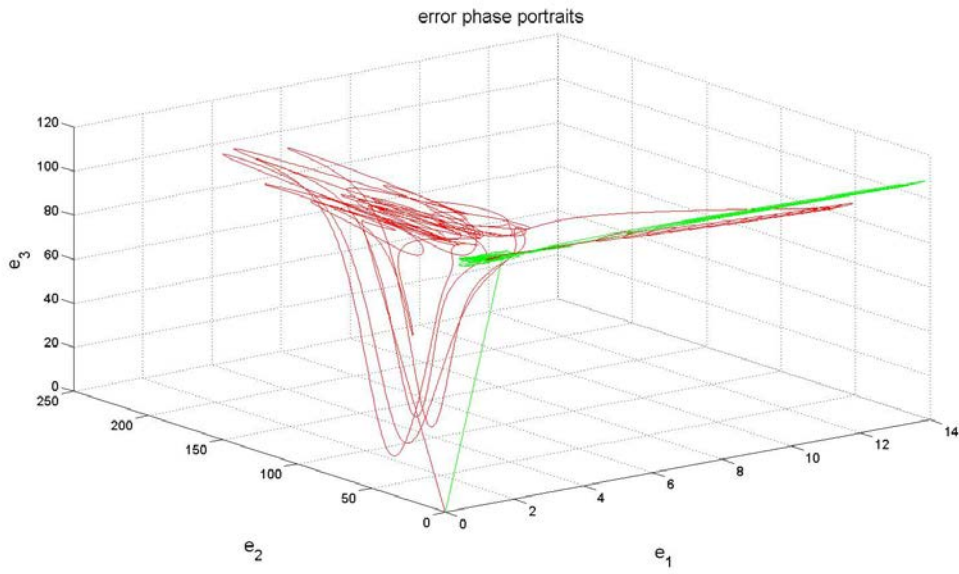
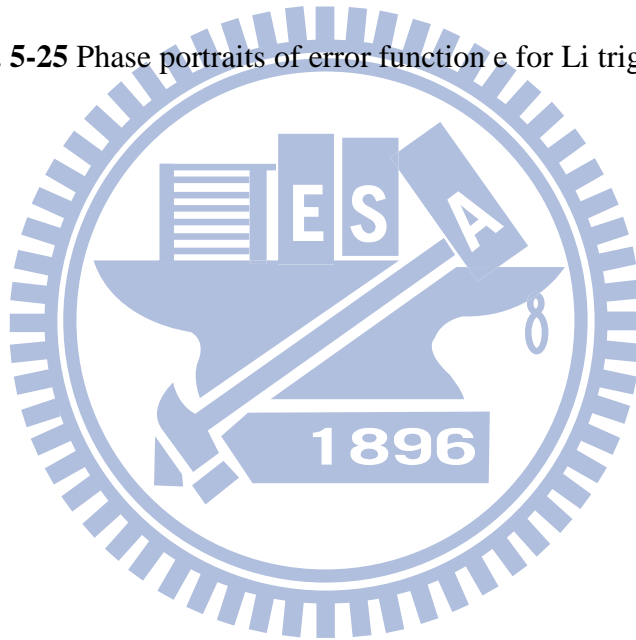


Fig. 5-25 Phase portraits of error function e for Li trigram.



Chapter 6

Kan-Li Hexagram Multiple Symplectic Derivative Synchronization by Partial Region Stability Theory

6-1. Preliminary

Hexagram, a part of Chinese philosophy, is advance of the eight trigram. It has two parts, upper and low. The two parts of Kan-Li hexagram both represent a trigram, Kan trigram and Li trigram, and they are used to complete a multiple symplectic derivative synchronization by three way, GYC partial region stability theory, Lyapunov function, and linear feedback method. At last, the efficiency of convergence for the three ways are compared.

This chapter is presented as follows. In Section 2, systems used in this chapter are shown and the Yang (normal) and Yin (historical) systems for Rössler System, Spott 22 system, and Spott C system are synchronized. In Section 3, the Kan-Li hexagram multiple symplectic derivative synchronization is presented by GYC partial region stability theory. In Section 4, the Kan-Li hexagram synchronization is proposed by traditional Lyapunov function. In Section 5, the Kan-Li hexagram synchronization is proposed by linear feedback method. In Section 6, the comparison of three synchronization ways is presented. In Section 7, summary is drawn.

6-2. Systems of Kan-Li hexagram synchronization

The Yang Rössler system is

$$\begin{cases} \dot{x}_1 = -x_2 - x_3 \\ \dot{x}_2 = x_1 + a_{11}x_2 \\ \dot{x}_3 = b_{11} + x_3(x_1 - c_{11}) \end{cases} \quad (6-1)$$

and the Yin Rössler system is

$$\begin{cases} \dot{x}_4 = x_5 + x_6 \\ \dot{x}_5 = -x_4 - a_{12}x_5 \\ \dot{x}_6 = -b_{12} - x_6(x_4 - c_{12}) \end{cases} \quad (6-2)$$

where $a_{11}=0.15$, $b_{11}=0.2$, $c_{11}=10$, $a_{12}=-0.15$, $b_{12}=-0.2$, $c_{12}=-10$ and the initial condition are $x_{10}=0.3$, $x_{20}=0.1$, $x_{30}=0.5$, $x_{40}=0.3$, $x_{50}=0.1$, $x_{60}=0.5$.

Set the Yin Rössler system be

$$\begin{cases} \dot{x}_4 = x_5 + x_6 & + k(x_1 - x_4) \\ \dot{x}_5 = -x_4 - a_{12}x_5 & + k(x_2 - x_5) \\ \dot{x}_6 = -b_{12} - x_6(x_4 - c_{12}) & + k(x_3 - x_6) \end{cases} \quad (6-3)$$

where x_1 , x_2 , and x_3 are states of Eq. (6-1), k is a positive constant, 100.

The Yang Spott 22 system is

$$\begin{cases} \dot{y}_1 = y_2 \\ \dot{y}_2 = y_3 \\ \dot{y}_3 = -a_{21}y_3 - y_2 - \sin y_1 \end{cases} \quad (6-4)$$

and the Yin Spott 22 system is

$$\begin{cases} \dot{y}_4 = -y_5 \\ \dot{y}_5 = -y_6 \\ \dot{y}_6 = a_{22}y_6 + y_5 + \sin y_4 \end{cases} \quad (6-5)$$

where $a_{21}=0.25$, $a_{22}=-0.25$ and the initial condition are $y_{10}=0.3$, $y_{20}=0.1$, $y_{30}=0.5$, $y_{40}=0.3$, $y_{50}=0.1$, $y_{60}=0.5$.

There are four types of linear feedback synchronizations of Spott 22 system for Li trigram synchronization.

(1) Set the Yang Spott 22 system be

$$\begin{cases} \dot{y}_{11} = y_{12} & + k(x_1 - y_{11}) \\ \dot{y}_{12} = y_{13} & + k(x_2 - y_{12}) \\ \dot{y}_{13} = -a_{21}y_{13} - y_{12} - \sin y_{11} & + k(x_3 - y_{13}) \end{cases} \quad (6-6)$$

where x_1 , x_2 , and x_3 are states of Eq. (6-1), k is a positive constant, 100.

(2) Set the Yang Spott 22 system be

$$\begin{cases} \dot{y}_{21} = y_{22} & + k(x_4 - y_{21}) \\ \dot{y}_{22} = y_{23} & + k(x_5 - y_{22}) \\ \dot{y}_{23} = -a_{21}y_{23} - y_{22} - \sin y_{21} & + k(x_6 - y_{23}) \end{cases} \quad (6-7)$$

where x_4 , x_5 , and x_6 are states of Eq. (6-2), k is a positive constant, 100.

(3) Set the Yin Spott 22 system be

$$\begin{cases} \dot{y}_{14} = -y_{15} & + k(z_1 - y_{14}) \\ \dot{y}_{15} = -y_{16} & + k(z_2 - y_{15}) \\ \dot{y}_{16} = a_{22}y_{16} + y_{15} + \sin y_{14} & + k(z_3 - y_{16}) \end{cases} \quad (6-8)$$

where z_1 , z_2 , and z_3 are states of Eq (6-10), k is a positive constant, 100.

(4) Set the Yin Spott 22 system be

$$\begin{cases} \dot{y}_{24} = -y_{25} & + k(z_4 - y_{24}) \\ \dot{y}_{25} = -y_{26} & + k(z_5 - y_{25}) \\ \dot{y}_{26} = a_{22}y_{26} + y_{25} + \sin y_{24} & + k(z_6 - y_{26}) \end{cases} \quad (6-9)$$

where z_4 , z_5 , and z_6 are states of Eq. (6-11), k is a positive constant, 100.

The Yang Spott C system is

$$\begin{cases} \dot{z}_1 = z_2 z_3 \\ \dot{z}_2 = z_1 - a_{31} z_2 \\ \dot{z}_3 = b_{31} - c_{31} z_1^2 \end{cases} \quad (6-10)$$

and the Yin Spott C system is

$$\begin{cases} \dot{z}_4 = -z_5 z_6 \\ \dot{z}_5 = -z_4 + a_{32} z_5 \\ \dot{z}_6 = -b_{32} + c_{32} z_4^2 \end{cases} \quad (6-11)$$

where $a_{31}=1$, $b_{31}=1$, $c_{31}=1$, $a_{32}=-1$, $b_{32}=-1$, $c_{32}=-1$ and the initial condition are $z_{10}=0.3$, $z_{20}=0.1$, $z_{30}=0.5$, $z_{40}=0.3$, $z_{50}=0.1$, $z_{60}=0.5$.

Set the Yang Spott C system be

$$\begin{cases} \dot{z}_1 = z_2 z_3 & + k(z_4 - z_1) \\ \dot{z}_2 = z_1 - a_{31} z_2 & + k(z_5 - z_2) \\ \dot{z}_3 = b_{31} - c_{31} z_1^2 & + k(z_6 - z_3) \end{cases} \quad (6-12)$$

where z_4 , z_5 , and z_6 are states of Eq. (6-11), k is a positive constant, 100.

6-3. Kan-Li hexagram synchronization by GYC partial region stability theory

Define

$$G_1(x, \dot{x}, y, \dot{y}, z, \dot{z}, t) = G_1(\text{Kan}) - F_1(\text{Kan}) = \begin{bmatrix} (y_1 + \cos y_2 - \dot{x}_4) - (x_5 + y_1 + \cos \dot{y}_1 + x_6) \\ (y_2 + \sin y_3 + \dot{x}_5) - (x_4 + \dot{y}_1 + \sin \dot{y}_2) \\ (y_3 + \sin y_2 - \dot{x}_4 - x_5) - (x_6 + \dot{y}_2) \end{bmatrix}, \quad (6-13)$$

where $G_1(\text{Kan})$ is Eq. (5-13), and $F_1(\text{Kan})$ is Eq. (5-14).

$$F_1(x, \dot{x}, y, \dot{y}, z, \dot{z}, t) = G_1(\text{Li}) - F_1(\text{Li}) = \begin{bmatrix} (y_{14} + y_{15}y_{16} - y_{11}\dot{y}_{11} - y_{11}y_{13}) - (y_{11}y_{12} + \dot{y}_{14} + \dot{y}_{15}) \\ (y_{15} + y_{16}y_{14} - y_{12}\dot{y}_{11}) - (y_{12}y_{13} - \dot{y}_{15} + \dot{y}_{15}y_{16} + y_{15}y_{16}) \\ (y_{15} + y_{16}y_{14} - y_{12}\dot{y}_{11}) - (y_{11}y_{13} + y_{15}^2 + y_{15}\dot{y}_{15}) \end{bmatrix}, \quad (6-14)$$

where $G_1(\text{Li})$ is Eq. (5-23), and $F_1(\text{Li})$ is Eq. (5-24).

Our purpose is to achieve the multiple symplectic derivative synchronization

$$G_1(x, \dot{x}, y, \dot{y}, z, \dot{z}, t) = F_1(x, \dot{x}, y, \dot{y}, z, \dot{z}, t) - K.$$

The state error is $e = G - F + K$ where $K = [83, 196, 43]^T$ such that error dynamics always exists in first quadrant.

$$e_{1i} = G_{1i} - F_{1i} + K_i \quad i = 1, 2, 3.$$

Our purpose is $\lim_{t \rightarrow \infty} e = 0$. We obtain the error dynamics:

$$\lim_{t \rightarrow \infty} \dot{e}_{1i} = \dot{G}_{1i} - \dot{F}_{1i} - u_{1i} \quad i = 1, 2, 3.$$

By partial region stability theory, we can choose a Lyapunov function in the form of a positive definite function in first quadrant:

$$V_1(e_1) = e_{11} + e_{12} + e_{13} \quad (6-15)$$

Its time derivative is

$$\dot{V}_1(e_1) = (\dot{G}_{11} - \dot{F}_{11} - u_{11}) + (\dot{G}_{12} - \dot{F}_{12} - u_{12}) + (\dot{G}_{13} - \dot{F}_{13} - u_{13})$$

We want to find u_1 such that \dot{V}_1 satisfies

$$\dot{V}_1(e_1) = -e_{11} - e_{12} - e_{13} < 0 \quad (6-16)$$

Choose the controller u_1 as

$$u_1 = \begin{bmatrix} u_{11} \\ u_{12} \\ u_{13} \end{bmatrix} = \begin{bmatrix} e_{11} + (y_2) - (\dot{y}_{15}) \\ e_{12} + (-0.15\dot{x}_5) - (2y_{12}\dot{y}_{12}) \\ e_{13} + (y_2\cos y_1) - (-10\dot{y}_{13}) \end{bmatrix} \quad (6-17)$$

which is negative definite function in first quadrant. Error states versus time and their time histories are shown in Fig. 6-1.

Define

$$G_2(x, \dot{x}, y, \dot{y}, z, \dot{z}, t) = G_2(\text{Kan}) - F_2(\text{Kan}) = \begin{bmatrix} (z_1 + z_2 - \dot{y}_5) - (y_6 + \cos y_4 - \dot{z}_2) \\ (z_2 + \dot{z}_2 + \cos \dot{y}_4) - (-y_5 + \cos y_5 - z_1) \\ (z_3 + y_4 + \cos \dot{y}_5) - (-\dot{z}_1/z_2 + \cos y_6) \end{bmatrix}, \quad (6-18)$$

where $G_2(\text{Kan})$ is Eq. (5-18), and $F_2(\text{Kan})$ is Eq. (5-19).

$$F_2(x, \dot{x}, y, \dot{y}, z, \dot{z}, t) = G_2(\text{Li}) - F_2(\text{Li}) = \begin{bmatrix} (y_{24} - y_{23} + y_{21}\dot{y}_{21} - y_{21}y_{23}) - (y_{21}y_{22} - \dot{y}_{25} - \dot{y}_{21} + y_{22}) \\ (y_{25} - y_{25} + \dot{y}_{21}y_{23} - y_{22}^2) - (y_{22}y_{23} - \dot{y}_{25} - \dot{y}_{21} + y_{23}) \\ (y_{26} - y_{21} - 10y_{23} - \dot{y}_{23}) - (y_{21}y_{23} - \dot{y}_{24}/y_{25} + \dot{y}_{22}) \end{bmatrix}, \quad (6-19)$$

where $G_2(\text{Li})$ is Eq. (5-28), and $F_2(\text{Li})$ is Eq. (5-29).

Our purpose is to achieve the multiple symplectic derivative synchronization

$$G_2(x, \dot{x}, y, \dot{y}, z, \dot{z}, t) = F_2(x, \dot{x}, y, \dot{y}, z, \dot{z}, t) - K.$$

The state error is $e = G - F + K$ where $K = [83, 196, 43]^T$ such that error dynamics always exists in first quadrant.

$$e_{2i} = G_{2i} - F_{2i} + K_i \quad i = 1, 2, 3.$$

Our purpose is $\lim_{t \rightarrow \infty} e = 0$. We obtain the error dynamics:

$$\lim_{t \rightarrow \infty} \dot{e}_{2i} = \dot{G}_{2i} - \dot{F}_{2i} - u_{2i} \quad i = 1, 2, 3.$$

By partial region stability theory, we can choose a Lyapunov function in the form of a positive definite function in first quadrant:

$$V_2(e_2) = e_{21} + e_{22} + e_{23} \quad (6-20)$$

Its time derivative is

$$\dot{V}_2(e_2) = (\dot{G}_{21} - \dot{F}_{21} - u_{21}) + (\dot{G}_{22} - \dot{F}_{22} - u_{22}) + (\dot{G}_{23} - \dot{F}_{23} - u_{23})$$

We want to find u_2 such that \dot{V}_2 satisfies

$$\dot{V}_2(e_2) = -e_{21} - e_{22} - e_{23} < 0 \quad (6-21)$$

Choose the controller u as

$$u_2 = \begin{bmatrix} u_{21} \\ u_{22} \\ u_{23} \end{bmatrix} = \begin{bmatrix} e_{21} + (-y_5 \sin y_4) - (-\dot{y}_{25}) \\ e_{22} + (-y_6) - (-\dot{y}_{24}) \\ e_{23} + (-y_5) - (-0.15\dot{y}_{22}) \end{bmatrix} \quad (6-22)$$

which is negative definite function in first quadrant. Error states versus time and their time histories are shown in Fig. 6-2.

At last, e_1 and e_2 are the components of error states e . Error states versus time and their time histories are shown in Fig. 6-3.

6-4. Kan-Li hexagram synchronization by traditional Lyapunov function

Define

$$G_1(x, \dot{x}, y, \dot{y}, z, \dot{z}, t) = G_1(\text{Kan}) - F_1(\text{Kan}) = \begin{bmatrix} (y_1 + \cos y_2 - \dot{x}_4) - (x_5 + y_1 + \cos y_1 + x_6) \\ (y_2 + \sin y_3 + \dot{x}_5) - (x_4 + \dot{y}_1 + \sin y_2) \\ (y_3 + \sin y_2 - \dot{x}_4 - x_5) - (x_6 + \dot{y}_2) \end{bmatrix}, \quad (6-23)$$

where $G_1(\text{Kan})$ is Eq. (5-13), and $F_1(\text{Kan})$ is Eq. (5-14).

$$F_1(x, \dot{x}, y, \dot{y}, z, \dot{z}, t) = G_1(\text{Li}) - F_1(\text{Li}) = \begin{bmatrix} (y_{14} + y_{15}y_{16} - y_{11}\dot{y}_{11} - y_{11}y_{13}) - (y_{11}y_{12} + \dot{y}_{14} + \dot{y}_{15}) \\ (y_{15} + y_{16}y_{14} - y_{12}\dot{y}_{11}) - (y_{12}y_{13} - \dot{y}_{15} + \dot{y}_{15}y_{16} + y_{15}y_{16}) \\ (y_{15} + y_{16}y_{14} - y_{12}\dot{y}_{11}) - (y_{11}y_{13} + y_{15}^2 + y_{15}\dot{y}_{15}) \end{bmatrix}, \quad (6-24)$$

where $G_1(\text{Li})$ is Eq. (5-23), and $F_1(\text{Li})$ is Eq. (5-24).

Our purpose is to achieve the multiple symplectic derivative synchronization

$$G_1(x, \dot{x}, y, \dot{y}, z, \dot{z}, t) = F_1(x, \dot{x}, y, \dot{y}, z, \dot{z}, t) - K.$$

The state error is $e = G - F + K$ where $K = [83,196,43]^T$.

$$e_{1i} = G_{1i} - F_{1i} + K_i \quad i = 1, 2, 3.$$

Our purpose is $\lim_{t \rightarrow \infty} e = 0$. We obtain the error dynamics:

$$\lim_{t \rightarrow \infty} \dot{e}_{1i} = \dot{G}_{1i} - \dot{F}_{1i} - u_{1i} \quad i = 1, 2, 3.$$

We can choose a Lyapunov function in the form of a positive definite function:

$$V_1(e_1) = e_{11}^2 + e_{12}^2 + e_{13}^2 \quad (6-25)$$

Its time derivative is

$$\dot{V}_1(e_1) = (\dot{G}_{11} - \dot{F}_{11} - u_{11}) + (\dot{G}_{12} - \dot{F}_{12} - u_{12}) + (\dot{G}_{13} - \dot{F}_{13} - u_{13})$$

We want to find u_1 such that \dot{V}_1 satisfies

$$\dot{V}_1(e_1) = -e_{11}^2 - e_{12}^2 - e_{13}^2 < 0 \quad (6-26)$$

Choose the controller u_1 as

$$u_1 = \begin{bmatrix} u_{11} \\ u_{12} \\ u_{13} \end{bmatrix} = \begin{bmatrix} e_{11} + (y_2) - (\dot{y}_{15}) \\ e_{12} + (-0.15\dot{x}_5) - (2y_{12}\dot{y}_{12}) \\ e_{13} + (y_2 \cos y_1) - (-10\dot{y}_{13}) \end{bmatrix} \quad (6-27)$$

which is negative definite function. Error states versus time and their time histories are shown in Fig. 6-4.

Define

$$G_2(x, \dot{x}, y, \dot{y}, z, \dot{z}, t) = G_2(\text{Kan}) - F_2(\text{Kan}) = \begin{bmatrix} (z_1 + z_2 - \dot{y}_5) - (y_6 + \cos y_4 - \dot{z}_2) \\ (z_2 + \dot{z}_2 + \cos \dot{y}_4) - (-y_5 + \cos y_5 - z_1) \\ (z_3 + y_4 + \cos \dot{y}_5) - (-\dot{z}_1/z_2 + \cos y_6) \end{bmatrix}, \quad (6-28)$$

where $G_2(\text{Kan})$ is Eq. (5-18), and $F_2(\text{Kan})$ is Eq. (5-19).

$$F_2(x, \dot{x}, y, \dot{y}, z, \dot{z}, t) = G_2(\text{Li}) - F_2(\text{Li}) =$$

$$\begin{bmatrix} (y_{24} - y_{23} + y_{21}\dot{y}_{21} - y_{21}y_{23}) - (y_{21}y_{22} - \dot{y}_{25} - \dot{y}_{21} + y_{22}) \\ (y_{25} - y_{25} + \dot{y}_{21}y_{23} - y_{22}^2) - (y_{22}y_{23} - \dot{y}_{25} - \dot{y}_{21} + y_{23}) \\ (y_{26} - y_{21} - 10y_{23} - \dot{y}_{23}) - (y_{21}y_{23} - \dot{y}_{24}/y_{25} + \dot{y}_{22}) \end{bmatrix}, \quad (6-29)$$

where $G_2(\text{Li})$ is Eq. (5-28), and $F_2(\text{Li})$ is Eq. (5-29).

Our purpose is to achieve the multiple symplectic derivative synchronization

$$G_2(x, \dot{x}, y, \dot{y}, z, \dot{z}, t) = F_2(x, \dot{x}, y, \dot{y}, z, \dot{z}, t) - K.$$

The state error is $e = G - F + K$ where $K = [83, 196, 43]^T$.

$$e_{2i} = G_{2i} - F_{2i} + K_i \quad i = 1, 2, 3.$$

Our purpose is $\lim_{t \rightarrow \infty} e = 0$. We obtain the error dynamics:

$$\lim_{t \rightarrow \infty} \dot{e}_{2i} = \dot{G}_{2i} - \dot{F}_{2i} - u_{2i} \quad i = 1, 2, 3.$$

We can choose a Lyapunov function in the form of a positive definite function:

$$V_2(e_2) = e_{21}^2 + e_{22}^2 + e_{23}^2 \quad (6-30)$$

Its time derivative is

$$\dot{V}_2(e_2) = (\dot{G}_{21} - \dot{F}_{21} - u_{21}) + (\dot{G}_{22} - \dot{F}_{22} - u_{22}) + (\dot{G}_{23} - \dot{F}_{23} - u_{23})$$

We want to find u_2 such that \dot{V}_2 satisfies

$$\dot{V}_2(e_2) = -e_{21}^2 - e_{22}^2 - e_{23}^2 < 0 \quad (6-31)$$

Choose the controller u as

$$u_2 = \begin{bmatrix} u_{21} \\ u_{22} \\ u_{23} \end{bmatrix} = \begin{bmatrix} e_{21} + (-y_5 \sin y_4) - (-\dot{y}_{25}) \\ e_{22} + (-y_6) - (-\dot{y}_{24}) \\ e_{23} + (-y_5) - (-0.15\dot{y}_{22}) \end{bmatrix} \quad (6-32)$$

which is negative definite function in first quadrant. Error states versus time and their time histories are shown in Fig. 6-5.

At last, e_1 and e_2 are the components of error states e . Error states versus time and their time histories are shown in Fig. 6-6.

6-5. Kan-Li hexagram synchronization by linear feedback method

Define

$$G_1(x, \dot{x}, y, \dot{y}, z, \dot{z}, t) = G_1(\text{Kan}) - F_1(\text{Kan}) = \begin{bmatrix} (y_1 + \cos y_2 - \dot{x}_4) - (x_5 + y_1 + \cos \dot{y}_1 + x_6) \\ (y_2 + \sin y_3 + \dot{x}_5) - (x_4 + \dot{y}_1 + \sin \dot{y}_2) \\ (y_3 + \sin y_2 - \dot{x}_4 - x_5) - (x_6 + \dot{y}_2) \end{bmatrix}, \quad (6-33)$$

where $G_1(\text{Kan})$ is Eq. (5-13), and $F_1(\text{Kan})$ is Eq. (5-14).

$$F_1(x, \dot{x}, y, \dot{y}, z, \dot{z}, t) = G_1(\text{Li}) - F_1(\text{Li}) = \begin{bmatrix} (y_{14} + y_{15}y_{16} - y_{11}\dot{y}_{11} - y_{11}y_{13}) - (y_{11}y_{12} + \dot{y}_{14} + \dot{y}_{15}) \\ (y_{15} + y_{16}y_{14} - y_{12}\dot{y}_{11}) - (y_{12}y_{13} - \dot{y}_{15} + \dot{y}_{15}y_{16} + y_{15}y_{16}) \\ (y_{15} + y_{16}y_{14} - y_{12}\dot{y}_{11}) - (y_{11}y_{13} + y_{15}^2 + y_{15}\dot{y}_{15}) \end{bmatrix}, \quad (6-34)$$

where $G_1(\text{Li})$ is Eq. (5-23), and $F_1(\text{Li})$ is Eq. (5-24).

Our purpose is to achieve the multiple symplectic derivative synchronization

$$G_1(x, \dot{x}, y, \dot{y}, z, \dot{z}, t) = F_1(x, \dot{x}, y, \dot{y}, z, \dot{z}, t)$$

The state error is $e = G - F$.

$$e_{1i} = G_{1i} - F_{1i} \quad i = 1, 2, 3.$$

Our purpose is $\lim_{t \rightarrow \infty} e_{1i} = 0$.

By linear feedback method, set that

$$\dot{G}_{1i} = \dot{F}_{1i} + K(G_{1i} - F_{1i}) \quad i = 1, 2, 3. \quad (6-35)$$

where K is a positive constant, 100.

Error states versus time and their time histories are shown in Fig. 6-7.

Define

$$G_2(x, \dot{x}, y, \dot{y}, z, \dot{z}, t) = G_2(\text{Kan}) - F_2(\text{Kan}) = \begin{bmatrix} (z_1 + z_2 - \dot{y}_5) - (y_6 + \cos y_4 - \dot{z}_2) \\ (z_2 + \dot{z}_2 + \cos \dot{y}_4) - (-y_5 + \cos y_5 - z_1) \\ (z_3 + y_4 + \cos \dot{y}_5) - (-\dot{z}_1/z_2 + \cos y_6) \end{bmatrix}, \quad (6-36)$$

where $G_2(\text{Kan})$ is Eq. 5-18, and $F_2(\text{Kan})$ is Eq. 5-19.

$$F_2(x, \dot{x}, y, \dot{y}, z, \dot{z}, t) = G_2(\text{Li}) - F_2(\text{Li}) =$$

$$\begin{bmatrix} (y_{24} - y_{23} + y_{21}\dot{y}_{21} - y_{21}y_{23}) - (y_{21}y_{22} - \dot{y}_{25} - \dot{y}_{21} + y_{22}) \\ (y_{25} - y_{25} + \dot{y}_{21}y_{23} - y_{22}^2) - (y_{22}y_{23} - \dot{y}_{25} - \dot{y}_{21} + y_{23}) \\ (y_{26} - y_{21} - 10y_{23} - \dot{y}_{23}) - (y_{21}y_{23} - \dot{y}_{24}/y_{25} + \dot{y}_{22}) \end{bmatrix}, \quad (6-37)$$

where $G_2(Li)$ is Eq. 5-28, and $F_2(Li)$ is Eq. 5- 29.

Our purpose is to achieve the multiple symplectic derivative synchronization

$$G_2(x, \dot{x}, y, \dot{y}, z, \dot{z}, t) = F_2(x, \dot{x}, y, \dot{y}, z, \dot{z}, t).$$

The state error is $e = G - F$.

$$e_{2i} = G_{2i} - F_{2i} \quad i = 1, 2, 3.$$

Our purpose is $\lim_{t \rightarrow \infty} e_{2i} = 0$.

By linear feedback method, set that

$$\dot{G}_{2i} = \dot{F}_{2i} + K(G_{2i} - F_{2i}) \quad i = 1, 2, 3. \quad (6-38)$$

where K is a positive constant, 100.

Error states versus time and their time histories are shown in Fig. 6-8.

At last, e_1 and e_2 are the components of error states e . Error states versus time and their time histories are shown in Fig. 6-9.

6-6. Comparison of synchronization ways

From the previous sections, we know that the synchronization way of the above three method are different. Tables and Figures (Fig. 6-10 ~ Fig. 6-12) for comparing the efficiency of convergence are given as follows. The superiority of new strategy is obvious. The error states of linear feedback method are most poor and of new strategy are much smaller and decay more quickly than that of traditional method.

Table 6-1 the value ($\times 10^{-4}$) of error dynamics at second 315 ~ 325 for new strategy.

t	Yang			Yin		
	e_1	e_2	e_3	e_1	e_2	e_3
315	0.01196	0.5917	0.07280	0.01196	0.5917	0.03737
316	0.00440	0.2177	0.02678	0.00440	0.2177	0.01375
317	0.00162	0.0801	0.00985	0.00162	0.0801	0.00506
318	0.00060	0.0295	0.00362	0.00060	0.0295	0.00186
319	0.00022	0.0108	0.00133	0.00022	0.0108	0.00068
320	0.00008	0.0040	0.00049	0.00008	0.0040	0.00025
321	0.00003	0.0015	0.00018	0.00003	0.0015	0.00009
322	0.00001	0.0005	0.00007	0.00001	0.0005	0.00003
323	0.00000	0.0002	0.00002	0.00000	0.0002	0.00001
324	0.0000	0.0001	0.00001	0.0000	0.0001	0.00000
325	0.0000	0.0000	0.00000	0.0000	0.0000	0.00000

Table 6-2 the value of error dynamics at second 315 ~ 325 for traditional Lyapunov function.

t	Yang			Yin		
	e_1	e_2	e_3	e_1	e_2	e_3
315	0.0022	0.1064	0.0131	0.0025	0.1506	0.0067
316	0.0013	0.0646	0.0079	0.0015	0.0913	0.0041
317	0.0008	0.0392	0.0048	0.0009	0.0554	0.0025
318	0.0005	0.0238	0.0029	0.0006	0.0336	0.0015
319	0.0003	0.0144	0.0018	0.0003	0.0204	0.0009
320	0.0002	0.0087	0.0011	0.0002	0.0124	0.0006
321	0.0001	0.0053	0.0007	0.0001	0.0075	0.0003
322	0.0001	0.0032	0.0004	0.0001	0.0045	0.0002
323	0.0000	0.0019	0.0002	0.0000	0.0028	0.0001
324	0.0000	0.0012	0.0001	0.0000	0.0017	0.0001
325	0.0000	0.0007	0.0001	0.0000	0.0010	0.0000

Table 6-3 the value of error dynamics at second 315 ~ 325 for linear feedback method.

t	Yang			Yin		
	e_1	e_1	e_2	e_3	e_2	e_3
315	-0.0025	-0.2797	0.0033	0.0025	0.0009	0.0052
316	-0.0015	0.0631	0.0023	0.0008	0.0014	0.0010
317	0.0049	0.2410	-0.0000	-0.0002	0.0005	-0.0047
318	0.0021	-0.4044	-0.0074	-0.0010	0.0013	-0.0067
319	0.0004	-0.0410	0.0009	-0.0039	0.0086	-0.0025
320	0.0016	0.4661	0.0013	-0.0039	-0.0121	0.0047
321	0.0041	-0.5133	0.0083	0.0089	-0.0086	0.0083
322	0.0010	-0.2801	-0.0013	0.0032	0.0072	0.0043
323	-0.0034	0.7818	0.0107	-0.0026	0.0038	-0.0044
324	-0.0023	-0.5340	0.3319	-0.0016	-0.0013	-0.0101
325	-0.0008	-0.3440	-0.0655	-0.0002	-0.0012	-0.0069

6-7. Summary

In this chapter, hexagram, advance of the eight trigrams, is first studied with chaotic system. Kan-Li hexagram synchronization is combination of Kan trigram synchronization and Li trigram synchronization. The error dynamics have three stages. Firstly, in 0 ~ 150 sec. no control is applied. And then, the synchronization of Yang and Yin system appears in second 151 ~ 300. Finally, after second 301, error dynamics achieve synchronization. At last, the comparison of section 6 proves again that synchronization by GYC theory is much better than other synchronization way.

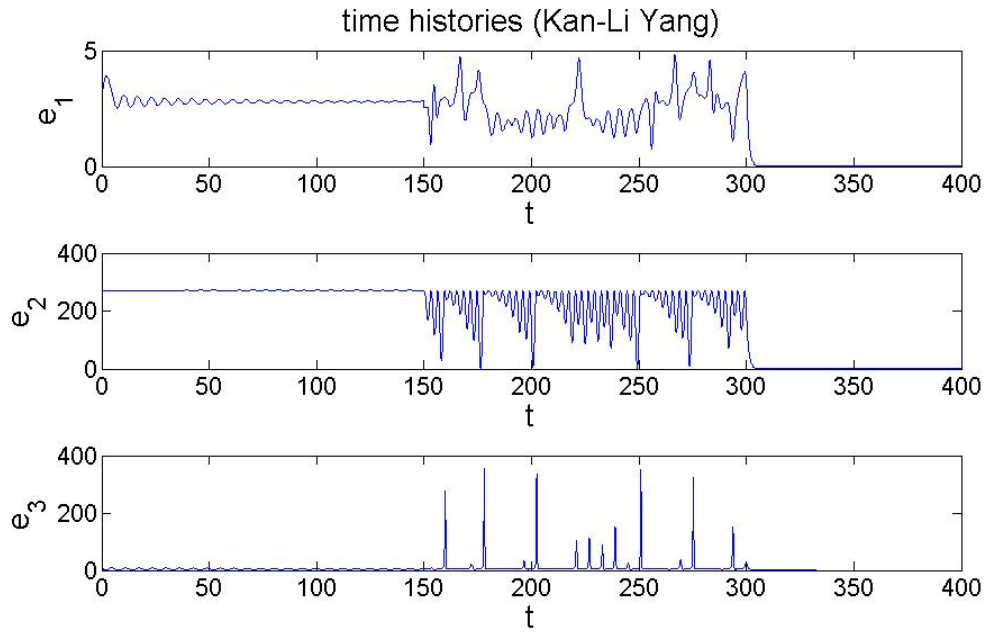


Fig. 6-1 Time histories of Yang error function for Kan-Li hexagram synchronization by GYC theory.

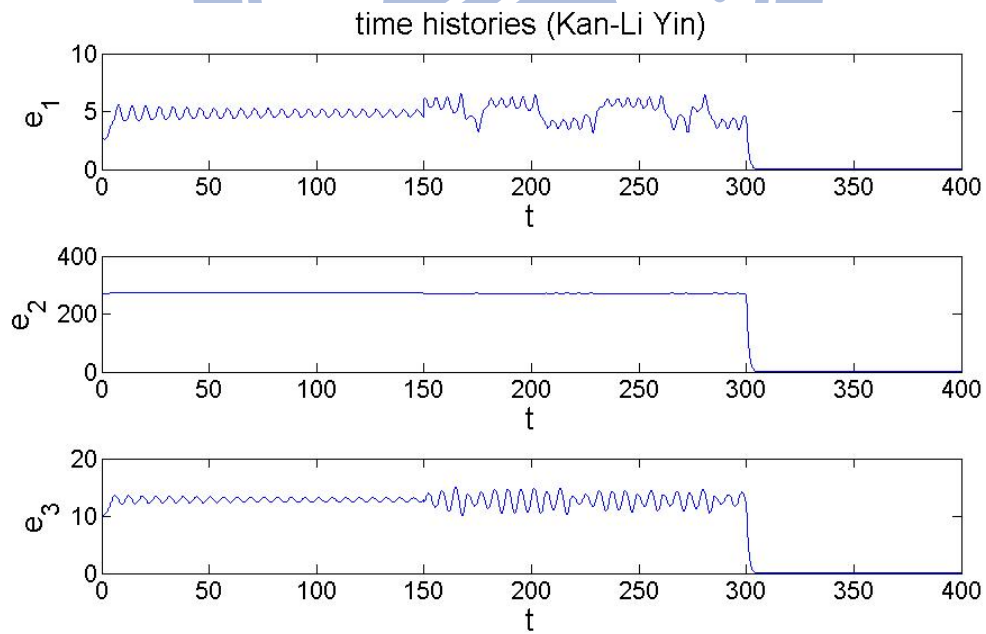


Fig. 6-2 Time histories of Yin error function for Kan-Li hexagram synchronization by GYC theory.

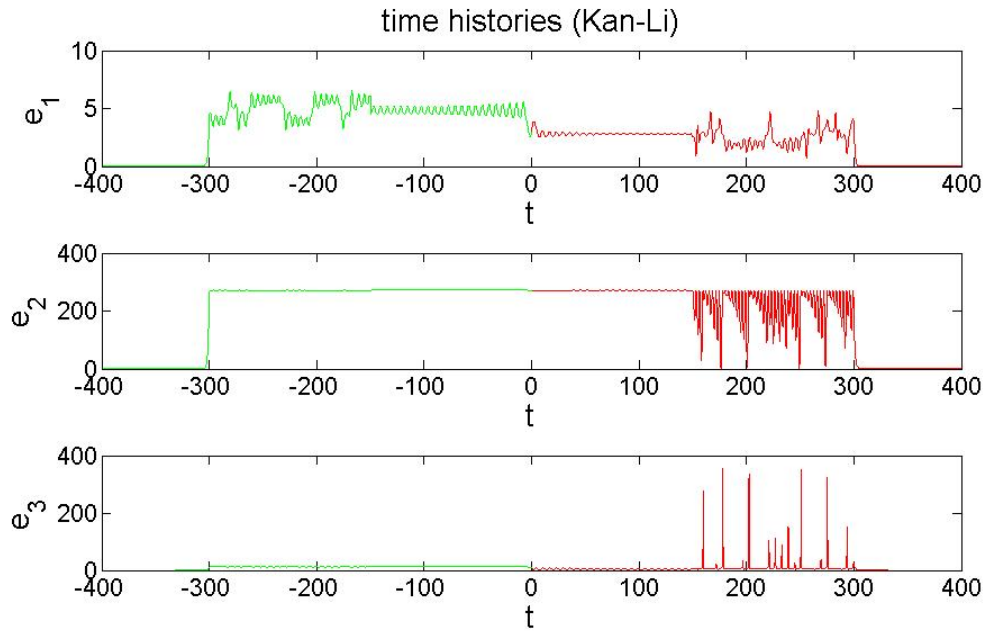


Fig. 6-3 Time histories of error function for Kan-Li hexagram synchronization by GYC theory.

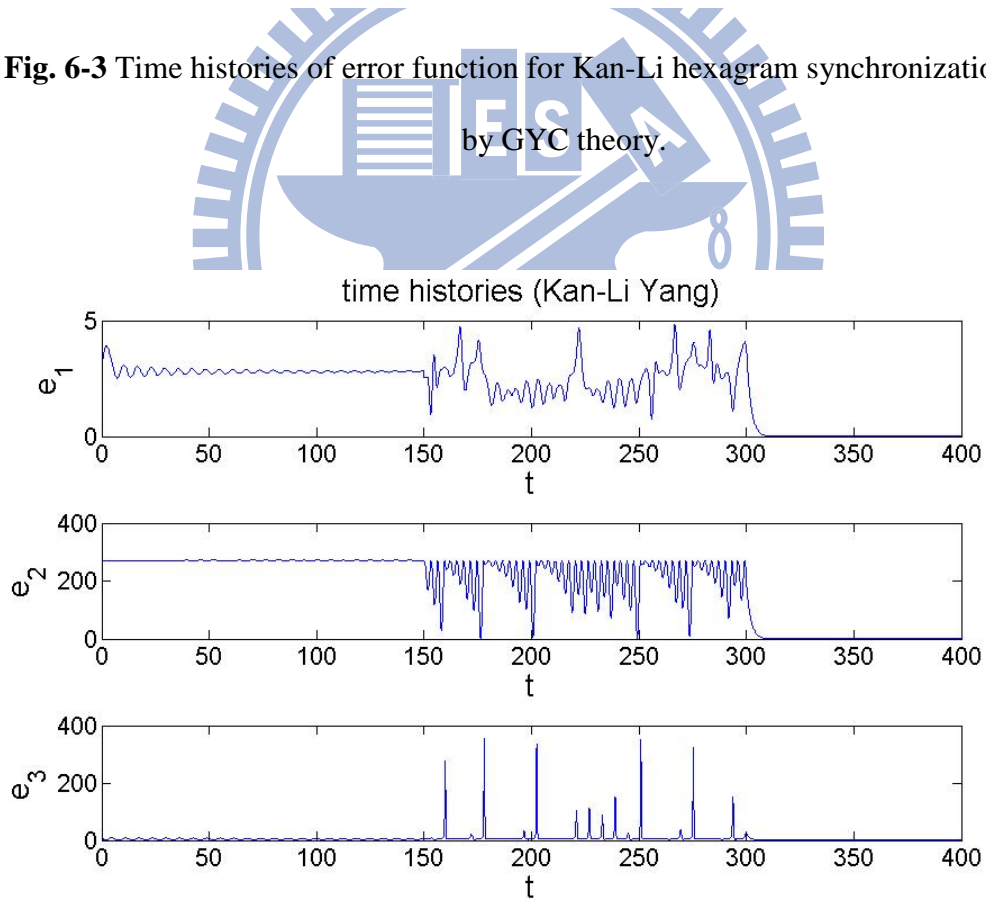


Fig. 6-4 Time histories of Yang error function for Kan-Li hexagram synchronization by Lyapunov function.

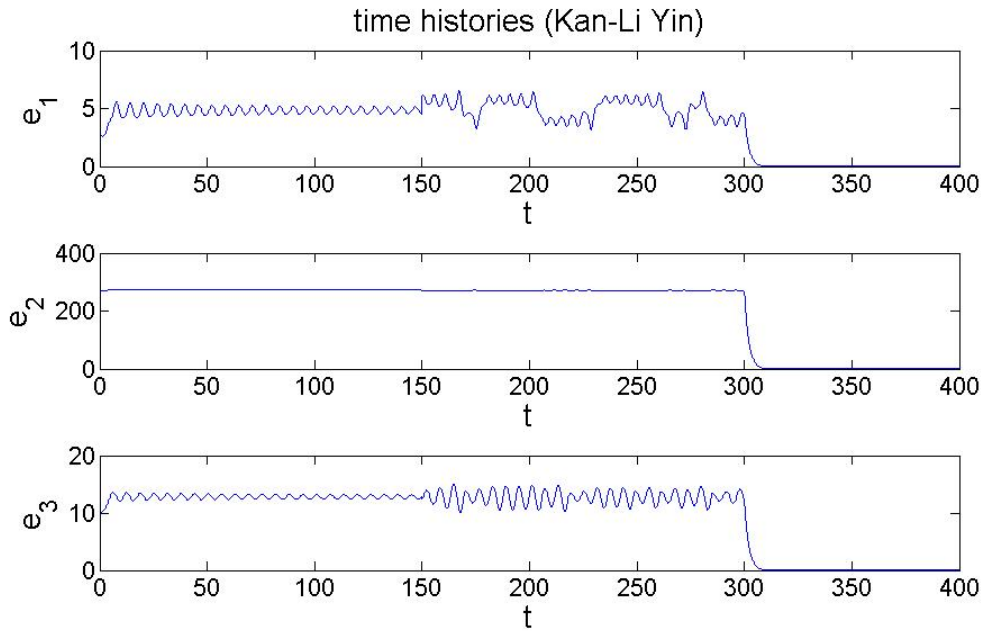


Fig. 6-5 Time histories of Yin error function for Kan-Li hexagram synchronization by Lyapunov function.

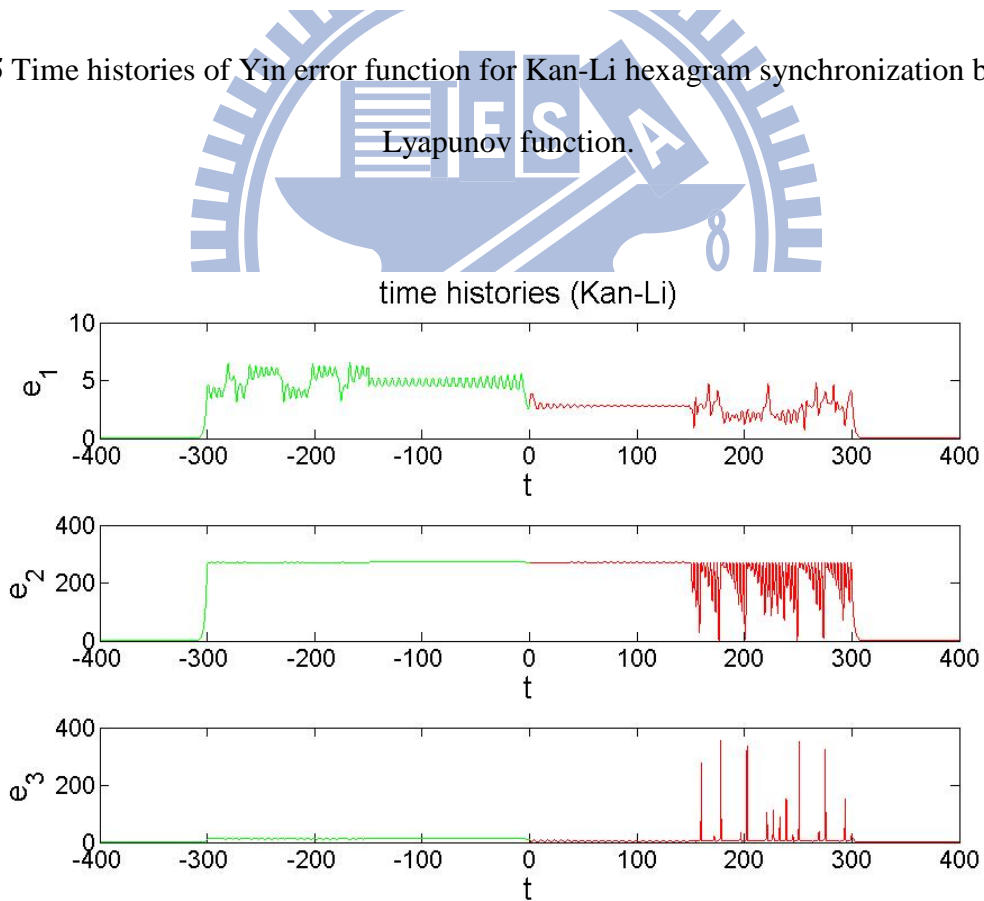


Fig. 6-6 Time histories of error function for Kan-Li hexagram synchronization by Lyapunov function.

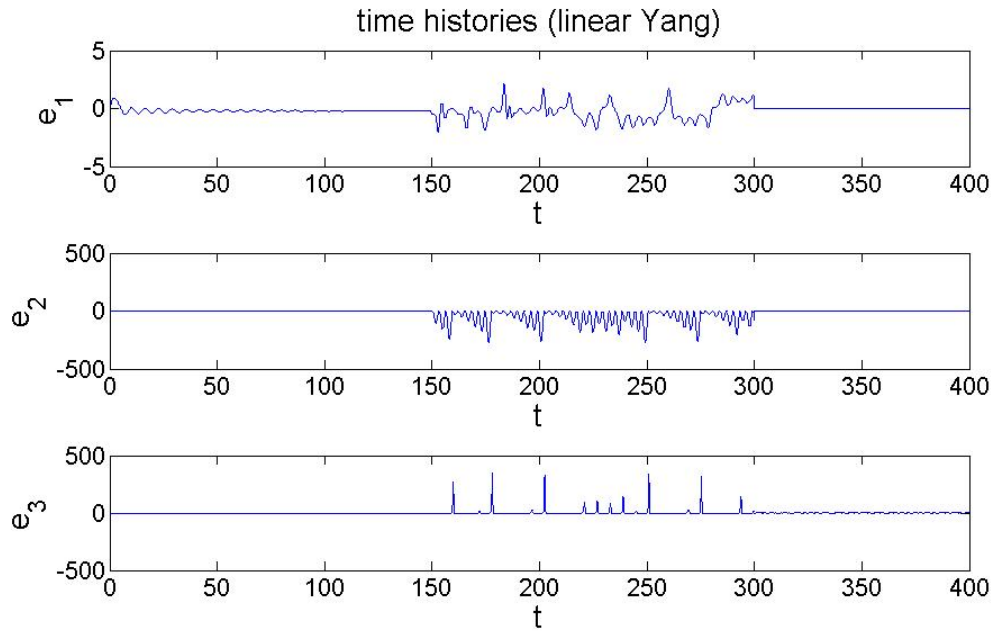


Fig. 6-7 Time histories of Yang error function for Kan-Li hexagram synchronization by linear feedback method.

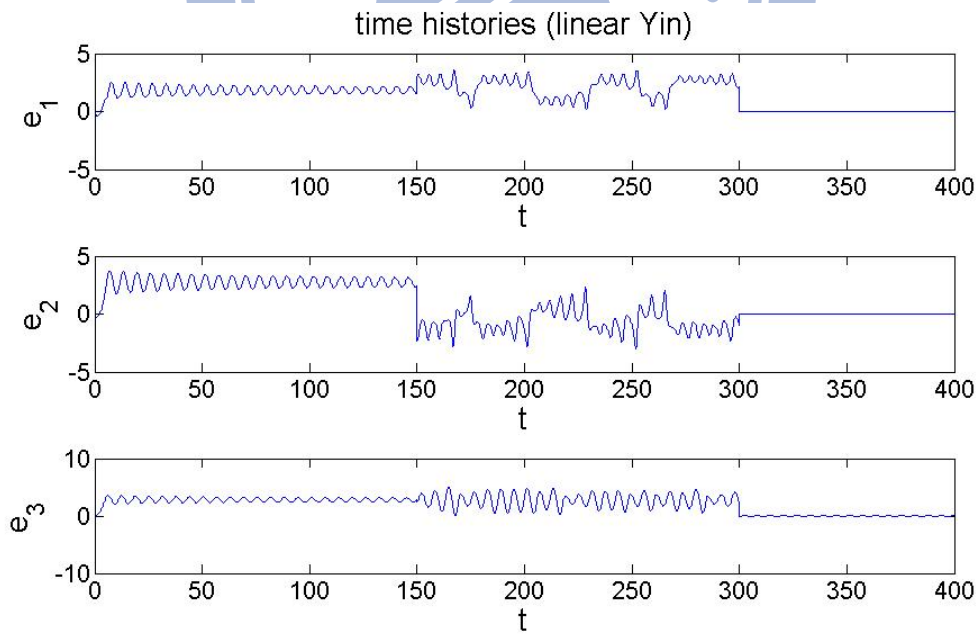


Fig. 6-8 Time histories of Yin error function for Kan-Li hexagram synchronization by linear feedback method.

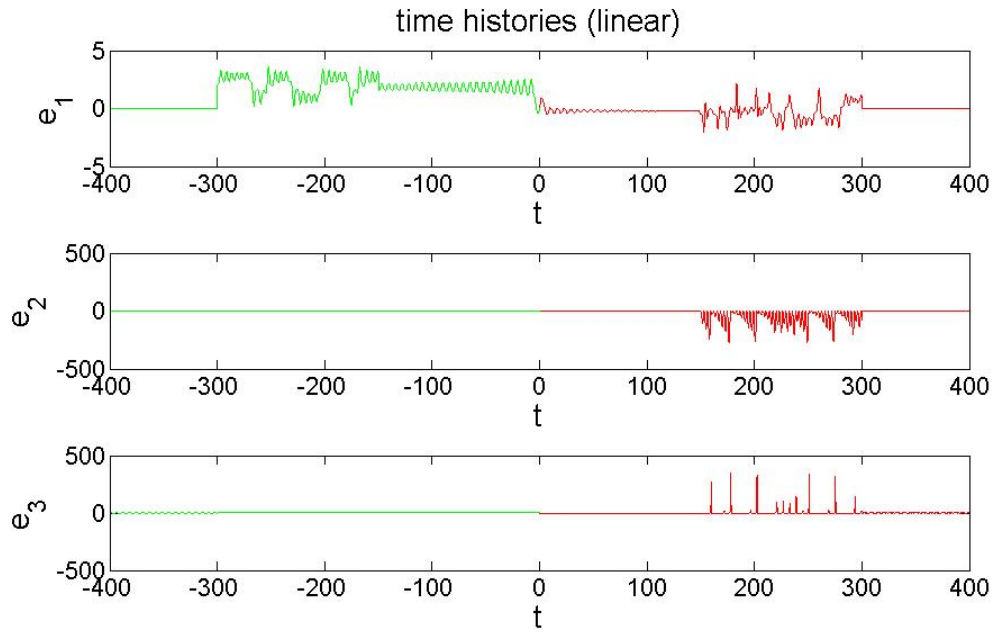
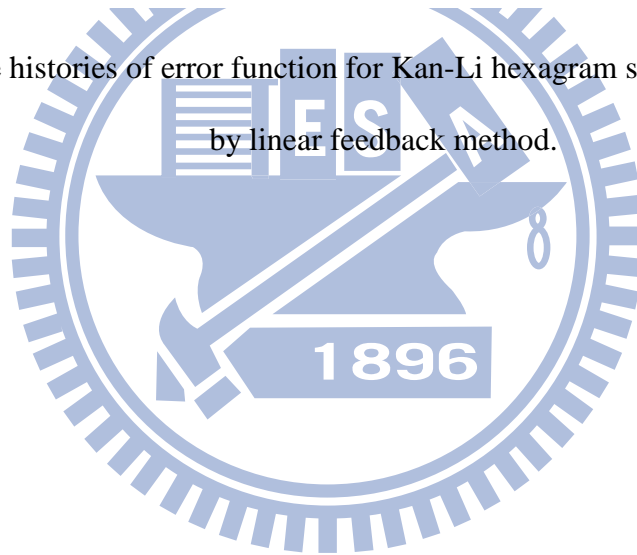


Fig. 6-9 Time histories of error function for Kan-Li hexagram synchronization by linear feedback method.



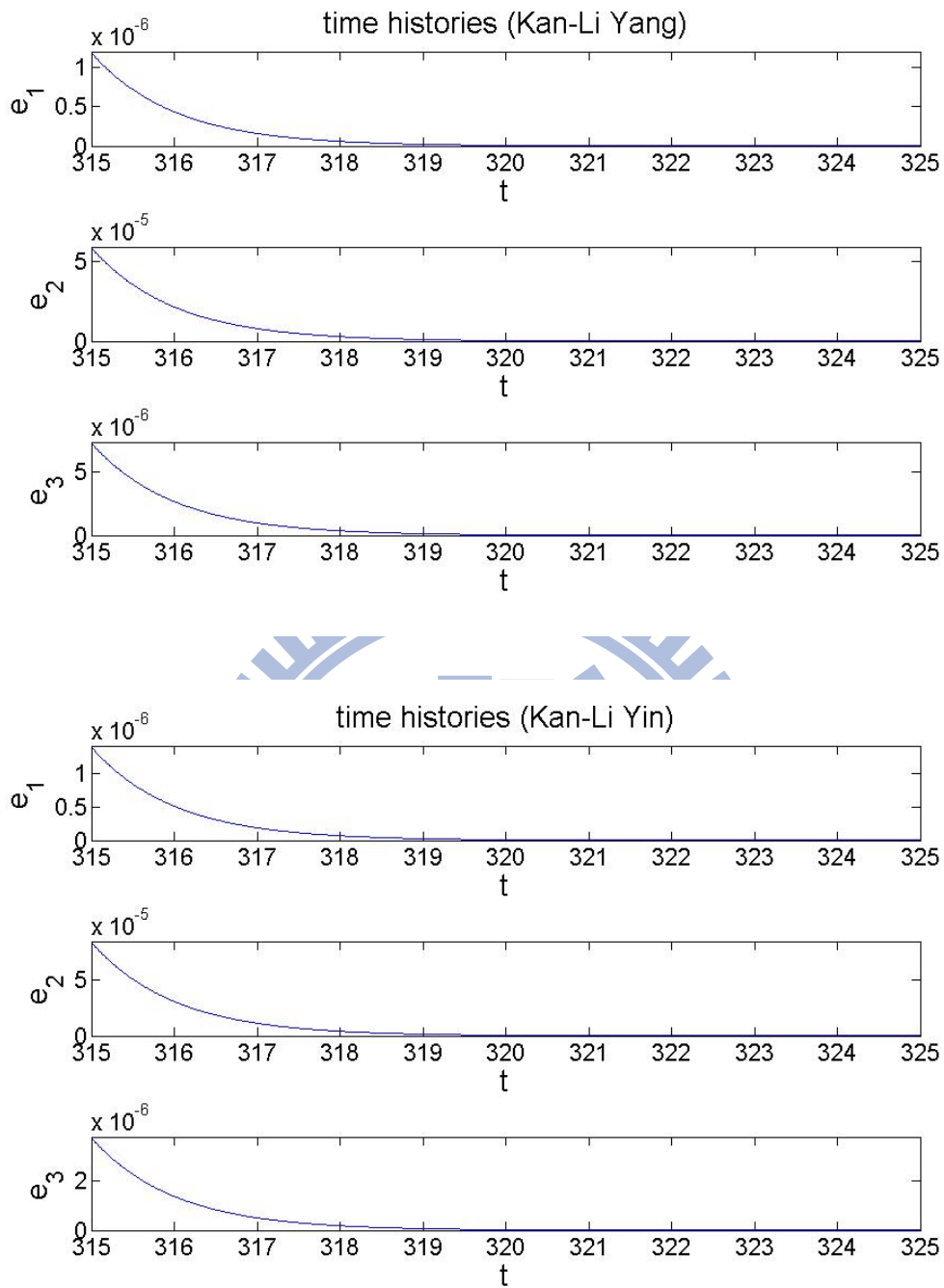


Fig. 6-10 Time histories of error function for Kan-Li hexagram synchronization by GYC theorem in 315 ~ 325 seconds.

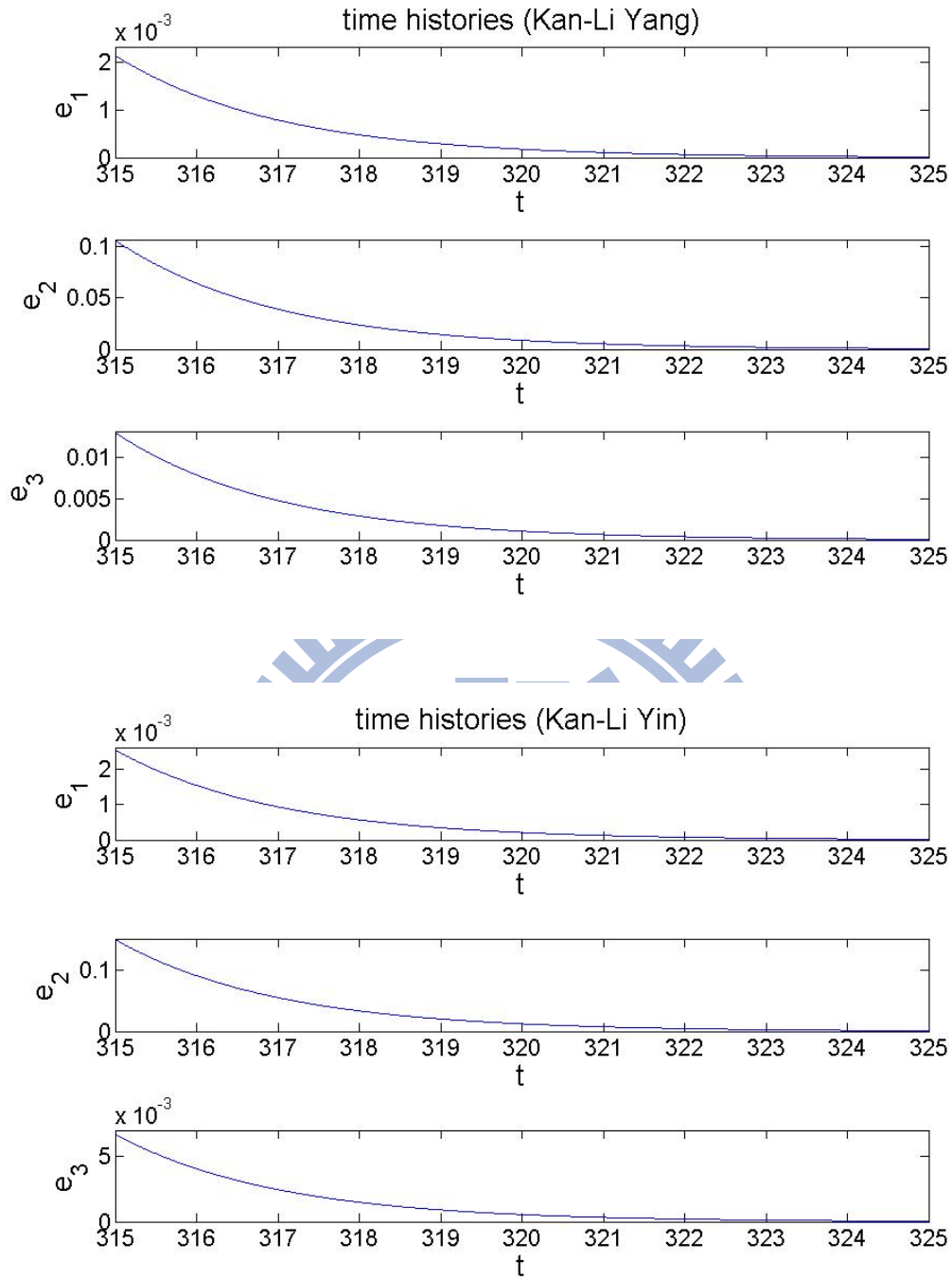


Fig. 6-11 Time histories of error function for Kan-Li hexagram synchronization by Lyapunov function in 315 ~ 325 seconds.

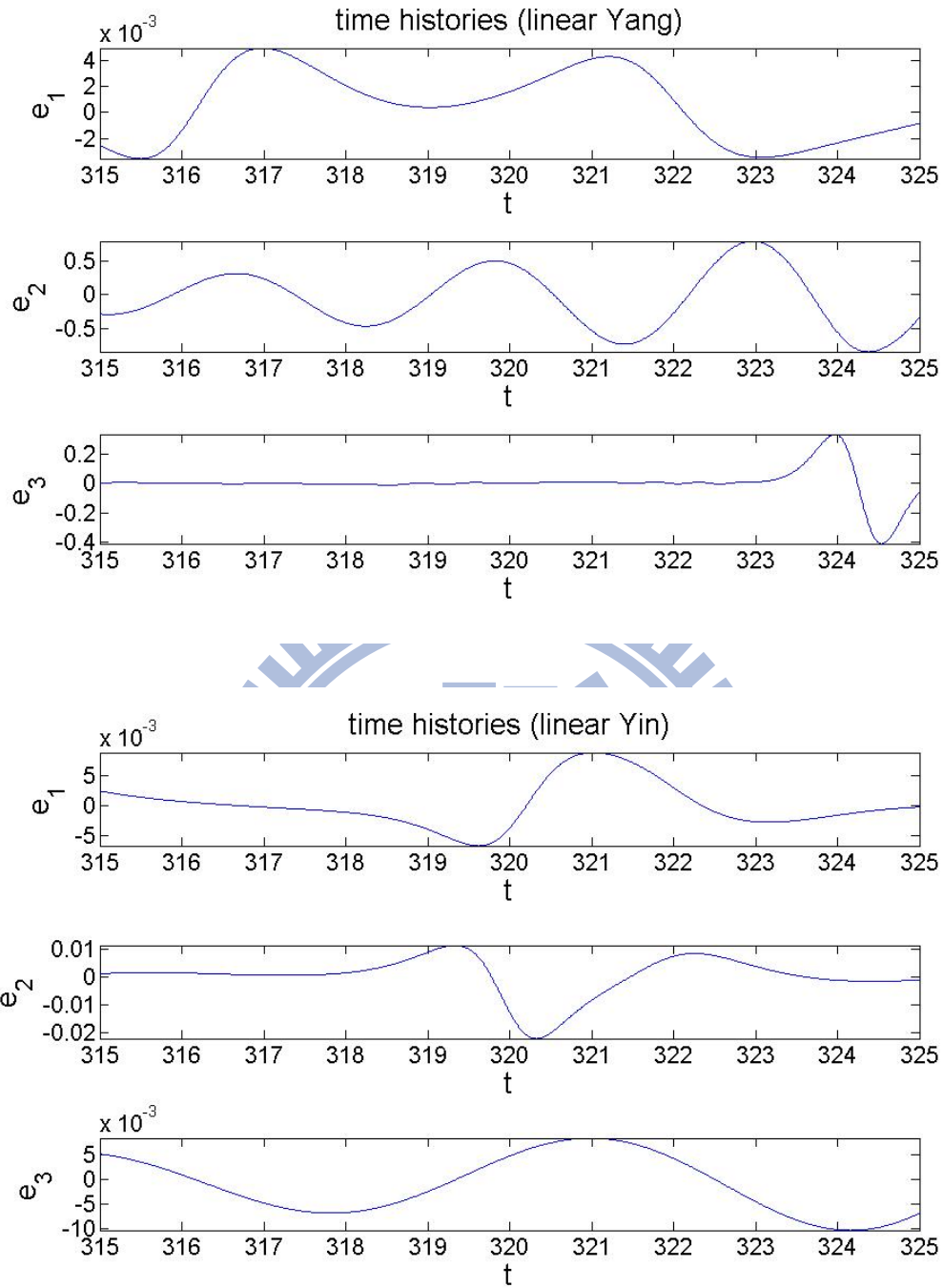


Fig. 6-12 Time histories of error function for Kan-Li hexagram synchronization by linear feedback method in 315 ~ 325 seconds.

Chapter 7

Conclusions

In this thesis, a new chaotic study is studied, the combination of chaos and Chinese philosophy is presented by chaos systems, chaos synchronization, and multiple symplectic derivative synchronization.

In Chapter 2, the chaotic behavior of Tai Ji Rössler system, combination of Yang Rössler system and Yin Rössler system, is studied by phase portraits, time history, Lyapunov exponent, bifurcation diagrams.

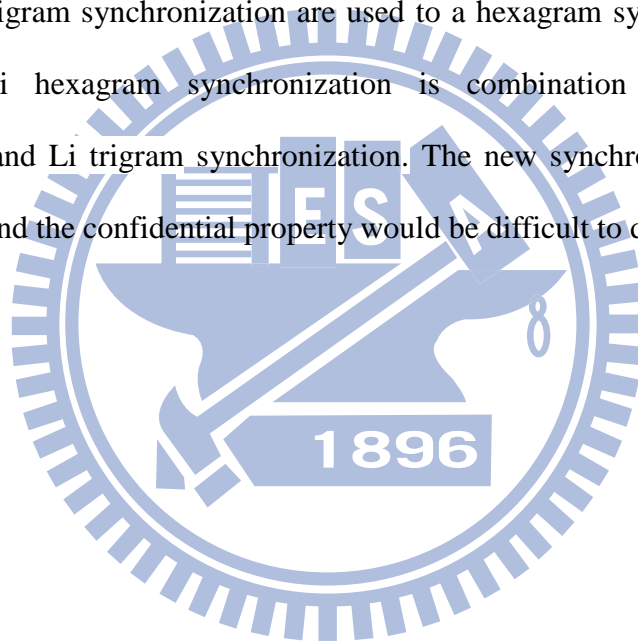
In Chapter 3, a new multiple symplectic derivative synchronization is presented. The variables and their derivatives in two given synchronization functions are used to achieve chaos control by GYC partial region stability theory. By this way, the Lyapunov function is a simple linear homogeneous function of error states and the controllers are more simple and have less simulation error because they are in lower order than that of traditional controllers. Finally, Tables and Figures in Chapter 3 are given to prove that the new strategy do synchronize system more quickly.

In Chapter 4, time scales of two partner functions are different, which for partner A is t and for partner B is τ where τ is a variable time scale, $\tau = \tau(t)$. Moreover, multiple symplectic derivative synchronization by GYC partial region stability theory is further used to change the space of error dynamics. The new synchronization in this chapter is rather complex, but the confidential property is better than common methods.

In Chapter 5, the eight trigrams, one of Chinese philosophy, are first studied with chaotic system. The figure of trigrams is used to complete a different kind of multiple

symplectic derivative synchronization. By this way, chaos synchronization could be more complex. The error dynamics have three stages. Firstly, no control is applied. And then, the synchronization of Yang and Yin system appears. Finally, error dynamics achieve synchronization. It seems very complex, but it is full compliance with figures of the eight trigram. Also GYC partial region stability theory is used for searching controller easily and synchronizing system quickly.

In Chapter 6, the eight trigrams synchronization is advanced to complete hexagram synchronization in three different ways. By the relation of trigram and hexagram, two trigram synchronization are used to a hexagram synchronization. For example, Kan-Li hexagram synchronization is combination of Kan trigram synchronization and Li trigram synchronization. The new synchronization could be rather complex, and the confidential property would be difficult to decipher.



References

- [1] Lorenz, E.N., “Deterministic non-periodic flows”, *J. Atmos.* **20**, 130–141 (1963).
- [2] Yuming Shi, Pei Yu, “Chaos induced by regular snap-back repellers”, *J. Math. Anal. Appl.* **337** 1480–1494 (2008).
- [3] Risong Li, “A note on the three versions of distributional chaos”, *Commun Nonlinear Sci Numer Simulat* **16** 1993–1997(2011).
- [4] Marc Gerritsma, Jan-Bart van der Steen, Peter Vos, George Karniadakis, “Time-dependent generalized polynomial chaos”, *Journal of Computational Physics* **229** 8333–8363 (2010).
- [5] Lacitignola, D., Petrosillo, I., Zurlini, G., “Time-dependent regimes of a tourism-based social–ecological system: period-doubling route to chaos”, *Ecol. Complex.* **7**, 44–54 (2010).
- [6] Elnashaie, S.S.E.H., Grace, J.R., “Complexity, bifurcation and chaos in natural and man-made lumped and distributed systems”, *Chem. Eng. Sci.* **62**, 3295–3325 (2007).
- [7] Jovic, B., Unsworth, C.P., Sandhu, G.S., Berber, S.M., “A robust sequence synchronization unit for multi-user DS-CDMA chaos-based communication systems”, *Signal Process.* **87**, 1692–1708 (2007).
- [8] Ge, Z.M., Chen, C.C., “Phase synchronization of coupled chaotic multiple time scales systems”, *Chaos Solitons Fractals* **20**, 639–647 (2004).
- [9] Ge, Z.M., Cheng, J.W., “Chaos synchronization and parameter identification of three time scales brushless DC motor system”, *Chaos Solitons Fractals* **24**, 597–616 (2005).
- [10] Wang, Y., Wong, K.W., Liao, X., Chen, G., “A new chaosbased fast image encryption algorithm”, *Appl. Soft Comput.* (in press).

- [11] Fallahi, K., Leung, H., “ A chaos secure communication scheme based on multiplication modulation. Commun”, *Nonlinear Sci. Numer. Simul.* **15**, 368–383 (2010).
- [12] Yu, W., “ A new chaotic system with fractional order and its projective synchronization”, *Nonlinear Dyn.* **48**, 165–174 (2007).
- [13] Chen, H.K., Sheu, L.J., “ The transient ladder synchronization of chaotic systems”, *Phys. Lett. A* **355**, 207–211 (2006).
- [14] Fujisaka H. and Yamada T., “Stability Theory of Synchronized Motion in Coupled-Oscillator Systems”, *Prog. Theor. Phys.*, 69, 32 (1983).
- [15] L.-M. Pecora and T.-L. Carroll, “Synchronizations in chaotic systems”, *Physical Review Letters*, 64 821-824 (1990).
- [16] A. Kittel, J. Parisi and K. Pyragas, “Generalized synchronization of chaos in electronic circuit experiments”, *Physica D*, 112 459-471 (1998).
- [17] R. Mainieri and J. Rahacek, “Projection synchronization in three-dimensional chaotic systems”, *Phys. Rev. Lett.* 82 3042-3045 (1999).
- [18] M. Hu, and Z. Xu, “Adaptive feedback controller for projective synchronization”, *Nonlinear Analysis: Real World Applications*, 9 1253-1260 (2008).
- [19] H.-K. Chen, “Synchronization of two different chaotic system: a new system and each of the dynamical systems Lorenz, Chen and Lü”, *Chaos, Solution & Fractals*, 25 1049-1056 (2005).
- [20] N. Vasegh and F. Khellat, “Projection synchronization of chaotic time-delayed system via sliding mode controller”, *Chaos, Solution & Fractals*, 42 1054-1061 (2009).
- [21] J. Zhou and Z.-H. Liu, “Synchronized patterns induced by distributed time delays”, *Physical Review E*, 77 056213-1-5 (2008).

- [22] G.-J. Peng and Y.-L. Jiang, "Generalized projective synchronization of a class of fractional-order chaotic systems via a scalar transmitted signal", *Physics Letters A*, 372 3963-3970 (2008).
- [23] M. Juan and X.-Y. Wang, "Generalized synchronization via nonlinear control" *Chaos*, 18 023108-1-5 (2008).
- [24] Z.-M. Ge and C.-H. Yang, "Symplectic synchronization of different chaotic system", *Chaos, Solution & Fractals*, 40 2532-2543 (2009).
- [25] Kittel A., Parisi J. and Pyragas K., "Generalized synchronization of chaos in electronic circuit experiments", *Physica D*, 112, pp.459-471 (1998).
- [26] Boccaletti S., "The synchronization of chaotic systems", *Phys. Rep.*, 366, pp.1-101 (2002).
- [27] Rosenblum M., Pikovsky A. and Kurths J., "Phase synchronization of chaotic oscillators", *Physical Review Letters*, 76, pp.1804-1807 (1996).
- [28] Rosenblum M., Pikovsky A. and Kurths J., "Synchronization in a population of globally coupled chaotic oscillators", *Europhys. Lett.*, 34, pp.165-170 (1996).
- [29] Sivaprakasam S., Shahverdiev E.-M. Spencer P.-S. and Shore K.-A., "Experimental demonstration of anticipating synchronization in chaotic semiconductor laser with optical feedback", *Physical Review Letters*, 87, 154101 (2001).
- [30] Chen J.-Y., Wong K.-W., Cheng L.-M. and Shuai J.-W., "A secure communication scheme based on the phase synchronization of chaotic systems", *Chaos*, 13, pp.508-514 (2003).
- [31] Pikovsky A.-S., Rowenblum M.-G., Osipov G.-V. and Kurths J., "Phase synchronization of chaotic oscillators by external driving", *Physica D*, 104, pp.219-238 (1997).

- [32] Barsella A. and Lepers C., “Chaotic lag synchronization and pulse-induced transient chaos in lasers coupled by saturable absorber”, *Opt. Commun.*, 205, pp.397-403 (2002).
- [33] Ge, Zheng-Ming, Li, Shih-Yu, “Yang and Yin parameters in the Lorenz system”, *Nonlinear Dyn.* 62: 105–117 (2010)
- [34] Rössler O.E., “An equation for hyperchaos”, *Physics Letters A*, 71 (1979) 155.
- [35] Letelliee C., Dutertre P. & Maheu B., “Unstable periodic orbits and templates of the Rössler system: toward a systematic topological characterization”, *Chaos*, , 5(1), 271(1995).
- [36] Gilmore R., Lefranc M., *The topology of chaos*, Wiley, (2002).
- [37] Ge, Z. M., Tsai, S. E., “Double symplectic synchronization for Ge-Ku-van der Pol System”, *Nonlinear Analysis : Theory, Methods & Applications* (2009).
- [38] J.C. Sprott, “Some simple chaotic flows”, *Physical Review E*, 2 5 (1994).
- [39] Z.-M. Ge, C.-Y. Ho, S.-Y. Li and Chang C.-M., “Chaos control of new Ikeda–Lorenz systems by GYC partial region stability theory”, *Mathematical Methods in the Applied Sciences*, 32 1564-1584 (2009).